An Electron Resonance Study of Myoglobin Single Crystals

Thesis submitted for the Degree of

Doctor of Philosophy at the

University of Birmingham

by

G. A. HELCKÉ

Department of Physics

University of Keele,

May, 1963

TEXT BOUND CLOSE TO THE SPINE IN THE ORIGINAL THESIS

MISSING PRINT

Synopsis

The g-value and line width variations of the electron resonance spectrum, from single crystals of acid met myoglobin, have been measured in both 'high spin' and 'low spin' derivative form. The g-value variation is discussed in conjunction with the present structural knowledge of the myoglobin molecule obtained from X-ray measurements. Directions in the crystal, of importance in the electron resonance study are found to be closely parallel to features in the molecular structure. It is found that the direction of the maximum g-value in the azide derivative, which is also the direction of the crystalline electric field at the iron atom, makes an angle of 9° with the normal to the haem plane as calculated from electron resonance and X-ray measurements on the 'high spin' complex. This point is discussed in connection with a possible process whereby molecular groups may be exchanged at the sixth coordination point of the iron atom.

The line width variation of from 40 to 800 gauss has been explained in terms of a scatter in the orientation of the principal g values, due to some form of disorder in the crystal structure. On this hypothesis, theoretical line width variations have been fitted to the experimentally observed line width variations. Values for the standard deviation in the orientation of the principal axes have been obtained in this way.

Acknowledgments

The author would like to thank:-

Professor D. J. E. Ingram for his continued encouragement and supervision of this work;

Dr. R. M. Deal, Jr., for his help and encouragement in the early part of this work;

The members of the Microwave Group and technical staff of the University of Keele for much cooperation and assistance;

Dr. K. Munday for supplying the myoglobin crystals;

The Royal Society for a grant towards equipment;

The Medical Research Council for a maintenance grant;

Miss V. M. Cook for her care in typing this thesis.

CONTENTS

Chapter 1

INTRODUCTION

The work described in this thesis concerns the study of one of the iron-containing haemoproteins, using the techniques of electron resonance. These proteins are of sufficient biological importance to justify their study by all available means, whilst the magnetic complex is of considerable interest in itself. In order, therefore, to relate the two aspects of the work, a very general discussion follows which aims at introducing the magnetic study of haemoproteins in a logical fashion.

1.1. The magnetic properties of matter

More than one hundred years ago, Faraday concluded that all matter has magnetic properties. These have subsequently been explained in terms of two basic magnetic effects, diamagnetism and paramagnetism, which are atomic or molecular in origin. Diamagnetism is present in all matter but the term "diamagnetic" is reserved for substances in which it is the predominant magnetic effect. The presence of paramagnetic ions or molecules in a substance can lead to various magnetic properties depending on the degree of magnetic interaction between them. If the interaction is weak, the substance is classed as paramagnetic, whilst strong interactions lead to ferromagnetic, antiferromagnetic and ferrimagnetic

effects. For the purpose of this thesis the case of strong interactions will not be considered. A description of diamagnetism and paramagnetism will show how the measurement of the magnetic properties of a substance can give information of direct interest in connection with chemical structure.

1.2 Diamagnetism and Paramagnetism

Classically considered, diamagnetism arises from the orbital acceleration or Larmor Precession of an electron due to a magnetic field. Thus an increase in magnetic field increases the angular momentum of the electron. A corresponding magnetic moment is induced, the direction of which opposes the applied field. The diamagnetic contribution to the magnetic susceptibility is negative and temperature independent to a first approximation. From this reasoning every electron orbit should contribute to diamagnetism through the Larmor Precession and all matter should therefore be diamagnetic.

An atomic electron has an angular momentum due to its orbital motion, and an intrinsic angular momentum known as its spin. Each of these has its corresponding magnetic moment, both of the same order of magnitude. An assembly of non-interacting atoms, each possessing a magnetic moment, would not show a permanent magnetic moment in the absence of an external magnetic field, due to the random orientation of the magnetic dipoles. However a magnetic field

induces a bulk magnetic moment, due to its orienting effect on the magnetic dipoles, which is parallel to the magnetic field. This paramagnetism will be temperature dependent as thermal motion will be the chief de-orienting agent.

Temperature dependent paramagnetism can only be found in substances whose molecules possess a magnetic moment. Such substances are relatively rare, because in most compounds the electron spins are paired with opposite orientations, while the orbits tend to form closed shells. The total angular momentum and therefore the magnetic moment is then zero. The magnetic moment possessed by certain nuclei is always very much smaller than that due to the electron and is detected as a hyperfine splitting in the paramagnetic resonance spectrum to be discussed later.

1.3 Chemical Structure

The previous discussion described the close relationship existing between the presence of unpaired electrons in a substance and its magnetic properties. It was mentioned that in a closed atomic shell, the electron spins are paired with opposite spin orientations so that the magnetic effects of their spins cancel. At the same time the orbital angular momentum of a closed shell is zero and there is no orbital contribution to the magnetic moment. Atoms and ions with this rare gas configuration must therefore be diamagnetic. Conversely it must be the valence electrons of most

atoms which provide the magnetic properties.

Though the interaction of atoms in molecules or in solids is not essentially influenced by magnetic effects, the spin plays an important part because opposite spin orientations for two electrons allow them to occupy the same orbit. Thus in a "covalent" bond the electron spins will cancel with a consequent reduction in the magnetic moment.

Magnetic measurements on the various chemical compounds formed by an element can therefore give information directly concerning chemical structure. The magnetic effects of the orbital motion complicate this situation considerably, but the same effects may yield valuable information about the electron orbits.

Many atoms and ions have incomplete electron shells and hence a permanent magnetic moment. However, compounds containing these atoms are often diamagnetic because the valence electrons have formed bonds in which the spins are paired. There are two major exceptions to this general rule, (i) atoms in which the shells inside the valency electrons are not filled and (ii) compounds in which some of the normal bonds have been broken or modified to leave unpaired electrons scattered throughout the sample.

The second of these groups contains such cases as organic free radicals, irradiated crystals and structures with many dislocations or breaks, and will not be considered in this thesis. The first comprises the so-called 'transition elements'.

1.4 The Transition Group Elements

As stated above the requirement of an incomplete electron shell, restricts the occurrence of paramagnetism in normal compounds to certain well-defined regions of the periodic table, known as the transitions groups. In these elements there is an incomplete shell separated by one or more complete shells from the surroundings of the atom. The electrons in these shells are therefore not necessarily involved in the chemical bonding.

The iron group elements have an incomplete 3d shell so that the magnetic electrons will play a greater part in the chemical bonding here than in the rare earth elements. In the last named group there is an incomplete 4f shell separated from the surroundings by two or three complete shells. It is not surprising therefore that the magnetic properties of the rare earths resemble those of free atoms and ions.

The magnetic properties of these two groups have been extensively studied but much less is known about those of the palladium (4d), platinum (5d) and uranium (5f - 6d) groups.

Salts of the iron group elements with which this thesis is primarily concerned, exhibit rather unexpected magnetic properties. These are more like those which would result from electron spin only rather than from an agglomeration of free ions. This lack of an orbital contribution to the magnetic moment is known as orbital "quenching" and will be discussed at a later stage. However, it

may be mentioned that this is due to the presence of strong crystalline electric fields into which the orbital motion is locked. It is then unable to make its proper contribution to the magnetic susceptibility. Another effect is that the magnetic field associated with the orbital motion will have directional properties determined by the crystalline electric field. A competition then arises between this magnetic field and the external magnetic field for the orientation of the spin magnetic moment. This magnetic moment sets itself along the resultant of the two and magnetic anisotropy results. Measurements on single crystals will therefore yield more detailed information than powders or solutions in which the anisotropy will be averaged out.

1.5 Magnetic Measurements

The main phenomenon in any paramagnetic substance is its susceptibility, which is defined by the relation

$$I = xH$$

where I is the intensity of magnetization or magnetic moment per unit volume, x the susceptibility per unit volume, and H the magnetic field.

Susceptibility is essentially a bulk property and is a measure of the net effects of the diamagnetic and paramagnetic contributions. The latter is itself a sum of the contributions from the magnetic moments due to the electron orbital motion, electron spin, and

nuclear spin. However, for salts of the iron group, the orbital motion is largely quenched. Ignoring the small contribution from the diamagnetism and nuclear spin the susceptibility may then be compared with that expected from electron spins only. In this way an estimate of the number of unpaired electrons present can be obtained.

Two facts often prevent susceptibility measurements from yielding precise experimental data. Firstly except at temperatures below 1 ^{o}K a number of levels are populated and the susceptibility is an average over these levels. Secondly the unit cell in a single crystal may contain several paramagnetic ions whose axes of anisotropy are differently oriented. The net anisotropy is then a sum of the individual contributions.

Bearing in mind these two problems therefore, it follows that any technique which yields information on the magnetic electrons in the ground state and can give precise data for each ion will be of great value. Such a technique is Magnetic Resonance.

1.6 Magnetic Resonance

Magnetic Resonance may be roughly divided into four types:- nuclear, ferromagnetic, antiferromagnetic and electron resonance. As the name implies nuclear resonance is concerned with nuclear dipoles. whilst the others are concerned with electronic dipoles. Ferromagnetic and antiferromagnetic resonance is observed in magnetic

systems in which the electronic dipoles are strongly coupled together by exchange forces. However electron resonance, with which this thesis will be concerned, is confined to loosely coupled systems where the paramagnetic units may be regarded as individuals.

The term "resonance" refers to the analogy between a microscopic magnetic carrier, with an angular momentum precessing about the magnetic field direction, and the numerous macroscopic examples of resonance. In the latter a system performing a periodic motion absorbs power from a periodic driving force; this is greatest when the frequency of the driving force and the natural frequency of the system are equal. If the magnetic carrier is an electron situated in a constant magnetic field then its periodic motion is the Larmor precession. The driving force in magnetic resonance is a periodic magnetic field applied at right angles to the constant magnetic field. When the frequency of the driving force approaches that of the Larmor precession, power will be absorbed from it.

In spectroscopic terms the principle of the method is again very simple. A constant magnetic field is applied to the paramagnetic ions and the electronic energy levels undergo Zeeman splittings. Simultaneously, a small radio-frequency magnetic field is also applied. The splittings can be measured directly and very accurately by finding the frequencies which induce transitions between the Zeeman levels.

The technique of paramagnetic resonance has proved very valuable in the study of transition group ions, giving four main types of

information:

(i) As mentioned earlier, the bulk properties of single crystals, that is the susceptibility and specific heat, are averages over several populated energy levels at normal temperatures. At very low temperatures, these properties depend only on the energy levels within a few cm^{-1} of the ground level. These are the levels studied by electron resonance, so that information obtained can be used when studying the bulk properties at low temperatures.

(ii) The magnetic anisotropy in a single crystal has a symmetry related to that of the crystalline electric field. This in turn is related to the symmetry of the environment of the paramagnetic ion in the crystal. The electron resonance results will reflect the magnetic anisotropy and hence can provide information on the symmetry of the surrounding of each ion; also about the nature and strength of the binding between the ion and its diamagnetic neighbours.

(iii) The broadening of electron resonance absorbtion lines can occur in a variety of ways, the majority of which can be divided roughly into two groups. The first being those which broaden the actual energy levels between which the resonance absorbtion takes place. The second being macroscopic effects, such as the spatial variation of the external constant magnetic field over the paramagnetic sample.

The broadening of energy levels is closely related to the

relaxation time of the level by Heisenberg's uncertainty principle. Line width measurements can therefore give information on the various interactions between the magnetic carriers and the crystal lattice, and between the magnetic carriers themselves.

(iv) Whilst electron resonance concerns electronic transitions, the interaction between the electrons and nucleus can cause a splitting of the electronic energy levels. From measurements on such splittings, information on the nucleus of the paramagnetic ion can be obtained, for example; the nuclear spin and approximate values for the nuclear magnetic dipole and electric quadrupole moments.

1.7 Transition Group Studies

In a study of the magnetic properties of the transition group elements the paramagnetic ions are usually inserted as impurities into diamagnetic single crystals. This magnetic dilution allows better resolution of the spectrum, which in the undiluted crystal is broadened by dipolar interactions.

The commonest method has been to grow mixed crystals such as potassium zinc sulphate $\left[K_2Zn(SO_4)_2,\ 6H_2O\right]$. The zinc ions can then be replaced by paramagnetic ions to give the required paramagnetic concentration. In the majority of the crystals which have been used in the study of the transition group ions, the magnetic complex may be regarded as approximately octahedral. The central paramagnetic

ion is surrounded by six neighbours, for example water molecules in the above salt. Another salt used with the iron group is potassium cobalticyanide $\left[K_3Co(CN)_6\right]$. Here the trivalent cobalt ion has no paramagnetic moment due to its $3d^6$ electrons being paired. The paramagnetic ion to be investigated can be substituted, and in this complex will be surrounded by an octahedron of CN molecules.

The nature of the six surrounding atoms or molecules will govern the strength of the crystalline electric field which the paramagnetic ion experiences. To study the effect of this on the magnetic properties it is therefore necessary to grow two different crystal hosts for the same element.

Whilst a knowledge of the host lattice from X-ray measurements aids the interpretation and understanding of the resonance results, the latter are so sensitive to the symmetry of the magnetic complex that distortions can be detected which are not observable with X-rays.

1.8 The Haemo-Proteins

A slightly different situation is faced in the study of the haemo-proteins. These are large protein molecules known to contain iron in an octahedral environment. Single crystals can be grown from these proteins but unlike the crystals mentioned above, the magnetic dilution is fixed. However, there is in fact sufficient dilution for the paramagnetic ions to be only loosely coupled.

The detailed structure of the haemo-proteins is lately unknown

with the notable exceptions of Sperm Whale Myoglobin and Haemoglobin. Even the structure of these was as yet incompletely determined when the first electron resonance investigations began. In this case therefore the resonance measurements were able to provide structural information from their symmetry which supplemented the X-ray measurements. Now, however, detailed structural information from X-ray measurements is available for Myoglobin which greatly aids interpretation of the resonance results.

A peculiarity of crystals of the haemo-proteins is their loose water filled structure. Due to this, chemical changes may be made to the surroundings of the iron atom without disturbing the overall crystal structure. In fact the ligand at the sixth co-ordination point may be exchanged for various molecular groups with subsequent changes in the crystal field and bonding of the iron atom. Any consequent local structural changes will also be detected in the resonance results.

It can be seen from this description that the haemo-proteins form an interesting system for investigation on purely academic grounds. However, the haemo-proteins are of great interest biologically. Haemoglobin itself is the pigment responsible for the colour of red blood corpuscles. The most important function of haemoglobin is that of combining with oxygen at the lungs and releasing oxygen wherever it is needed. This reaction is a bonding of the oxygen molecule to the iron atom which is the para-

magnetic unit studied by electron resonance. The effects of various reactions of the iron atom which are of such great interest biologically can thus be studied minutely whilst ignoring the greater part of the diamagnetic protein molecule.

Chapter 2

Basic Theory

2.1. The Free Ion

Historically it was found necessary to add the property of spin to the fundamental electronic properties of mass and charge, in order to explain such features as multiplet splittings in atomic spectroscopy. Spin corresponds to the classical conception of a material particle rotating on its axis. This rotation gives rise to a spin angular momentum, whilst the rotation of the charge gives rise to a magnetic moment. In addition, an electron belonging to an atom or ion will have an orbital angular momentum and magnetic moment. The electronic state is then labelled by the quantum numbers L and S, which represent the angular momentum measured in units of $h/2\pi$. The corresponding magnetic moments are

$$\bar{\mu}_L = -\beta\bar{L} \quad \text{and} \quad \bar{\mu}_S = -g\beta\bar{S} \qquad 2.1$$

where β is the Bohr magneton $\frac{eh}{4\pi mc}$, and the factor g is the Landé "g" factor, first introduced in connection with the anomalous Zeeman effect. The "g" factor has the value 2 (more precisely 2.0023) for electron spin only and 1 for orbital motion only.

These magnetic moments will interact with an external magnetic field $\bar{H}$, the total interaction being

$$-\bar{H}(\bar{\mu}_L + \bar{\mu}_S) = \beta H(\bar{L} + 2\bar{S}) \qquad 2.2$$

In order to derive the resonance condition, the simplest possible situation to consider is that of an electron in an S orbital, as in the hydrogen atom. Here there is no orbital angular momentum, so that the interaction is just $g\beta\bar{H}.\bar{S}$. If the magnetic field is in the z direction the interaction can be written $g\beta H_z S_z$. The spin quantum number of an electron is $\frac{1}{2}$, and its spin component in the direction of the magnetic field has the eigen values M_s of $\frac{1}{2}$ and $-\frac{1}{2}$. The magnetic energy of the electron is then $-\frac{1}{2}g\beta H_z$ or $\frac{1}{2}g\beta H_z$, which corresponds to the electron spin being aligned parallel or anti-parallel to the field. The energy of the parallel or (α) spin is lowered by $\frac{1}{2}g\beta H_z$, whilst the energy of the anti-parallel or (β) spin is raised by $\frac{1}{2}g\beta H_z$. The energy difference between the two spin levels is then $g\beta H_z$. In the case of a free ion the splitting is independent of the direction of the applied magnetic field, and it may therefore be written as $g\beta H$.

Magnetic dipole transitions can be induced between these levels by applying an oscillating magnetic field in a direction perpendicular to the main field H_z, with a frequency ν such that

$$h\nu = g\beta H. \qquad 2.3$$

The selection rule for the transition is that $\Delta M_s = \pm 1$. This is the general resonance condition.

The frequency of resonance is thus proportioned to the magnetic field, so that either may be varied to achieve resonance. In

practice it is more convenient to vary the magnetic field and to keep the frequency constant. The spectrum is then presented as a relation between absorption and magnetic field for a given frequency.

The spectrum for atomic hydrogen, the simple case under discussion, actually shows two electron resonance lines. This is due to the spin of the proton which, like that of the electron, has a magnitude of $\frac{1}{2}$. Due to the greater mass, however, the magnetic moment of the proton is only about 10^{-3} Bohr magnetons. This magnetic moment interacts both with the external field and with the magnetic field of the electron, the latter interaction being considerably larger than the former. The proton spin is usually denoted by $\bar{I}$, the total magnetic interaction being of the form

$$g\beta\bar{H}.\bar{S} + A\bar{S}.\bar{I} + B\bar{H}.\bar{I} \qquad 2.4$$

where B depends on the magnetic moment of the proton, and A depends also on the quantum mechanical probability of the electron being at the position of the proton.

As with the electron spin the nuclear spin is quantized by the external magnetic field. The spin component in the z direction having eigen values $M_I = \pm \frac{1}{2}$, the magnetic energies of the electron are then

$\frac{1}{2}g\beta H_z + \frac{1}{4}A + \frac{1}{2}BH_z$ and $\frac{1}{2}g\beta H_z - \frac{1}{4}A - \frac{1}{2}BH_z$

$-\frac{1}{2}g\beta H_z + \frac{1}{4}A - \frac{1}{2}BH_z$ and $-\frac{1}{2}g\beta H_z - \frac{1}{4}A + \frac{1}{2}BH_z$.

Neglecting the term BH_z in comparison with A, two transitions occur with the selection rules $\Delta M_S = \pm 1$ and $\Delta M_I = 0$, as shown in the diagram Fig. (2.1).

The resonance conditions for the two transitions are

$$h\nu = g\beta H_1 + \tfrac{1}{2}A \quad \text{and} \quad h\nu = g\beta H_2 - \tfrac{1}{2}A.$$

The separation between the two transitions corresponds to a field change of

$$H_2 - H_1 = \frac{A}{g\beta} \qquad 2.5$$

The splitting of the resonance spectrum is known as Hyperfine Structure. In general, if the nuclear spin of a paramagnetic atom or ion is I, the nucleus has 2I + 1 orientations in the magnetic field produced by each of the 2S + 1 orientations of the electronic moment. Each electronic energy level is therefore subdivided into 2I + 1 components, giving 2I + 1 equally spaced lines of equal intensity, as long as the external field is very much greater than that produced by the nucleus.

So far the discussion has considered an electron in an S orbit, having no orbital angular momentum. If the electron has $l \neq 0$, it has two types of angular momenta represented by the quantum numbers s and l. The interaction between the corresponding spin

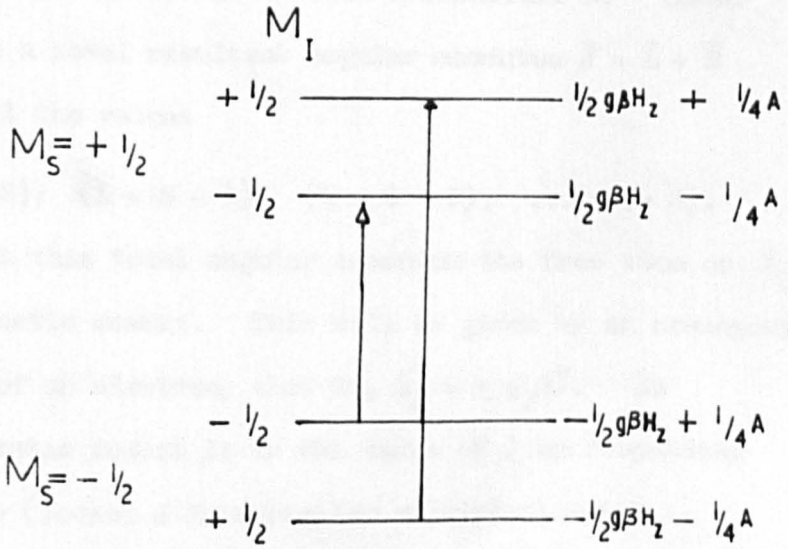
M_I
$+ 1/2$
$1/2\,g\beta H_z + 1/4\,A$
$M_S = + 1/2$
$- 1/2$
$1/2\,g\beta H_z - 1/4\,A$
$- 1/2$
$-1/2\,g\beta H_z + 1/4\,A$
$M_S = - 1/2$
$+ 1/2$
$-1/2\,g\beta H_z - 1/4\,A$

FIG. 2.1.

and orbital magnetic moments, known as spin-orbit interaction, couples these together, to form a resultant total angular momentum $j.\left(\frac{h}{2\pi}\right)$.[*] For more than one electron the total angular momentum can be derived using the Russell-Saunders coupling, which supposes that the individual spin momenta couple, to form a resultant spin angular momentum S, and the orbits to form a resultant L. These then couple to form a total resultant angular momentum $\bar{J} = \bar{L} + \bar{S}$ where $\bar{J}$ can have all the values

$$(L + S);\ (L + S - 1);\ (L + S - 2);\ \ldots (L - S).$$

Associated with this total angular momentum the free atom or ion will have a magnetic moment. This will be given by an analogous expression to that of an electron, that is, $\bar{\mu}_J = - g_J \beta \bar{J}$. In calculating the magnetic moment it is the value of J corresponding to the lowest energy (lowest J in a regular multiplet) which is usually most important, since the lowest levels have the greatest population at normal temperatures. Calling this value of the total angular momentum J_o, the associated magnetic moment can be written as

$$\bar{\mu}_{J_o} = - g_{J_o} \beta \bar{J}_o \ , \qquad 2.6$$

---

[*] NOTE: The quantum numbers l, s and j are the projections of the precessing vectors $\sqrt{l(l+1)}$, $\sqrt{s(s+1)}$ and $\sqrt{j(j+1)}$, along the z direction. The value of the total angular momentum, therefore, should really be written as $\sqrt{j(j+1)}\ h/2\pi$, but the single letters are used for convenience.

but the magnetic moment of the free atom may be written as

$$\bar{\mu} = \bar{\mu}_L + \bar{\mu}_S \quad . \qquad 2.7$$

Remembering that

$$\bar{\mu}_L = -\beta\bar{L}$$

and

$$\bar{\mu}_S = -2\beta\bar{S} \qquad 2.1$$

it is evident that as

$$\bar{\mu} = -\beta(\bar{L} + 2\bar{S}) \qquad 2.8$$

and

$$\bar{J} = \bar{L} + \bar{S} \qquad 2.9$$

$\bar{\mu}$ cannot be parallel to $\bar{J}$ (or to $\bar{\mu}_J$), but can be considered as precessing uniformly around $\bar{J}$.

Writing $\bar{\mu} = \bar{\mu}_{\parallel} + \bar{\mu}_{\perp}$, where $\bar{\mu}_{\parallel}$ and $\bar{\mu}_{\perp}$ are components respectively parallel and perpendicular to $\bar{J}$, it can be seen from the diagram, Figure (2.2), that

$$\bar{\mu}_{\parallel} = \bar{\mu}_L \cos(\bar{L}, \bar{J}) + \mu_S \cos(\bar{S}, \bar{J}) = -g_J\beta\bar{J} \qquad 2.10$$

where

$$g_J = \frac{3}{2} + \frac{S(S+1) - L(L+1)}{2J(J+1)} \qquad 2.11$$

g_J, the Landé "g" factor has the value 2 when L = 0, and 1 when S = 0. However, it may be noted that g_J need not lie between these values; for example, in a $^2P_{\frac{1}{2}}$ state $g = \frac{2}{3}$ and in a $^4P_{\frac{1}{2}}$ state

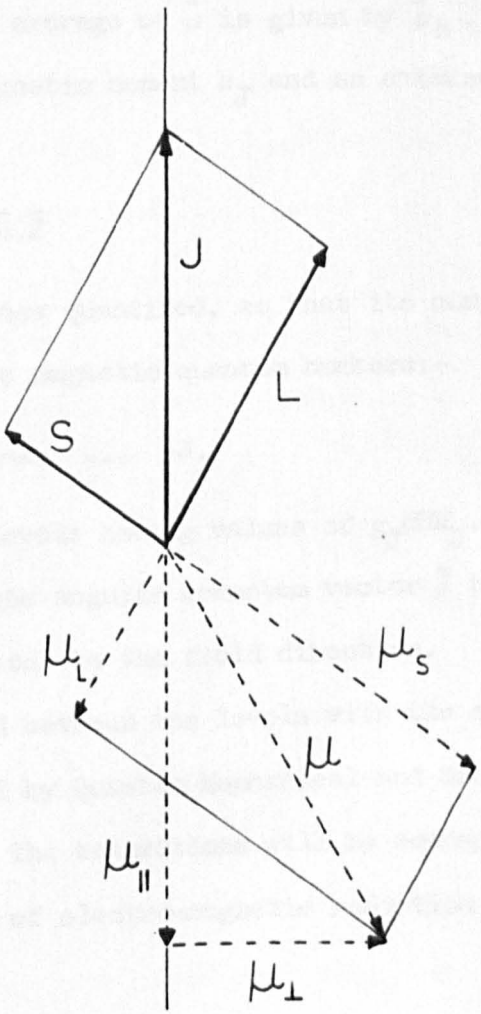

FIG. 2.2

COUPLING OF SPIN AND ORBITAL ANGULAR MOMENTA IN A FREE ATOM OR ION

$$g = \frac{8}{3} .$$

The time average of $\mu_{\perp}$ vanishes due to the uniform precession of $\bar{\mu}$ about $\bar{J}$, so that the time average of $\bar{\mu}$ is given by $\bar{\mu}_{\parallel}$.

The interaction of the magnetic moment μ_J and an external magnetic field H_z is

$$- \bar{\mu}_J \bar{H} = g_J \beta \bar{H} . \bar{J} \qquad 2.12$$

The total angular momentum is now quantized, so that its components in the field direction have the magnetic quantum numbers:-

$$M_J = J; \quad J-1; \quad J-2; \quad \ldots \quad -J.$$

There are thus $2J + 1$ energy levels having values of $g_J \beta H M_J$. These correspond to the picture of the angular momentum vector $\bar{J}$ taking on $(2J + 1)$ discreet orientations to the field direction. Magnetic dipole transitions are allowed between the levels with the selection rule $\Delta M_J \pm 1$, which is imposed by Quantum Mechanical and Group Theoretical considerations. The transitions will be accomparied by the emission or absorption of electro-magnetic radiation following the condition

$$h\nu = g_J \beta H \quad . \qquad 2.13$$

The electron resonance spectrum will, therefore, consist of one line only.

Free atoms and ions are not found naturally but can be produced in discharge tubes, the dissociated atoms being passed in a stream through an electron resonance absorption cavity.

2.2. The Paramagnetic Ion in a Crystal Lattice

When the paramagnetic ion is situated in a crystal lattice, the bonding, which takes place between it and the neighbouring diamagnetic ions, must affect profoundly the energies of the orbital levels involved. In the iron group transition metals therefore, the effects are most pronounced upon the 3d and 4s orbitals. The relative energies and the separations between these orbital levels are, therefore, of fundamental importance in determining the electron distribution between the levels, and the subsequent spin pairing in a particular complex.

Two main theories, the Electrostatic Crystal Field Theory and the Molecular Orbital Theory, have been developed to predict the orbital energies in complexes.

The first of these theories considers only the effect on the paramagnetic ion of the electrostatic field produced by the ligands; no other participation of the ligand electrons is considered. The second theory, however, attempts to find orbitals fulfilling the same function for molecules as the s, p, d orbitals do for atoms. The electronic structure of a molecule is then described by assigning electrons, both central atom and ligand, two at a time, to the orbitals, in order of increasing energy. The ligand electrons are thus considered as participating in the bond, which makes this theory particularly suitable for the description of covalent bonding. Conversely, the Electrostatic Theory is best suited to the description

of ionic bonding. However, since few complexes can be classed as purely ionic or purely covalent, both theories should really be considered for the best description of a complex. The name Ligand Field Theory is used for such a discussion using both Crystal Field and Molecular Orbital Theories. In qualitative discussions the process is simplified, because the principal features of the (d) orbital energy level diagram are the same in both electrostatic and molecular orbital theory.

The effect of the crystalline field on the orbitals of the central atom is similar to that of the Stark field in atomic spectroscopy. The discussion, therefore, extends from that of the free ion, in the previous section, to that of the ion perturbed by an electrostatic field. The actual behaviour of the ion will depend upon the relative strengths of the crystalline field and the inter-electronic couplings.

On this basis the complexes can be divided into three broad classes.

(1) Weak fields - e.g. hydrated 4f group ions.

The magnetic 4f electrons lie well inside the ion, and are thus shielded from the crystalline electric field. This field interaction with the magnetic electrons is then weaker than the Russell-Saunders (s.s and l.l) coupling and the spin orbit (L.S) coupling, so that $\bar{J}$ has the same importance as in the free ion; that is, J is still a good quantum number. The effect of the crystalline field is to lift the M_J degeneracy either wholly or partly.

(2) Medium fields - e.g. most hydrated 3d group ions.

The magnetic electrons are in 3d orbits, which approach the negative ligands fairly closely, exposing them strongly to the crystalline electric field. The interaction of this with the magnetic electrons is now sufficiently strong to uncouple $\bar{L}$ and $\bar{S}$, but not to overcome the (s.s and l.l) coupling. The crystalline field can then interact directly with $\bar{L}$, so leading to a quenching of the orbital magnetic moment. The factors affecting the removal of the overall orbital degeneracy of an ion by a crystalline field will be discussed at a later stage.

(3) Strong field, or covalent bonding - e.g. the cyanides of 3d group ions.

Here, the internal fields are sufficiently strong to prevent the formation of $\bar{L}$ and $\bar{S}$. This results in a reduced spin magnetic moment from that of the free ion, in addition to the reduction in orbital magnetic moment.

These classifications consider the effects of fields which differ only in intensity, so that the effect on the orbital energies is only a matter of degree. The important property of the field in determining the type of splitting of the orbital levels, is the symmetry. The $(2L + 1)$-fold degeneracy of multiplet terms, and the $(2l + 1)$-fold degeneracy of orbitals is closely connected with the assumption of spherical symmetry, surrounding a gaseous

atom or ion. The symmetry of most crystalline fields will be considerably lower than spherical, so that the spatial degeneracy of the orbitals will be removed. However, it is useful to discuss the effect on d orbitals, of fields of fairly high symmetry in purely physical terms. Such a discussion allows many of the properties of transition ions in complexes to be understood.

In the majority of the crystals which have been used in the electron resonance study of 3d group ions, the magnetic complex may be regarded as approximately octahedral, with the central atom (M) surrounded by six neighbours (X). In some complexes, (for example, Cu^{2+}), the chemical evidence suggests a planar complex of four neighbours instead of six, meaning that two neighbours are somewhat more distant from the central ion than the other four. Their effect could, therefore, be neglected in the first approximation. However, this could still be regarded in terms of a distorted octahedron and, in fact, the interpretation of the resonance results. in most cases, favours the concept of an octahedral complex.

In the Electrostatic Crystal Field Theory, the six nearest neighbours (negative ions) are regarded as point charges, or dipoles with their negative ends pointed towards the central ion. The symmetry of the crystalline field so produced at the central ion, therefore, depends on the distortion of the array from that of a regular octahedron.

If the central ion (M) is at the origin of a Cartesian system of coordinates (x', y', z'), the six neighbours can be given the coordinates ($\pm$p, 0, 0), (0, $\pm$ q, 0), (0, 0, $\pm$r). The various symmetries of the complex are then:-

(1) Cubic.

p = q = r, giving a regular octahedron.

(2) Tetragonal.

p = q $\neq$ r, giving an elongation or compression of the octahedron along the z' axis.

(3) Trigonal.

The octahedron is stretched or compressed along a line through the centre of opposite faces - e.g. along [111].

(4) Orthorhombic.

p $\neq$ q $\neq$ r.

(5) Lower than orthorhombic.

Such distortions may arise, if the atom or molecule, at say (+p, 0, 0), is not at the same distance from M as that approximately at (-p, 0, 0), or if they lie off the axis, or if they are not of the same nature.

In order to see the effect of the crystalline field on the d orbital energies, the simplest case of cubic symmetry will be considered.

The five 3d orbitals of M have the form indicated in the diagram, Figure (2.3), in which the coordinate axes lie along the

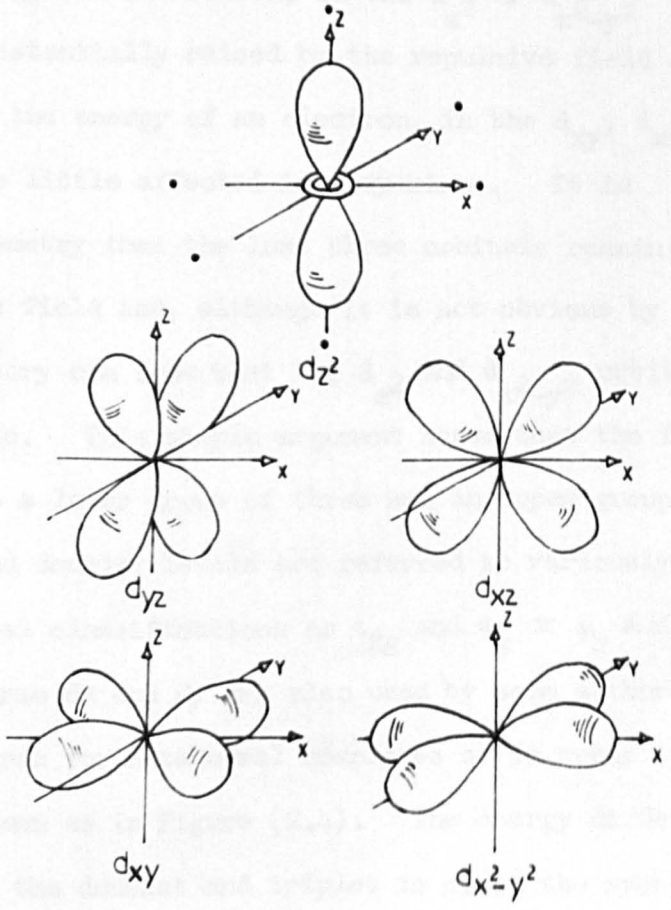

FIG. 2.3 CHARGE CLOUDS ASSOCIATED WITH d-ORBITALS.

MX bond directions. It can be seen that the d_{z^2} and $d_{x^2-y^2}$ orbitals have substantial amplitudes in the direction of the ligands, but that the orbitals d_{xy}, d_{yz} and d_{zx} tend to avoid them. It follows that the energy of an electron, in the d_{z^2} or $d_{x^2-y^2}$ orbitals, will be substantially raised by the repulsive field of the ligands, whereas the energy of an electron, in the d_{xy}, d_{xz}, d_{yz} orbitals, will be little affected in comparison. It is apparent from the symmetry that the last three orbitals remain degenerate in a cubic field and, although it is not obvious by inspection, group theory can show that the d_{z^2} and $d_{x^2-y^2}$ orbitals also remain degenerate. This simple argument shows that the five d orbitals split into a lower group of three and an upper group of two. The triplet and doublet levels are referred to variously by their group theoretical classifications as t_{2g} and e_g or γ_5 and γ_3 respectively; the terms dε and dγ are also used by some authors. The energy level diagram for octahedral complexes of 3d group ions can, therefore, be drawn as in Figure (2.4). The energy difference, or splitting, between the doublet and triplet is given the symbol Δ.

On the basis of this result alone, several of the magnetic properties of 3d group ions can be discussed.

A physical description of the quenching of orbital moments can be given, taking a $3d^1$ (that is, one 3d electron) complex, such as Ti^{3+}, as an example. In the ground state the d electron will be in the t_{2g} levels, thus having a three-fold orbital degeneracy. This

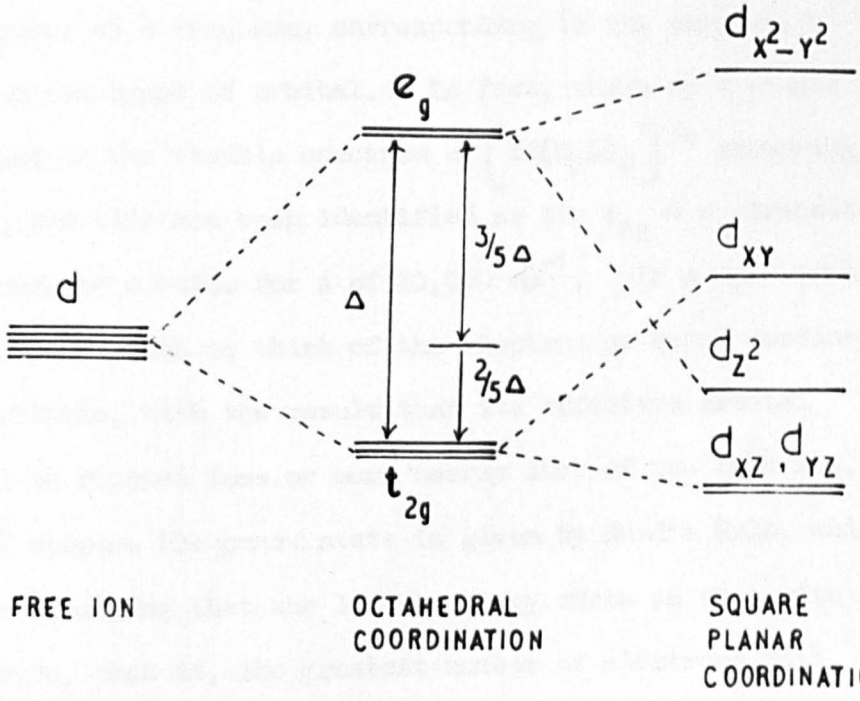

FIGS. 2.4 & 2.5

ENERGY LEVEL SCHEMES

implies an orbital moment of $l' = 1$ where $2l' + 1 = 3$, l' being called the "effective" orbital moment. The orbital moment has been effectively lowered or partially quenched. For the case of a $3d^1$ complex, there should be an electronic transition, in which the electron is transferred from the t_{2g} to the less stable e_g orbital; this should occur at a frequency corresponding to the separation Δ between the two types of orbital. In fact, there is a single absorption band in the visible spectrum of $\left[Ti(H_2O)_6\right]^{3+}$ occurring at 5000A [1], and this has been identified as the $t_{2g} \rightarrow e_g$ transition. This corresponds to a value for Δ of 20,000 cm^{-1}. If Δ were smaller it would be less correct to think of the electron as being confined to the t_{2g} orbitals, with the result that its effective orbital momentum will be reduced less or more nearly that of the free ion.

In a $3d^2$ complex the ground state is given by Hund's Rule, which can be stated as saying that the lowest energy state is that with the highest spin, that is, the greatest number of electrons with parallel spins. There are two factors which cause the spins to align themselves in this way. One is the Coulomb repulsion between charged particles, which causes two electrons to avoid each other, as far as possible; this they can do by entering different orbits. The other is the Quantum Exchange Interaction, which tends to keep the spins of neighbouring electrons aligned parallel. (This interaction will be discussed at a later stage.) Thus, in $3d^2$

and $3d^3$ complexes the electrons will be in separate members of the t_{2g} level. The effective orbital moment of a d^3 complex will depend on the size of Δ. If Δ is large the orbital degeneracy is 1, as there will be three electrons in the t_{2g} levels; if Δ is small the degeneracy is that of the free ion.

However, the fourth electron in $3d^4$ complexes has a choice of two possibilities. To obey Hund's Rule requires raising the electron into the e_g level. This can only be done if the Coulomb and Exchange energies are greater than Δ; otherwise, the fourth electron must remain in the t_{2g} level with its spin anti-parallel to the three already there. Thus, the resulting spin can be, in the first case, $4 \times \frac{1}{2}$ and, in the second, $2 \times \frac{1}{2}$. The same cases occur for $3d^5$ complexes with two possible spins of $\frac{5}{2}$ and $\frac{1}{2}$, and similarly for $3d^6$ and $3d^7$; but with $3d^8$, $3d^9$ and $3d^{10}$ complexes there are respectively two, three and four electrons in the e_g level, and Hund's rule again applies.

The two types of complex possible in $3d^4$, $3d^5$, $3d^6$ and $3d^7$ compounds are known as "high spin" and "low spin" complexes. In octahedral compounds of lower symmetry an intermediate configuration can occur, in which $3d^5$ and $3d^6$ complexes have three and two unpaired spins respectively. Electron Resonance studies have shown that in Ferric Porphyrin Chloride the central ion has only three unpaired spins.(2) (3)

For a particular ion, high spin or low spin complexes will result according to the strength of the crystalline field. Since this is produced by the ligand ions, it is interesting to see which ions are associated with the largest splittings. In the case of the ferric ion [4], for example, the complex $[FeF_6]^{3-}$ has been shown to have a high spin $\frac{5}{2}$ with $\Delta = 10{,}000\ cm^{-1}$, whilst $[Fe(CN)6]^{3-}$ has a low spin $\frac{1}{2}$ with $\Delta = 30{,}000\ cm^{-1}$. In the Ferric Haemoglobin and Myoglobin complexes the ion is surrounded by five nitrogen atoms, the sixth ligand being interchangeable. With a water molecule in this position a spin of $\frac{5}{2}$ is found, whilst with a cyanide group there is a spin of $\frac{1}{2}$.

It has been found empirically that many of the more frequent ligands can be arranged in a series, such that Δ increases along the series for a particular central metal atom. This is known as the "spectrochemical" series which is, in order of increasing Δ,

I^-, Br^-, Cl^-, F^-, C_2H_5OH, H_2O, NH_3 ethylenediamine, No_2^-, CN^- .

The examples above fit into this series in order.

Whilst discussing the high and low spin classification of compounds, it is relevant to mention Pauling's Magnetic Criterion for Bond Type. Pauling classified the high and low spin compounds as "essentially ionic" and "essentially covalent". He argued that the filling of the t_{2g} orbitals, at the expense of reducing the spin, can only be enforced by the use of the e_g orbitals in covalent

bonding. This argument cannot, of course, apply to octahedral ions with less than four, or more than seven, d electrons.

This sharp division between ionically and covalently bonded compounds is a necessary result of the Valence Bond Theory. Such a division does not correspond to the situation as revealed by experiment, which shows a more gradual transition. However, the classification of low spin complexes as "covalent" is not without some foundation. In the Electrostatic Theory the absence of e_g electrons exposes the ligands more completely to the metal ion, and so increases the extent to which their σ electrons are polarized. This is the closest approach in an electrostatic theory, to the idea of a more "covalent" bond.

It can be seen, from the above discussion, that not only is there no sharp division betwen "ionic" and "covalent" complexes, but also there is no sharp division between "ionic" and "covalent" bonds. It is customary to ascribe a degree or percentage of covalency to a particular bond. The experimental quantity most closely related to this is the electron density distribution, a high degree of electron delocalization being the physical property described by the term "covalent".

One of the most useful methods for determining the degree of electron delocalization is that of electron resonance. The spectrum of single crystals of copper phthalocyanine, for example, shows a hyperfine structure, due to the nuclear spin of the copper;

but, in suitably diluted crystals, there is a second hyperfine structure from the nuclear spin of the surrounding four nitrogen atoms in the planar molecule. Such an effect can only result if the magnetic electrons are delocalized, to a considerable extent, from the central atom onto the ligands, where they can interact with the nuclear spins. At the same time, their interaction with the nuclear spin of the central atom should be reduced.

The appearance of this double hyperfine structure is, therefore, a strong justification for classifying the bonding of a complex as "covalent". Conversely, when other information points to covalent bonding, hyperfine structure from the ligands might be expected in the electron resonance spectrum.

So far, no further splitting of the d orbitals, other than that by a cubic field, has been considered. For ions other than those in which the effective orbital momentum is zero ($L' = 0$), the t_{2g} degeneracy is reduced by small components of the crystal field, that are of lower symmetry, and spin orbit coupling. Before the expected electron resonance spectrum can be discussed for a particular complex, the orbital splittings and remaining degeneracy of the ground states must be known.

Two theorems are very helpful in determining the degeneracy of the ground state of the ion.

(i) Kramer's Theorem.[5]

This theorem states that in a system containing an odd number

of electrons, an electric field, no matter what its symmetry, cannot completely lift the degeneracy of the system. It will leave each level with an even degeneracy in spin.

(ii) Jahn-Teller Theorem.[6]

This theorem states that, apart from linear complexes, a complex which has a degenerate ground state will spontaneously distort, in such a way, that the degeneracy is removed. A Kramer's degeneracy will, however, remain unaffected.

Whilst the Kramer's theorem is quite general inside the limits quoted, the Jahn-Teller effect is expected to produce larger splittings for certain 3d complexes than for others.

The reason for the distortions is that the regular octahedral environment is only the most favourable one for a spherical positive ion surrounded by six negative ions. In the 3d group the spherical ions are $3d^3$, $3d^5$ (high spin), $3d^6$ (low spin), $3d^8$ and $3d^{10}$. The removal of an electron from any of these will obviously result in a non-spherical charge distribution around the central ion.

In $3d^9$ complexes, for example, there are two possible e_g electron configurations -

$$(d_{x^2-y^2})^2 (d_{z^2})^1 \quad \text{or} \quad (d_{x^2-y^2})^1 (d_{z^2})^2 .$$

In the first configuration the ligands along the Z axis will be more strongly attracted by the central atom, than those in the

XY plane. A more stable environment will, therefore, result if the octahedron distorts so that $p = q > r$. The second should, in the same way, cause a distortion so that $p = q < r$. The symmetry of the resulting field is tetragonal. Which distortion will occur in a d^9 complex cannot be predicted by such considerations. Experimentally, however, the most common distortion is the second.

The preceding argument for the presence of a Jahn-Teller distortion depends only on there being an odd number of e_g electrons. The distortions should be expected, therefore, in the compounds of the following ions:

$d^4 (t_{2g})^3 (e_g)^1$ Cr^{2+}, Mn^{3+} (high spin)

$d^7 (t_{2g})^6 (e_g)^1$ Co^{2+}, Ni^{3+} (low spin)

$d^9 (t_{2g})^6 (e_g)^3$ Cu^{2+}, Ag^{2+} .

Converse arguments can show that, as the two ligands along the Z axis are removed further from the central atom, the energy of the d_{z^2} orbital goes down, with respect to the $d_{x^2 - y^2}$ orbital. Moving the ligands still further along the Z axis produces the limiting case of a square planar complex, with the d orbital diagram as shown in Figure (2.5).

Finally, the case of ions with t_{2g} shells, which are neither filled nor half-filled, must be considered. Since the t_{2g} orbitals

interact much less strongly with the ligands than do e_g orbitals, their unsymmetrical occupation should produce much smaller distortions. Where there is π bonding present, however, somewhat larger distortions might be expected.

The net result of these two theorems is that systems with an even number of electrons have singlet ground states, and those with an odd number of electrons have doublet ground states. This refers to the total degeneracy, spin plus orbital.

Thus, paramagnetic resonance should only be observed where there is an odd number of electrons. As an example, the splitting of the Cr^{3+} ion illustrates several points. Figure (2.6).

The free ion has a ^4F ground state, that is, $L = 3$ and $S = \frac{3}{2}$ so that

the orbital degeneracy $2L + 1 = 7$

and the spin degeneracy $2S + 1 = 4$

The total degeneracy is therefore 7×4.

As the strength of the crystalline cubic field increases, the free ion ground state is split into three: two orbital triplets with an orbital singlet lowest. The four-fold spin degeneracy is then split according to Kramer's Theorem to leave a minimum even degeneracy, that is, two spin doublets. The splitting between these is a product of the combined Jahn-Teller distortions and spin orbit coupling. Since Cr^{3+} is a d^3 ion,

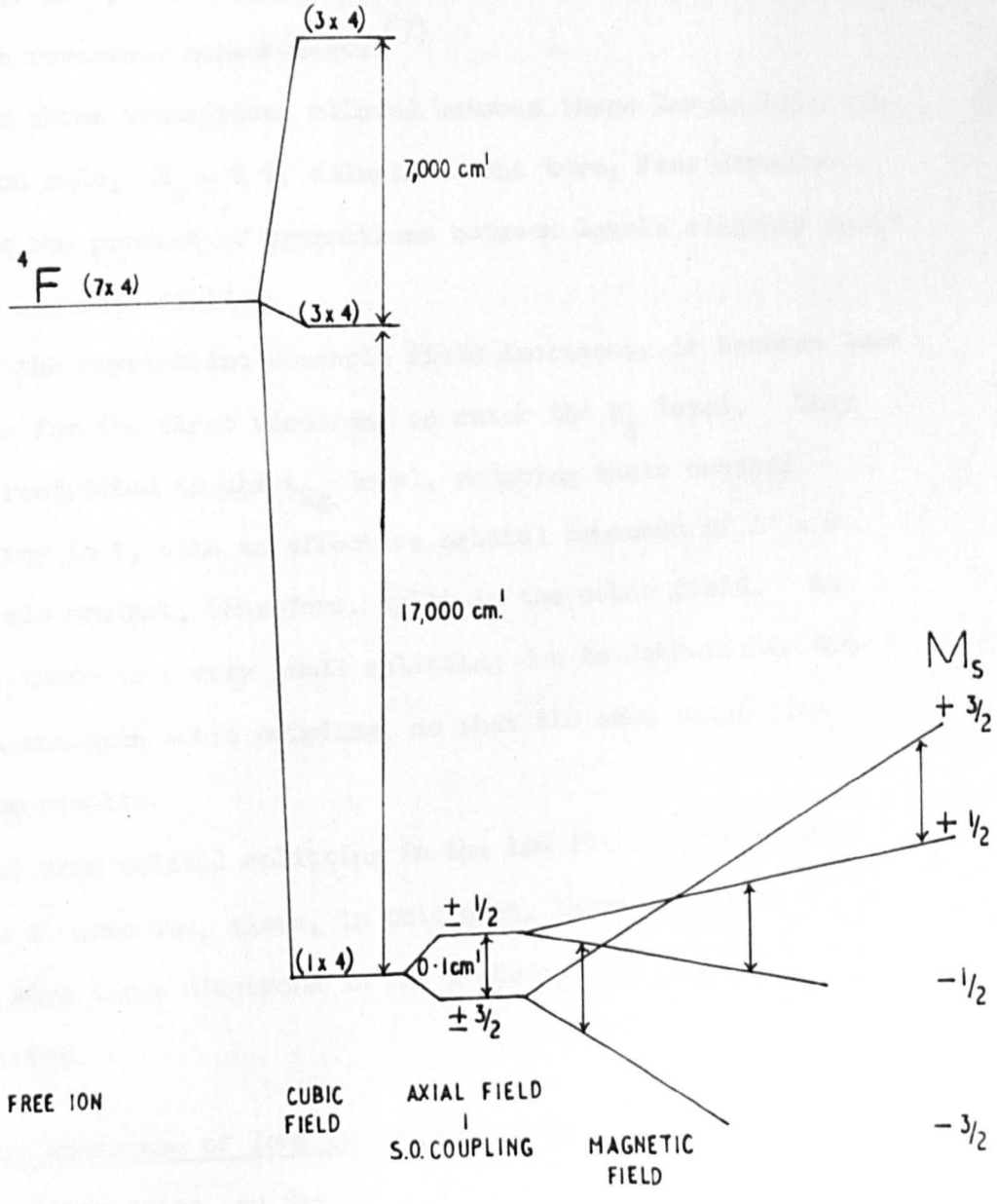

FIG. 2.6. ENERGY LEVEL DIAGRAM of Cr^{3+} IN AN AXIAL FIELD.

however, only a very small splitting should be produced by the Jahn-Teller effect. In fact, the splitting is only of the order 0.1 cm^{-1}, which brings both doublets within the range of electron resonance measurements.(7)

The three transitions allowed between these levels with the selection rule, $M_s = \pm 1$, illustrate the term, Fine Structure, which is the product of transitions between levels slightly split in zero magnetic field.

As the crystalline electric field increases, it becomes less possible for the three electrons to enter the e_g level. They become restricted to the t_{2g} level, reducing their orbital degeneracy to 1, with an effective orbital momentum of $L' = 0$. The levels are not, therefore, split in the cubic field. As before, there is a very small splitting due to Jahn-Teller distortion and spin orbit coupling, so that the same three line spectrum results.

The same orbital splitting in the low field is obtained also in d^7 ions but, since, in this case, there are three holes rather than three electrons in the d shell, the order of levels is inverted.

2.3. Electron Resonance of Ions in the Crystal Lattice

The discussion, so far, has given a general outline of the magnetic behaviour and energy levels of the paramagnetic ions, in their environment in crystals. It has shown that it is possible

to say in which compounds electron resonance should be observed, and to explain the appearance of fine structure.

The main features of the electron resonance spectrum from crystals are the g value, fine structure, hyperfine structure and line width. The last will be discussed in the next chapter.

2.3.1 g value

Since the orbital momentum is often reduced to an effective L', the g value is no longer that of atomic spectroscopy, and is called the "spectroscopic splitting factor". Moreover, since the orbital component of the g value is dependent on the interaction with the crystalline field, it will possess the symmetry of this field. The g value is, therefore, usually anisotropic as are the paramagnetic properties as a whole.

If an ion is situated in a cubic field, the magnetism is isotropic; in a tetragonal field, the magnetism is axially symmetric about the tetragonal axis, which, therefore, defines an axis of principal g value. In the orthorhombic field, three axes of principal g value are defined by the orthorhombic axes.

In general, an anisotropic g value can be represented by three principal values, g_x, g_y, g_z along the principal axes of the complex. If the magnetic field H has the direction cosines (l, m, n) with respect to (X, Y, Z), the g value measured is given by

$$g^2 = l^2 g_x^2 + m^2 g_y^2 + n^2 g_z^2 \qquad 2.14$$

In the case of axial symmetry, when a $g_{\parallel}$ and a $g_{\perp}$ are defined as g values parallel and perpendicular to the crystalline field axis, the formula reduces to the form

$$g_{\theta}^2 = g_{\parallel}^2 \cos^2\theta + g_{\perp}^2 \sin^2\theta \qquad 2.15$$

where θ is the angle between the magnetic field $\bar{H}$ and the crystal field axis.

This can be derived as follows. The magnetic field H has components H cos θ and H sin θ respectively along, and normal to, the symmetry axis. Figure (2.7). The components of the magnetic moment in these directions are, therefore, proportional to $g_{\parallel} H \cos\theta$ and $g_{\perp} H \sin\theta$.

Compounding these shows that the resultant magnetic moment of the electron is not parallel to the magnetic field, but makes an angle ϕ with the Z axis. The g value is proportional to the length of this vector and has the value

$$g_{\theta}^2 = g_{\parallel}^2 \cos^2\theta + g_{\perp}^2 \sin^2\theta \quad .$$

Since g is not parallel to $\bar{H}$, the subscript in g_{θ} must not imply a direction for g. A double subscript $g_{\theta\phi}$ is less ambiguous, in that it implies the tensor g acting between θ and ϕ. The g values, measured in experiments on single crystals, are really only the magnitudes of g measured with the field in direction θ. A resonance is obtained with the condition $h\nu = g\beta H$, from which a g value is calculated without any direction other than that of

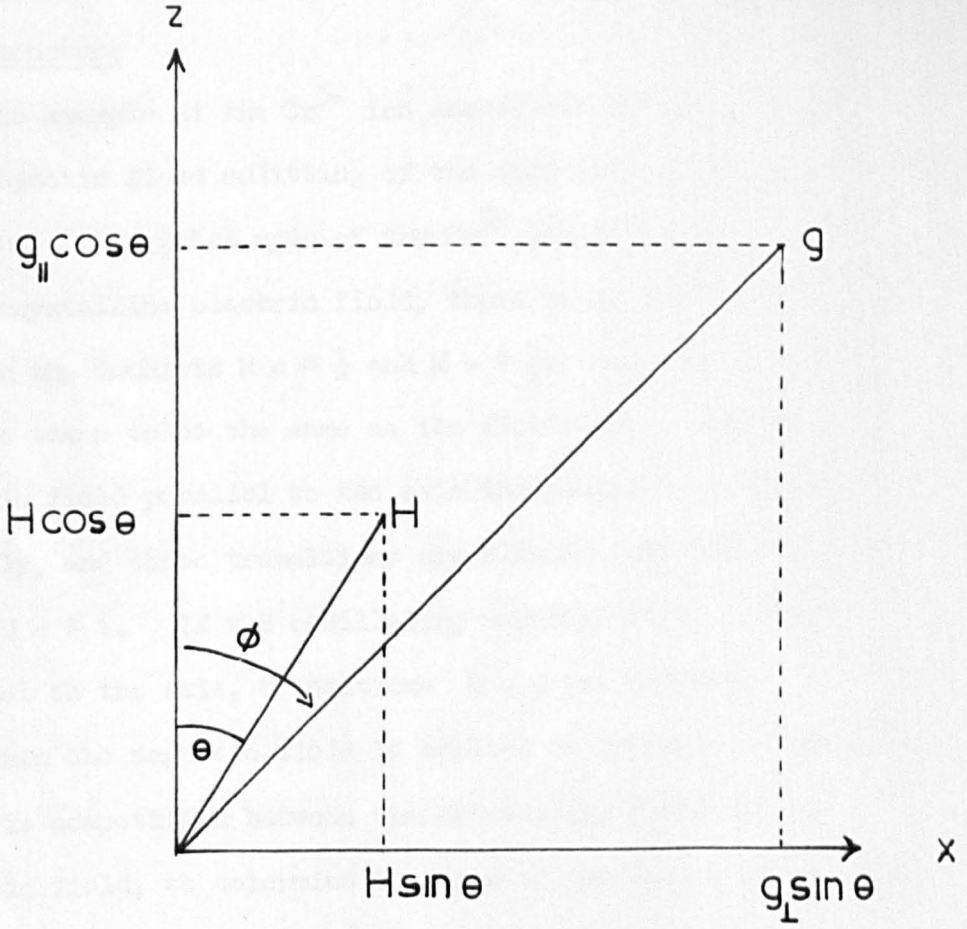
z
$g_{\parallel}\cos\theta$
g
$H\cos\theta$
H
ϕ
θ
x
$H\sin\theta$
$g_{\perp}\sin\theta$

FIG. 2.7

the field being ascribed to it.

2.3.2 Fine Structure

The example of the Cr^{3+} ion showed the effect of a small zero magnetic field splitting of the spin levels, on the resonance spectrum. The total spin of the Cr^{3+} ion is $S = \frac{3}{2}$. Due to the axial crystalline electric field, there is an initial splitting between the doublets $M = \pm \frac{1}{2}$ and $M = \pm \frac{3}{2}$; the axis of quantization is taken to be the same as the field axis. Applying a magnetic field parallel to the axis the energy levels diverge linearly, and three transitions are allowed with the selection rule $M = \pm 1$. If the oscillating magnetic field is also parallel to the axis, transitions $M = 0$ are allowed.

When the magnetic field is applied at an angle to the axis, there is competition between the crystalline field and the magnetic field, to determine the axis of precession of the spin. In this case the lines no longer diverge linearly, unless the magnetic field is very much greater than the crystalline field.

The first order variation of the spectrum [8] has been shown to follow a $\left\{ 3 \frac{g_{11}}{g}^{2} \cos^2\theta - 1 \right\}$ law, so that the splittings collapse to zero when $\theta = \cos^{-1}\left(\frac{1}{\sqrt{3}} \frac{g}{g_{11}} \right)$. The g value of the lines is taken to be that of the centre line, the $+\frac{1}{2} -\frac{1}{2}$ transition in the example. This is known as a true g value, since g remains constant, independent of the radiation frequency used. The total

spin $S = \frac{1}{2}$ and there are three transitions; in general, there are 2S transitions in the fine structure.

The magnitude of the zero field splitting (2D) can be determined from the separation between the outer transitions, when the magnetic field is parallel to the crystalline field axis [8]. The size of the splitting varies usually in the range zero to a few cm^{-1}.

2.3.3 Hyperfine Structure

The splitting of the resonance spectrum, due to interactions between the magnetic moments of the electron and the magnetic moment of the nucleus. has been mentioned already. A hyperfine structure can be expected, owing to the nuclear spin of the central ion and, in certain cases, from the nuclear spins of ligand ions.

In general, the nuclear magnetic moment produces a magnetic field at the electron. This gives rise to the following interactions:-

(a) Dipolar interaction between the electronic and nuclear spins. The magnitude of the interaction falls off with the third power of the dipolar separation. The splitting itself follows as $(3\cos^2\theta - 1)$ variation, where θ is the angle between the magnetic field and the line joining the dipoles.

(b) The interaction of the nucleus with the field produced by the orbital motion of the electrons at the nucleus. This also varies as $\frac{1}{r^3}$

(c) The Fermi contact interaction. The interaction requires the electron to have a finite probability density at the nucleus. In the case of hyperfine structure from ligand nuclear magnetic moments, the dipolar interaction will be reduced considerably by the $\frac{1}{r^3}$ term. However, for a covalent complex, in which the central metal electron may be said to have a finite probability density at the ligand nucleus, this becomes the most important interaction. These hyperfine splittings are isotropic, which distinguishes them from the dipolar splittings.

Since the magnetic moments of the nuclei also interact with the magnetic field, the total magnetic interaction with the nuclei is given by

$$A\bar{S}.\bar{I} + B\bar{H}.\bar{I} \quad . \qquad 2.4$$

If H is not very large, the spacing between the lines may vary with the direction of the field; also A is usually anisotropic when g is anisotropic. In this case, three principal values A_x, A_y and A_z are defined as the values of A along the X, Y and Z axes, respectively. The interaction is given by

$$A_x S_x.I_x + A_y S_y.I_y + A_z S_z.I_z \quad . \qquad 2.16$$

The interaction of the nuclear moment with the magnetic field is of the order 10^{-4} cm^{-1}, and is usually negligible. However, in combination with the nuclear electric quadrupole moment it has been used to determine the relative signs of the

zero field and hyperfine splitting parameters D and A. [8] Experimentally, the structure constant A is found to have values between 10^{-1} and 10^{-3} cm^{-1} for many transition group ions in crystals.

Besides magnetic nuclear interactions, electric interactions exist with the nuclear electric quadrupole moment. However, these will not be discussed here, as they have no direct bearing on the results.

2.4 Spin-Hamiltonian

The description of the resonance properties of ions has been greatly simplified by the use of the so-called spin-Hamiltonian, introduced by Abragam and Pryce. [9] The spin-Hamiltonian describes the rather complicated behaviour of the lowest energy levels of the ion, in terms of a relatively small number of parameters, which can be determined experimentally by electron resonance. The form of the spin-Hamiltonian can frequently be guessed with little detailed knowledge of the crystalline field. Experiment is, therefore, aimed at finding the spin-Hamiltonian, and theory at passing from a model to a spin-Hamiltonian, or in the reverse direction.

A normal Hamiltonian expresses, mathematically, the various interaction energies and factors which influence the ion. For example, the Hamiltonian

$$\mathcal{H} = \beta\bar{H}.(\bar{L} + 2\bar{S}) + \lambda\bar{L}.\bar{S} \qquad 2.17$$

expresses the interaction between the magnetic field and the orbital and spin magnetic moment, and the spin-orbit coupling. Using a Hamiltonian of this form, it is possible to calculate the splittings of the levels of an ion in a magnetic field. However, it was shown, by Abragam and Pryce [9], that these splittings are just the same as those, which would be obtained by ignoring the orbital angular momentum, and replacing its effect with an anisotropic coupling between electron spin and magnetic field of the form

$$\beta\bar{H}.g.\bar{S} = \beta g_{\parallel} H_z S_z + \beta g_{\perp}(H_x S_x + H_y S_y) \quad . \qquad 2.18$$

For a particular ion, there can be derived a relation between the g value and the orbital angular momentum. In the tetrahedral environment of Ti^{3+}, for example, [10] the splitting of the ground state has been shown to be $2\beta H_z$, when the magnetic field is parallel to the tetragonal axis, and $2\beta H_x(1 - \frac{3\lambda}{\Delta})$ when it is perpendicular. This can be expressed in terms of

$$g_{\parallel} = 2$$

and $$2.19$$

$$g_{\perp} = 2(1 - \frac{3\lambda}{\Delta})$$

where λ is the spin orbit coupling, and Δ the tetragonal field splitting.

The spin-Hamiltonian can be used even in cases where the lowest level is orbitally degenerate. If transitions between $2S' + 1$ levels are observed experimentally, S' is defined as the "effective" or fictitious spin, and is used in the spin-Hamiltonian. With an orbital singlet state lowest, the splitting of the spin degeneracy is usually fairly small; the effective spin is, therefore, equal to the actual spin. For an orbitally degenerate state, however, components of the crystalline field of lower symmetry and spin orbit interaction usually produce a splitting, of the order of 100 cm^{-1}. In accordance with Kramer's and the Jahn-Teller Theorems, no resonance would be expected if the number of electrons is even, and the effective spin would be $\frac{1}{2}$ if the number of electrons is odd.

A sufficiently general spin-Hamiltonian can be written in the component form as

$$\mathcal{H} = \beta(g_z H_z S_z + g_x H_x S_x + g_y H_y S_y) + D\left\{S_z^2 - \tfrac{1}{3}S(S+1)\right\} + E(S_x^2 - S_y^2) \qquad 2.20$$

The first term in the brackets represents the splitting of the $(2S + 1)$ multiplets by the applied magnetic field. In this term $g_x g_y g_z$ are the values along the principal axis. The term $D\left\{S_z^2 - \tfrac{1}{3}S(S+1)\right\}$ represents the initial splittings, in zero magnetic field, of the spin multiplet, by an axially symmetric

component of the crystalline field. The term $E(S_x^2 - S_y^2)$ represents possible initial splitting by the crystalline field components of lower symmetry.

2.5. S state ions

For half filled shells, the ground state is an orbital singlet. This occurs in the iron group for $3d^5$ high spin complexes, that is Mn^{2+} and Fe^{3+}, with a ground state of $^6S_{5/2}$. With no orbital contribution to the magnetic moment, isotropic magnetic properties are expected with a susceptibility corresponding exactly to the spin only value. In most complexes of these ions, however, slight departures from the expected behaviour are observed, which require explanation.

Van Vleck and Penney [11] derived a possible mechanism for a splitting of the ^6S state. The crystalline field cannot split the S state, nor can spin-orbit coupling alone remove the six-fold spin degeneracy. They showed, however, that on going to a high order in perturbation theory, the combination of a cubic crystalline field and spin-orbit coupling could produce small splittings of the spin levels.

Exact comparison with experimental data awaited the electron resonance investigation of Mn^{2+} by Bleaney & Ingram [13] which showed that small splittings did exist. Abragam & Pryce [12] showed that these splittings are in fact too large to be explained

by the above process. They suggested a mechanism depending on the distortion of the otherwise spherical electron-cloud distribution by the tetragonal (or trigonal) component of crystalline field. If, for example, the distribution is slightly ellipsoidal, the dipole-dipole energy of the spins will vary with their orientation with respect to the axes of the ellipsoid. The spin levels are therefore no longer degenerate.

In Mn^{2+} the small splitting $\sim 0.1\ cm^{-1}$ leaves three Kramers doublets. These are all populated at normal temperatures so that on application of a magnetic field, electron resonance transitions can occur between the six spin levels with the selection rule $\Delta M = \pm 1$. A fine structure of five lines is observed. Superimposed on this is a large isotropic hyperfine structure, from the nuclear spin 5/2 of the manganese ion. This is unexpected since d orbitals have nodes of zero electron probability at the nucleus with the result that the Fermi contact term is zero. This leaves only the much weaker anisotropic dipolar interaction. Abragam & Pryce suggested that the origin of the hyperfine structure lies in a configurational interaction of the form $3s3d^5 4s$ with $3s^2 3d^5$. Since s electrons have a finite probability density at the nucleus their contribution to the hyperfine splitting through the Fermi contact term is considerable; only a small amount of configurational interaction may be necessary to explain the splitting.

Measurements on Fe^{3+} show a similar small splitting except for ferric haemoglobin and myoglobin. The g value anisotropy in these complexes indicates a very large splitting of the spin states $\sim 10\ cm^{-1}$, which requires the presence of strong asymmetric crystalline fields. This subject will be discussed more fully at a later stage.

REFERENCES

(1) L. E. Orgel, An Introduction to Transition Metal Chemistry, Methuen (1960).

(2) J. S. Griffith, Disc. Farad. Soc. 26 (1958) p. 81.

(3) J. E. Bennett, Ph.D. Thesis, Southampton University.

(4) C. A. Coulson, Valence, Oxford Univ. Press (1961)

(5) H. A. Kramers, Proc. Acad. Sci. Aust. 33.

(6) H. A. Jahn and E. Teller, Proc. Roy. Soc. A 161 (1937) p. 220.

(7) D. M. S. Bagguley and J. H. E. Griffiths, Nature Lond. 160 (1947) p. 532 and Proc. Roy. Soc. A 204 (1950) p. 188.

(8) B. Bleaney, Phil. Mag. 42 (1951) p. 441.

(9) A. Abragam and M. H. L. Pryce, Proc. Roy. Soc. A 205 (1951) p. 135.

(10) A. Carrington and H. C. Longuet-Higgins, Quart. Rev. 14 (1960) p. 427.

(11) J. H. Van Vleck and W. G. Penney, Phil. Mag. 17 (1934) p. 961.

(12) B. Bleaney and D. J. E. Ingram, Proc. Roy. Soc. A 205 (1951) p. 336.

Chapter 3

Mechanisms for the Line Broadening of the Electron Resonance Spectrum of Single Crystals

3.1. Introduction

All electron resonance lines have a finite width known, in the limiting case, as the natural width. This arises from Heisenberg's uncertainty principle

$$\Delta E \cdot \tau \sim \hbar \quad .$$

The spins in all levels except the lowest one have a finite 'lifetime' because of the probability of spontaneous emission. Thus all such levels have a finite energy spread, which gives rise to the finite widths of the corresponding transitions. These line widths are quite negligible, compared with other factors at the radiation frequencies used in electron resonance, however.

Line widths are usually expressed as the frequency separation between half-power points. Since very often it is the derivative curve that is experimentally traced, it is much easier to measure the frequency separation of the maximum slope points of the absorption curve and this is frequently quoted as the line width.

The shape of an absorption line, as a function of frequency in a fixed magnetic field, can be described by means of a normalized function $g(\nu)$, where ν is frequency and

$$\int_0^\infty g(\nu)d\nu = 1 \quad .$$

For absorption lines of similar shape, the maximum value of the shape function, $g(\nu)_{max}$, will be large for narrow and small for broad lines. The line width can therefore be defined as

$$\Delta(\nu) = \frac{1}{\left[g(\nu)\right]_{max}} \quad .$$

Line shapes are difficult to calculate theoretically. Generally, different moments are calculated for comparison with experiment. The n^{th} moment is defined as

$$\langle (\Delta\nu)^n \rangle = \int_{-\infty}^{+\infty} g(\nu - \nu_o)(\nu - \nu_o)^n \, d(\nu - \nu_o)$$

where ν_o is the frequency of the centre of the line.

Theoretically the expressions for line width are frequently derived on the assumption that the magnetic field is kept constant and the measuring frequency is varied, whereas experimentally it is the field that is varied and the frequency kept constant. It is easy to relate the line widths when the energy levels diverge linearly with magnetic field, but where this is not so the relation is complicated. The levels are known to diverge linearly in Haemoglobin and Myoglobin complexes but this is not the case where resonance takes place, at low field values, between levels

which are split in zero magnetic field.

Assuming that the levels diverge linearly the relation between the energy and field is

$$\Delta E = g\beta \Delta H \quad .$$

It follows that even when the actual energy line width ΔE is constant, if the crystal has an anisotropic g value, the line width (in gauss) ΔH measured by electron resonance will vary inversely with g. Line widths measured by electron resonance can therefore be compared either by converting to a ΔE or by simply multiplying by g or g/g_e, where g_e is the free spin value.

3.2. Homogeneous and Inhomogeneous Broadening

The line width in electron resonance spectra of single crystals is caused by a number of different mechanisms. It is customary to classify these into two groups, after Portis [1] as homogeneously or inhomogeneously broadened lines. In homogeneously broadened lines the absorbed energy is distributed over all the spins. Examples of such broadening are dipole-dipole interactions between like spins and spin-lattice interactions. Inhomogeneous broadening exists when energy is transferred only to those spins whose local fields satisfy the resonance condition. Examples of this broadening are, hyperfine interactions, impurities and defects near the paramagnetic ion and mosaic structure in nearly perfect crystals.

3.3.1. Spin-lattice Relaxation

In a paramagnetic ion with effective spin $S' = \frac{1}{2}$, electron resonance is observed when absorptive transitions are stimulated between the two lowest spin levels, by the incident radiation. It has been shown by Einstein that in this case both absorptive and emissive transitions have equal probability for a particular electron. However, since at normal temperatures, in a system at thermal equilibrium, the lower state has a greater population, there will be a greater absorption than emission of energy. The relative population of the levels at thermal equilibrium is given by Maxwell-Boltzmann statistics, for a particular temperature of the crystal lattice $T^{o}K$, as:-

$$\frac{n_{upper}}{n_{lower}} = e^{-\left(\frac{\Delta E}{KT}\right)}$$

where ΔE is the energy difference between spin levels. If, due to induced absorptive transitions, the population of the upper state increases, the population ratio becomes equivalent to a temperature T_S greater than that of the lattice T. This temperature is known as the spin temperature. Unless the spin temperature is to remain permanently higher than that of the lattice, there must be some form of relaxation mechanism between the spins and the lattice. This relaxation mechanism must allow the spins to "feel" the thermal motion of the lattice, thus inducing transitions between the spin levels so that equilibrium is reached. In this

way the lifetime of the spins in the energy levels will be reduced and through Heisenberg's uncertainty principle the levels will be broadened.

The time taken for the spin temperature to relax back to that of the lattice is known as the spin-lattice relaxation time, usually given the symbol T_1. An expression for the relaxation time in a two level system can be derived simply as follows.

Let the number of spins per cubic centimetre in the upper level be N_- and in the lower level N_+. Let the upward and downward transition probabilities be W_+ and W_- respectively. Then if the whole system of spins and lattice is at thermal equilibrium at temperature T, the number of transitions upwards and downwards must be equal and

$$W_+ N_+ = W_- N_- \quad . \tag{1}$$

But N_+ and N_- are related at equilibrium by the Boltzmann factor, so that

$$\frac{W_-}{W_+} = \frac{N_+}{N_-} = e^{\left(\frac{\Delta E}{KT}\right)} \approx 1 + \frac{\Delta E}{KT} \tag{2}$$

if $\frac{\Delta E}{KT} \ll 1$ which is the case if ΔE the magnetic splitting is due to fields of less than 10k gauss and if T is greater than $20^{\circ}K$.

Therefore W_- and W_+ can be written as

$$\left.\begin{aligned} W_- &\approx W\left(1 + \frac{\Delta E}{2KT}\right) \\ W_+ &\approx W\left(1 - \frac{\Delta E}{2KT}\right) \end{aligned}\right\} \tag{3}$$

where W = mean of W_+ and W_- = $\frac{W_+ + W_-}{2}$.

The above expressions state that the upward transition probability is less than the downward. Unlike the radiation stimulated transitions, the transitions stimulated by interaction with the lattice do not have equal probabilities up and down.

If the spin system is no longer at equilibrium with the lattice, but has a spin temperature $T_s \neq T$, the excess number of electrons $n = N_+ - N_-$ in the lower level will be reduced. The relaxation process will therefore tend to increase n, which changes by 2 with each transition. The rate of change of n is given by

$$\frac{dn}{dt} = 2N_-W_- - 2N_+W_+ \quad . \tag{4}$$

Using the equations (3) above this becomes

$$\frac{dn}{dt} = 2W(n_o - n) \tag{5}$$

where

$$n_o = N\frac{\Delta E}{2KT} \quad . \tag{6}$$

n_o is the excess number of electrons at equilibrium and $N = N_+ + N_-$.

Integrating gives

$$n_o - n = (n_o - n_i)e^{-2Wt} \tag{7}$$

where n_i is the value of n at time $t = 0$. Thus the approach to

equilibrium is seen to be exponential with a characteristic time of $\frac{1}{2W}$. The relaxation time is therefore inversely proportional to the mean transition probability

$$T_1 = \frac{1}{2W} \quad . \tag{8}$$

3.3.2. Saturation Factor

In the absence of radiation, the differential equation governing the time variation of the excess number n of electrons in the lower level, is given by a combination of equations 5 and 8

$$\frac{dn}{dt} = \frac{n_o - n}{T_1} \quad . \tag{9}$$

When radiation is present, however, another term must be added to account for the upward transitions which correspond to the net absorption of energy. This gives the equation

$$\frac{dn}{dt} = \frac{n_o - n}{T_1} - 2nP \tag{10}$$

since P is the same for upward and downward transitions and is the probability per unit time of a transition between the levels under the influence of the radiation. A steady state is reached when $dn/dt = 0$, and in this condition the steady state value n_s is given from (10) by

$$\frac{n_s}{n_o} = \frac{1}{1 + 2PT_1} \quad . \tag{11}$$

Since the population of the lower level is always the greater at normal temperatures, at thermal equilibrium there will be more upward radiation induced transitions than downward. Therefore n_s will be less than n_o by an amount depending on the transition probability. From radiation theory and for the case of $S = \frac{1}{2}$, the transition probability is given by

$$P = \tfrac{1}{4}\gamma^2 H_1^{\,2}\, g(\nu) \qquad (12)$$

where H_1 is the high frequency magnetic field which is perpendicular to the d.c. magnetic field, so that

$$\frac{n_s}{n_o} = \frac{1}{1 + \frac{1}{2}\gamma^2 H_1^{\,2} T_1\, g(\nu)} \quad . \qquad (13)$$

If the spin-lattice relaxation time T_1 is large, and if the amplitude H_1 of the high frequency magnetic field is large, the factor n_s/n_o will be small and since, from equation (6), $n_s = N\Delta E/2KT_s$, the spin temperature T_s will be high.

In this condition there will be fewer upward radiation induced transitions and the net absorption of energy will be reduced; the spin system is said to be saturated. For this reason the expression n_s/n_o is called the Saturation Factor, given the symbol Z.

It can be shown, using equation (6), that the spin temperature of the steady state is related to the lattice temperature by the expression

$$T_s = T/Z \qquad (14)$$

and also, by integrating equation (10), that the approach of the spin system to the steady state follows the exponential relation

$$(n_s - n) = (n_s - n_i)\, e^{-\frac{t}{T_1 Z}} \quad . \qquad (15)$$

Comparison with the approach to thermal equilibrium in the absence of radiation shows that the characteristic time is now $T_1 Z$ instead of T_1.

3.3.3. The Nature of the Spin-lattice Relaxation Mechanism

According to Kronig [2], the thermal motion of the lattice alters the crystalline electric field and thus acts on the spin system through spin-orbit coupling. There are two mechanisms whereby the spins can exchange energy with the lattice. They can either exchange a whole quantum with a lattice vibration or phonon of the appropriate frequency or transfer energy by scattering a quantum from the lattice and changing its value. This latter is known as the Raman process, while the former is the direct process, and will predominate at the higher temperatures.

In the case of $S = \frac{1}{2}$ the Raman process leads to an expression in which T_1 is proportional to $\Delta^6/\lambda^2 T^7$ for T smaller than the Debye temperature, and proportional to $1/T^2$ for T larger than the Debye temperature. Here Δ is the height of the next orbital above the ground state in cm^{-1}, λ is the spin-orbit coupling coefficient and T the absolute temperature. It follows that in "spin-only" magnetic substances there should be long relaxation times since Δ

is large. This is found to be so for most of the iron group complexes.

The direct process leads to a relaxation time proportional to $\Delta^4/\lambda^2 T$ and must be of importance at lower temperatures. However this process is not sufficient to explain the relaxation times actually observed. There would appear to be too few phonons of the appropriate frequency to transfer the energy at the rate indicated by the relaxation times.

Townes (3) has suggested that there are actually two kinds of relaxation mechanism at low temperatures, the usual spin-lattice relaxation and the lattice-bath relaxation. It is thought that in many crystals the latter mechanism predominates. In order to account for the high energy transport of the few phonons available with appropriate frequency, Townes suggested that the lattice modes are broadened by the interaction with the spins.

The theory of spin-lattice relaxation requires special treatment when applied to S state ions since here the orbital momentum is zero. It is necessary to introduce a configurational interaction between the ground state and excited states with non-zero orbital angular momentum. Theory (4) indicates that relaxation times for Mn^{2+} will be one hundred times longer than for non-S-state iron group salts.

Although much work is being done on the subject it is at the moment impossible to predict quantitatively what relaxation time

a given ion will have or how it is influenced by crystal field strength or crystal symmetries.

In general T_1 may vary from seconds to 10^{-11} seconds for various paramagnetic ions. Experimentally electron resonance measurements are made at temperatures which are sufficiently low for line widths to be due to interactions other than spin-lattice. Relaxation times longer than 10^{-7} seconds usually give a contribution to line width which is negligible compared with that from spin-spin interaction. If T_1 is longer than 10^{-5} seconds, however, undesirable saturation effects appear.

If spin-lattice relaxation is the major source of line broadening the line shape is similar to that of collision broadened lines in gaseous spectroscopy. This broadening has been treated theoretically by various authors, particularly Van Vleck and Weisskopf [5] who give an expression for the line shape. Using this expression the spin-lattice relaxation time could be calculated from the half width of the resonance absorption lines.

3.4. Spin-Spin Relaxation

Besides their interaction with the lattice, the ions interact with each other. From a semi-classical point of view, each ion can be regarded as a gyroscopic magnet; that is, its angular and magnetic moments are parallel. In the presence of a uniform, steady, external magnetic field $\bar{H}_o$, the magnet will precess around this direction at the larmor frequency, equal to $\gamma\bar{H}_o$. The magnet

can therefore be regarded as equivalent to a magnet fixed in the external field direction, together with a magnet rotating in a plane perpendicular to this.

In an assembly of such magnets, a particular magnet will experience not only the external magnetic field $\bar{H}_o$, but also a small local field $\bar{H}_{local}$ due to its neighbours. This local field will be of the order of μ/r^3 where μ is the magnetic dipole moment of the neighbouring magnet and r is the nearest neighbour distance. Each magnet then precesses about the resultant field $\bar{H}$. The value and orientation of $\bar{H}$ will vary from one magnet to another with the result that there will be a spread δw_o in the precessional frequencies. This spread in frequency will be of the order of $\gamma\bar{H}_{local}$. If two magnets have precessional frequencies differing by δw_o and are initially in phase, then they will be out of phase in a time $1/\delta w_o$.

This spread in precessional frequency will appear as a broadening of the resonant absorption line. The broadening does not depend on the magnets all having the same gyromagnetic ratios and may be termed "steady field" broadening.

The fields set up by the rotating magnets will also have a broadening effect. If two magnets have the same precessional frequencies, the rotating field from one will be at the right frequency to induce transitions in the other. If the precessional frequencies are different, however, the rotating fields will have

little effect. The broadening produced by this process is sometimes referred to as "resonant" broadening. Since the total energy of the interacting ions cannot change, the process may be considered as a mutual exchange of energy between the ions. The correct phasing for the transitions should occur periodically after a time interval of the order of $1/\delta w_o$. This can therefore determine the lifetime of a spin state so that using the uncertainty relation the order of energy spread of the levels will be

$$h\delta w_o \sim \hbar\gamma\bar{H}_{local} = \hbar\left(-g\frac{|e|}{2mc}\right)\bar{H}_{local} = -g\beta\bar{H}_{local}.$$

The broadening of the resonance line is therefore of the order of $\bar{H}_{local}$. The lifetime or phase memory time of the spin states can be described by a spin-spin relaxation time T_2 where $T_2 \sim 1/\delta w_o$. This relaxation time is more precisely defined by the relation

$$T_2 = \tfrac{1}{2}\left[g(\nu)\right]_{max}$$

and since the line width is defined as

$$\Delta(\nu) = \frac{1}{\left[g(\nu)\right]_{max}}$$

the spin-spin relaxation time is approximately given by the inverse of the half-width of the absorption line if this width is caused only by spin-spin interactions.

The theory of spin-spin interaction has been developed by

Van Vleck [6] and by Pryce and Stevens [7]. Van Vleck treated in detail the case of free spins and derived an expression for the mean-square width of a line due to dipolar interaction between the spins. Written as a field width rather than a frequency width, this expression is

$$(\Delta H)^2 = \tfrac{3}{4}S(S+1)g^2\beta^2 \sum_k \left\{\frac{1-3\cos^2\theta}{r^3}\right\}^2_{jk} + \tfrac{1}{3}S'(S'+1)\frac{g'^4}{g^2}\beta^2 \sum_{k'} \left\{\frac{1-3\cos^2\theta}{r^3}\right\}^2_{jk'} .$$

The transition concerned is between the levels of ions with spin S, and spectroscopic splitting factor g, r being the distance apart of the j^{th} and k^{th} ion. The second term represents the contribution to the broadening by "dissimilar" ions of spin S' and spectroscopic splitting factor g'. The line width will be anisotropic following a $(3\cos^2\theta - 1)$ variation, where θ is the angle between the magnetic field and the line joining the dipoles. In the case where there are two identical ions in a unit cell differently oriented with respect to the crystal axes, the contribution from "dissimilar" ions will be $\sqrt{\frac{3}{4}/\frac{1}{3}} = \frac{2}{3}$ that from "similar" ions. The general case of ions other than free spins is more complicated. The line width depends considerably on the direction in the crystal along which it is measured. The $(3\cos^2\theta - 1)$ variation will no longer be true.

There are three types of spin-spin interaction which can occur. These are interactions between:-

(a) the electron spin magnetic moments of neighbouring ions,

(b) the electron spin of one ion and the nuclear spins in the same ion,

(c) the electron spins and nuclear spins in a neighbouring ion.

The magnitudes of effects (a) and (b) are often of the same order whereas that of (c) is very much smaller.

The magnitudes of the steady field broadening can be considerable in the case of paramagnetic ions. For example, the field of a nearest neighbour with magnetic moment of about 1 Bohr magneton at a distance of 3A is of order 350 gauss and the sum of nearest neighbours may be over five hundred gauss. However since the magnitude of the interaction varies inversely with the third power of the separation of the ions, the broadening will be very much reduced in dilute crystals. At 9A the field will have been reduced from 350 to 13 gauss.

In more concentrated samples, the broadened line is made up of a large number of lines from individual ions each with differing local fields. The resonance condition for these is

$$h\nu = g\beta(\bar{H} + \bar{H}_{loc}) \quad .$$

The actual resonance absorption curve is the envelope of the individual resonance lines so that its detailed shape will depend

on the arrangement of the neighbours. If this has high symmetry the line shape may approximate to gaussian.

Spin-spin interaction is independent to a first order of temperature and frequency (or magnetic field strength).

3.5.1. Exchange Interactions

Line width measurements in crystal, with a high concentration of paramagnetic ions, rarely agree with widths calculated on the assumption of dipolar broadening. One of the main reasons for this is the exchange interaction between electrons. These are the fictitious forces to which is attributed the exchange energy term in, for example, the bonding of the hydrogen molecule. This is a purely quantum mechanical effect which cannot be explained in classical terms.

As a result of the uncertainty principle it becomes impossible in quantum mechanics, to distinguish between identical particles such as electrons. If therefore two atoms, for example, hydrogen atoms, are so close to each other that the wave functions for their electrons overlap, the electrons in overlapping orbitals become indistinguishable. Each electron is then equally associable with both atoms. In the Valence Bond theory, this situation can be described as a resonance between two states of equal probability. One, in which electrons (1) and (2) are near atoms (1) and (2) respectively, and the other, in which electrons (1) and (2) are near atoms (2) and (1) respectively. The combination of these two states produces two new states, one of which has a higher

energy, and one a lower energy, than that of the original states. These states differ in the relative orientation of the electron spins. According to the Pauli exclusion principle, electrons with parallel spins avoid each other. Their orbitals will therefore overlap very little resulting in an anti-bonding state, the energy of which is greater than that of the original states. When the electron spins are anti-parallel, however, the overlap will be large and a bonding state results. The lowering of energy in this state is due to the fact that the electrons are under simultaneous attraction to two positive nuclei instead of one. This is known as the exchange interaction, and the energy decrease as the exchange energy. Using Plank's relation, $E = h\nu$, an exchange frequency can be associated with the interaction, although it must not be regarded as the frequency of an actual exchange.

The relative spin orientation of the electrons, governs the degree of overlap of the orbitals, which in turn determines the magnitude of coulomb interaction between the electrons. Due to this relation, therefore, the coulomb interaction between two electrons can be thought of as a strong interaction between their spins. Dirac [8] has shown that when all spin-orbit interactions are neglected, the coulomb interactions between electrons can, in fact, be replaced by an interaction between their spins of the form

$$\tfrac{1}{4}J(1 + \bar{S}_1 \cdot \bar{S}_2) \quad .$$

The constant term is usually neglected as of no interest. The

value of J, the exchange integral, depends on the degree of overlap of the orbital wave functions of electrons (1) and (2). Applied to crystals, the interaction need only be considered between nearest neighbour ions since J decreases very rapidly with distance. The scalar product $J\bar{S}_1 \cdot \bar{S}_2$ is known as the isotropic exchange interaction, its value depending only on the relative orientation of the spins. The sign of J is a subject of considerable controversy but the usual sign is negative as is necessary in order that a chemical bond may be found.

If spin-orbit coupling is taken into account, the interaction cannot be considered as isotropic. The orbital wave functions are rarely spherically symmetrical in crystals, and this asymmetry is felt by the spins through spin-orbit-coupling. The anisotropic exchange has been shown to give an expression similar to that for dipole-dipole [9] interaction. It is of importance in explaining the ferromagnetic-anisotropy in cubic crystals but has rarely been used in the discussion of line width measurements in concentrated paramagnetic crystals.

3.5.2. Exchange between identical spins with $S' = \frac{1}{2}$

The effect of isotropic exchange interactions on the line widths in electron resonance can be described, for this case, simply as follows.

In the presence of an external magnetic field, and in the absence of exchange interaction, the electron spins will line up randomly, parallel or anti-parallel to the field direction. The

dipolar interaction between the spins results in each spin experiencing, in addition to the external field H_o, a local field H_{loc} due to the neighbouring spins. This local field will not be the same at every spin site because of the random distribution of parallel and anti-parallel spins. The resonance condition

$$h\nu = g\beta(H_o + H_{loc})$$

will not, therefore, satisfy all spins in the lower spin state, together. Resonance will occur over a spread of external field values.

The effect of exchange interaction is to average H_{loc}. For example, exchange between two spins at whose sites H_{loc} is equal in magnitude but opposite in direction would mean that the electrons concerned see an average H_{loc} of zero. The effect of this averaging is to increase the number of individual resonances occurring at the central value corresponding to $H_{loc} = 0$, causing the line to be sharper at the centre. This peaking of the absorption line is known as exchange narrowing. The actual line width, however, is difficult to predict since exchange narrowing is always accompanied by dipolar broadening. The theory of Van Vleck [6] shows that, in this particular case of identical spins with $S' = \frac{1}{2}$, the exchange contributes to the fourth but not to the second moment of the line, with the result that the centre of the line is narrowed. Since the area must remain constant, the wings are broadened.

3.5.3. Exchange between non-identical spins and between dissimilar ions

The theory of Van Vleck [6] and also Pryce and Stevens [7] shows that in all cases but the above, exchange interaction will contribute to the second moment and the line will be broadened. The case of strong exchange interaction between two ions with the same effective spins but different g values, is of special interest, in that it provides a direct measure of the size of the interaction between dissimilar ions. In the absence of exchange interaction, two transitions will be observed corresponding to frequencies $h\nu' = g'\beta H$ and $h\nu'' = g''\beta H$. If however the exchange energy is such that $J >> (g' - g'')\beta H$ only one transition will be observed at a frequency given by $h\nu = \frac{1}{2}(g' + g'')\beta H$. With very strong exchange the one absorption line will be narrowed. This effect has been observed by Bagguley and Griffiths [10] in copper sulphate crystals. The lines from the two inequivalent copper ions per unit cell were not resolved at a frequency of 0.3 cm^{-1} but at a frequency of 0.8 cm^{-1} the lines were almost resolved. This corresponds to $|J| \sim (g' - g'')\beta H$ at a frequency of 0.8 cm^{-1}, giving the value of $|J| \sim 0.15$ cm^{-1}.

3.5.4. Exchange interaction between ions with nuclear spin

The production of a nuclear hyperfine structure in electron resonance spectra has been discussed in the previous chapter. The effect of exchange interaction on this, can be discussed, simply, in the same way as in the case of exchange between identical spins.

If the nuclear spin of each ion is $I = \frac{1}{2}$, these spins will be aligned either parallel or anti-parallel to the magnetic field produced by the electrons, at the nucleus. The effect of exchange interaction, on the system as a whole, is to average out the effect of the nuclear spins on the electrons. For example, if exchange occurs between the electrons of two ions whose nuclear spins are oppositely oriented, the electrons see an average field, due to the nuclear spins of zero. The appearance of the resonance spectrum will depend on the magnitude of the exchange interaction. If the exchange energy is smaller than the hyperfine splitting, the lines will merely be less well resolved. If the exchange energy is of the same order as the hyperfine splitting, the lines will be only just resolved and one broad line results. However, for larger exchange energies, only one transition occurs, at the central frequency. This corresponds to all the local fields due to the nuclear spins being averaged out to zero. The line will now appear much narrower since it is no longer the envelope of unresolved structure.

3.5.5. The magnitude of the exchange energy

The direct way of estimating this is to measure the mean square line widths and subtract the widths calculated from dipole-dipole interactions. This method has been used by Ishiguro, Kambi and Usui [11] in the case of nickel fluosilicate.

They assumed that the exchange interaction with other than nearest neighbours was negligible and found $|J| \sim 0.04\ cm^{-1}$. A similar procedure has been used for nickel ammonium selenate by Stevens [12] who found a value of $|J| \sim 0.025\ cm^{-1}$ with a sign usually associated with ferromagnetism.

Griffiths [13] et al. have observed an exchange in ammonium chloroiridate. In semidilute crystals, there is a reasonable chance that $(IrCl_6)^{2-}$ complexes occupy nearest neighbour positions. There is then an exchange interaction between neighbouring pairs of iridium ions because of the transfer of unpaired electrons to the intervening chlorine ions. They found an anisotropic exchange

$$J_x = \mp\ 0.84;\quad J_y = \pm\ 0.64;\quad J_z = \pm\ 0.20\ cm^{-1}.$$

Unless the exchange interaction itself is to be determined, magnetically dilute samples must be used for electron resonance study. Both dipolar and exchange interactions should then be reduced sufficiently for the resolution of any structure.

3.6. Delocalization Narrowing

This is the motional narrowing due to the delocalization of the unpaired electrons in a molecular orbital. If the electron passes over several atoms with a nuclear spin in its orbit, the motion may produce an averaging similar to the exchange interaction described above. This possibility has been investigated by Walter [14], who concluded that there is definite experimental

evidence for this effect.

3.7. Other Sources of Broadening

3.7.1. Defects, Dislocation and Mosaic Crystal Structure

At very large dilutions it may be expected that the dipolar and exchange contribution to the line width will be negligible. In practice, however, there is often in crystals a residual line width which cannot be attributed to any of the mechanisms so far considered. This line width is particularly great for crystals in which there is large magnetic anisotropy.

The residual line width can usually be attributed to small variations in the parameters of the spin Hamiltonian. Instead of the usual sharp values for g, D and E etc., there is a distribution of values. This can happen if the surroundings of the ions are not all the same, due to defects and dislocations, or if the symmetry axes of individual ions are not all parallel due to a mosaic crystal structure.

In dilute nickel fluosilicate [9] & [11], the dipolar width should be not more than 6 gauss, but the line width is found to be between 20 and 50 gauss, depending on the care with which the crystal was grown. It is thought that this is due to small variations in D since g is isotropic, E is zero whilst D is between 0.1 and 0.5 cm^{-1}.

The line width in Ruby [15] is considered to be due to the fact that the symmetry axis changes direction in some manner along the crystal and may show a curvature along the boule. The

deviation across a crystal about one inch in length may be several degrees. The angular behaviour of the $\pm\frac{3}{2} \rightarrow \pm\frac{1}{2}$ transition of Cr^{3+} in Al_2O_3 is given by

$$h\nu = g\beta H \pm D(3\cos^2\theta - 1) \quad .$$

Since g is isotropic, the differential of this expression is

$$\Delta H = \frac{D}{g\beta}\,\frac{3}{2}\sin 2\theta\,\Delta\theta$$

where ΔH is the half line width and θ is the angle between the magnetic field and crystal axis. This should show a maximum line width for $\theta = 45^\circ$. At this angle and for an angular spread of 0.5° the corresponding half line width is $\sim$ 50 gauss. This is larger than the spin-spin interaction for all Cr^{3+} with concentrations less than 0.2 mole percent of Cr^{3+}.

Shaltiel and Low [15] have discussed this example and in the same paper derive theoretical expressions for the line shape and width due to a mosaic structure in a single crystal of ThO_2 containing a small amount (less than 0.01 %) of Gd^{3+}. They assume that the nearly perfect crystal consists of a large number of perfect crystallites which differ only in that the crystal axes point in slightly different directions. A co-ordinate system is attached to each crystallite, in which the co-ordinate axes coincide with the crystal axes. The coordinates in this system are denoted by θ and ϕ. The frequency of the transition between any two paramagnetic levels in an external

magnetic field H can be described by

$$\nu = F(H, \theta, \phi) \quad .$$

Assuming a gaussian distribution of crystallite orientations about the average, and that the misorientation of the crystallite is small, they derived an expression for the half width at half intensity

$$\Delta H = \tfrac{1}{2} \cdot \frac{\partial F}{\partial \theta} \; \alpha_o \Big/ \frac{\partial F}{\partial H}$$

where α_o is the average misorientation of the various crystallites.

The calculated line widths were normalized to give a best fit to the experimental curves by choosing $\alpha_o = 0.12^o \pm 0.02$.

The effect of the mosaic structure is to cause variations in the parameters of the spin Hamiltonian, which for Gd^{3+} with an $^8S_{7/2}$ ground state has a number of new terms due to the high spin value. Small differences between theory and experiment were explained by supposing the presence of a small additional axial field along the principle cubic axes. This is described as a distribution of values of D centred around D = 0.

These line widths will be frequency dependent.

3.7.2. Unresolved Hyperfine Structure

If there is sufficient line broadening, due to any of the mechanisms discussed so far, the individual lines of a hyperfine structure may not be resolved. In the case of strong exchange interaction it has been mentioned that the structure

is replaced by a single exchange narrowed line. However, for all other mechanisms the overall line width will be governed by the splitting of the unresolved hyperfine lines, and will be frequency independent.

3.8. Experimental Sources of Line Broadening

3.8.1. Power saturation broadening

It has been shown in Section 3.3.2. that in systems which have long spin-lattice relaxation times, spins when excited, may not return to the ground level sufficiently quickly for thermal equilibrium to be maintained. This happens when the incident power is high. It can be seen from equation 3.13 that the saturation will be a maximum at the peak of the resonance curve, where $g(\nu)$ is a maximum, and falls off on both sides, the line will therefore be broadened on saturation.

This is not true of inhomogeneously broadened lines, however, because the spin packets will saturate individually and their peak heights will each be reduced by the same fraction. Hence the overall resonance curve which is the envelope of individual resonances will decrease in height but retain its shape.

In practice, the power density per absorbing atom or molecule, in the solid state is rarely high enough for saturation to occur at ordinary temperatures. Conditions must usually be adjusted in order to observe it.

3.8.2. Inhomogeneous Magnetic Field

If the magnetic field varies over the sample, the resonance

condition will not be satisfied for all ions together. A broadening of the line results.

3.8.3. Modulation Broadening

Karplus [16] showed that modulation of the source or of the magnetic field at the sample are equivalent, and if either is modulated sinusoidally at a frequency, ν, then side-bands appear on both sides of the true resonance, separated from it by the modulation frequency. Classically, a high frequency modulation of the magnetic field may be thought of as a modulation of the Larmor precession frequency which would produce side-bands. These would be resolved or contribute to the line width, only if ν is of the order of or greater than the line width, and if their magnitude is sufficient to produce a noticeable effect.

The phenomenon has been noticed experimentally, and accounted for, by various workers, for example Townes and Merritt [17], who observed the side-bands produced by high frequency Stark modulation of a molecular absorption.

REFERENCES

(1) A. M. Portis, Phys. Rev. 91 (1953) p. 1071.

(2) R. de L. Kronig, Physica 6 (1939) p. 33.

(3) J. A. Giordmaine, L. E. Alsop, F. R. Nash & C. H. Townes, Phys. Rev. 109 (1958) p. 302.

(4) M. Blume & R. Orbach, Phys. Rev. 127 (1962) p. 1587.

(5) J. H. Van Vleck & V. F. Weisskopf, Rev. Mod. Phys. 17 (1945) p. 227

(6) J. H. Van Vleck, Phys. Rev. 74 (1948) p. 1168.

(7) M. H. L. Pryce & K. W. H. Stevens, Proc. Phys. Soc. A63 (1950) p. 36.

(8) P. A. M. Dirac, The Principles of Quantum Mechanics (O.U.P.) (1947) p. 219.

(9) J. F. Ollom & J. H. Van Vleck, Physica 17 (1951) p. 205.

(10) D. M. S. Bagguley & J. H. E. Griffiths, Proc. Roy. Soc. A201 (1950) p. 366.

(11) E. Ishiguro, K. Kambe & T. Usui, Physica 17 (1951) p. 310.

(12) K. W. H. Stevens, Proc. Roy. Soc. A214 (1952) p. 237.

(13) J. H. E. Griffiths, J. Owen, G. Park & M. F. Partridge, Phys. Rev. 108 (1957) p. 1345.

(14) R. I. Walter, J. Chem. Phys. 25 (1956) p. 319.

(15) D. Shaltiel & W. Low, Phys. Rev. 124 (1961) p. 1062.

(16) R. Karplus, Phys. Rev. 73 (1948) p. 1027.

(17) C. H. Townes & F. R. Merritt, Phys. Rev. 72 (1947), p. 1266.

Chapter 4

The Spectrometer

4.1. General Considerations

The requirements for the observation of electron resonance are basically very simple. The sample containing unpaired electron spins must be placed in a uniform magnetic field H, which will split the spin levels by the amount $g\beta H$. If an oscillating magnetic field of frequency ν is then applied to the sample, at right angles to the direction of the uniform field magnetic dipole transitions will be induced between the levels when the condition

$$h\nu = g\beta H$$

is satisfied. A net absorption of energy from the oscillating field will occur as long as there is a greater population in the lower level. This has already been discussed in the section on spin-lattice relaxation. The magnitude of the absorption will be proportional to the difference in population (n) between the levels. This is given by equation 3.6, if Maxwell Boltzmann statistics are obeyed,

$$n = N\frac{h\nu}{2KT} \qquad \text{when} \quad \frac{h\nu}{KT} \ll 1$$

N is the total number of spins in the two levels and T the temperature of spin system and lattice at thermal equilibrium.

Since a large absorption of energy will be easier to detect than a small one, it is apparent from this relation that a sensitive system must employ a high frequency oscillating magnetic field and low temperatures. However a limit to the frequency which can be used, is set by the strength of the magnetic field required to satisfy the resonance condition. Practical considerations such as the size of the magnet and power required, at present limit the strength of magnetic fields, with sufficient homogeneity for electron resonance, to not much greater than 15,000 gauss. This corresponds to frequencies of between 9 and 30 kMc/s, which lie in the microwave region of the electromagnetic spectrum and are easily produced using the klystron valve. Recent developments in superconducting magnets and coherent infra-red sources may modify this situation in the near future.

The basic units of the electron resonance spectrometer are:-

1. Microwave Source.
2. Absorption Cell.
3. Detection and Display System.
4. Magnetic Field.

4.1.1. Microwave Source

The frequencies most commonly used for electron resonance spectrometers are 9, 24 and 36 kMc/s, corresponding to wavelengths of 3 cms, 1.25 cms and 0.8 cms respectively. These are usually classified as being in the X, K and Q bands respectively. The

microwave source is usually a reflex klystron, which, due to its high stability, more monochromatic output and ease of tuning, is preferred to a magnetron except when very high power is needed. The power output of the klystrons used is most often of the order of 20 to 200 milliwatts. The spectrum produced by the reflex klystron is highly monochromatic, so that, unlike optical spectrometers, no dispersive element is required.

4.1.2. Absorption Cell

According to equation 3.12 the transition probability between the levels $M_s = \pm \frac{1}{2}$ is proportional to H_1^2 where H_1 is the amplitude of the microwave magnetic field. In most spectrometers therefore the absorption cell is designed to increase the value of H_1 at the sample and, therefore, the magnitude of the observed resonance signal. A resonant cavity is frequently employed for this purpose, and the extent to which it concentrates the field at the sample is described by the "Q" factor. This can be defined as

$$Q = 2\pi \left(\frac{\text{Energy stored}}{\text{Energy Dissipated per cycle}} \right) .$$

The energy dissipated per cycle is that lost as heat in the walls by the currents which must flow in order to sustain the standing wave pattern plus any lost in dielectrics etc.. The heat produced will depend on the electrical conductivity of the walls, which are usually made of copper brass or silver, with

the result that the "Q" factor may be very large, of the order of 10^4.

The configuration of the magnetic and electric fields is known for most cavity designs, so that the sample can be placed in a position of maximum magnetic and minimum electric field. The last condition ensures a minimum dielectric loss or damping in the cavity and a maximum absorption of microwave energy by the spin system at resonance. The size of the sample must be such that it occupies as much of the region of maximum magnetic field as possible, whilst projecting as little as possible into the electric field.

This is expressed in terms of the filling factor, F, which is defined as the ratio of the magnetic energy in the sample to the magnetic energy in the whole of the cavity volume.

Thus

$$F = \frac{\int_S H_1^2 \, dV}{\int_C H_1^2 \, dV}$$

the integrals being taken over the sample volume and the cavity respectively.

4.1.3. Microwave Detection

The level of microwave power leaving the absorption cavity is nearly always detected with a silicon-tungsten crystal rectifier.

This converts the microwave radiation into a d.c. signal so that it would be possible to observe resonance as the change in deflection of a sensitive galvanometer. However it is a general principle that a.c. techniques are more convenient than d.c.. In the simplest spectrometer, therefore, the magnetic field is modulated with a small a.c. component so that the resonance condition is satisfied twice in every field cycle. The output from the detecting crystal is therefore modulated with an intermediate frequency twice that of the field modulation, and can be amplified and displayed on an oscilloscope screen. With a suitably phased sweep on the X plates the resonance signal appears as a dip in the trace.

Such an arrangement is known as Crystal Video detection. Most spectrometers can operate in this way since it is convenient for a first examination of untried samples. It is not, however, the most sesitive detection system, and a means must be found of increasing the signal-to-noise ratio. A simple method of doing this with the crystal video spectrometer is to photograph the signal trace on the oscilloscope screen. The noise is then averaged over the time of the exposure which can be made long, with consequent improvement in the signal-to-noise ratio.

In general to improve the signal-to-noise ratio the signal must be made as large as possible and the noise as small as possible. Assuming that the conditions of high radiation frequencies and low

temperatures have been fulfilled, there is an upper limit to the power which can be absorbed during resonance by a particular sample in a given cavity. The signal cannot be increased further and the noise must therefore be reduced.

With a good klystron, the largest single source of noise in a spectrometer, such as the one described here, is the detecting crystal. The noise generated in the crystal varies inversely with the intermediate frequency, so that wherever possible a high frequency field modulation is used for the greatest sensitivity. The frequency of the field modulation which can be used is limited by the broadening it will produce and by the difficulty of producing a large sweep amplitude at the sample. A good compromise is found by using a modulation frequency of 100 kc/s, whilst to use higher intermediate frequencies a superhetrodyne detection system must be employed.

The sensitivity of detection can then be improved still further by reducing the bandwidth of the system until only noise at the intermediate frequency remains. Since the actual resonance absorption signal is carried as a slow amplitude modulation on the intermediate frequency, a very narrow band amplifier, tuned to this frequency, can be used without losing any information. The bandwidth of the system can be reduced still further by the use of phase-sensitive detection which allows only noise components which are in phase with the signal to pass through. There is a d.c.

output proportional to the first derivative of the absorption curve. After d.c. amplification this is passed to some form of pen recorder. The great advantage of this method of detection is that the signal-to-noise ratio is only dependent on the band-width of the last recording stage, the noise components of previous stages being eliminated.

4.1.4. Magnetic Field

Since the resonance condition is usually satisfied by varying the magnetic field strength whilst keeping the microwave frequency constant, the magnet is usually an electro-magnet. In the study of free radicals, which give signals very close to the free spin g value, a permanent magnet is often used. For the most general application, however, the magnet must be able to produce fields continuously variable from zero to those corresponding to g values of less than 2. The magnetic field must be uniform over the sample and must not vary with time. This requires that the ratio of pole piece diameter to gap width must be as large as possible, the magnet fed from a good current stabilized power supply and the temperature of the coils regulated with water cooling. The first requirement is, however, frequently a compromise between the need for a homogeneous field and the necessity for having a wide enough gap to accommodate dewars for low temperature measurements. The actual degree of homogeneity and stability of magnetic field required in electron resonance is determined by

the minimum line width expected. Line widths of less than 0.1 gauss are uncommon so that a homogeneity over the sample and stability of 1 part in 10^5 may be needed.

4.2. The Spectrometer

4.2.1. Special Requirements for the Study of Haemo-proteins

In the study of single crystals of haemo-proteins there are three main considerations which influence the choice of spectrometer to be used. These are:-

1. The small size of the crystals (1 or 2 mms. across).
2. The nature of the crystal, which is only stable when wet.
3. The very broad lines obtained (up to 700 gauss peak to peak).

A small crystal makes it necessary to use a small sample cavity in order that there will be a good filling factor. This requires the use of Q or K band frequencies.

The water content of the crystal will damp the cavity at room temperature so that all measurements must be carried out below $0^{\circ}C$.

The broad lines observed make it impracticable to display the absorption on an oscilloscope screen as this requires magnetic field modulation with an amplitude exceeding the total line width. A modulation amplitude of between 500 and 1000 gauss is therefore needed to display the broadest lines, otherwise only a tilting of the trace will be seen. Because of this it is more convenient

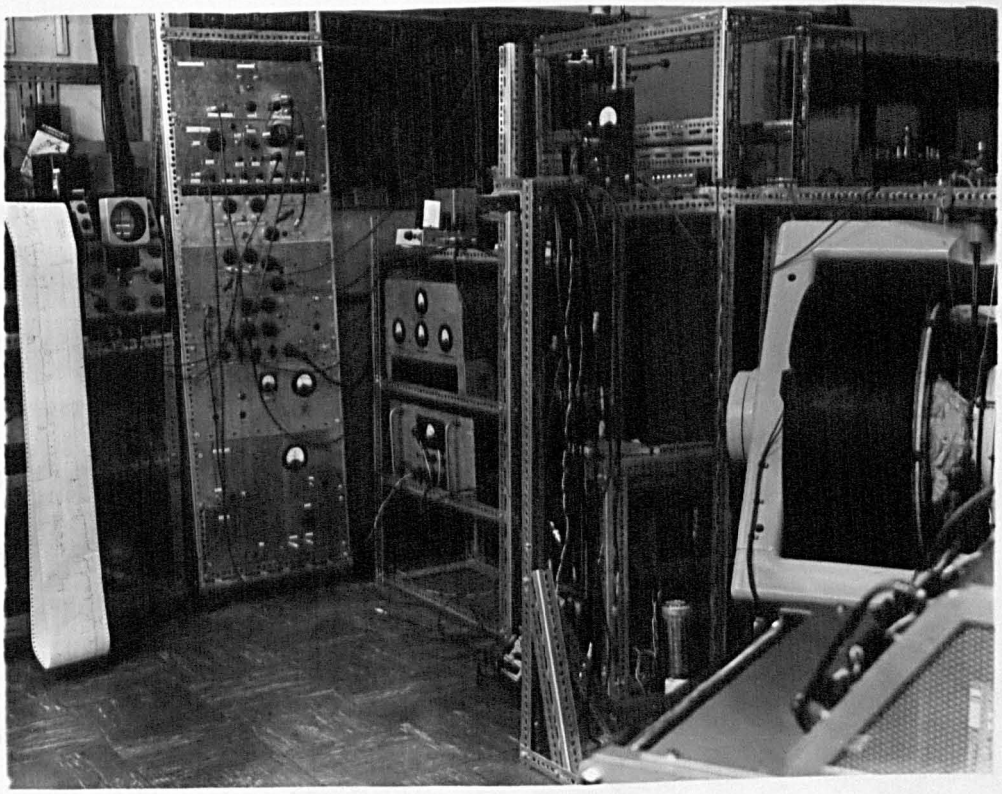

GENERAL VIEW OF SPECTROMETER

to trace out the absorption line by a pen recorder as the magnetic field is swept slowly through resonance. This suggests the use of phase sensitive detection with say, a field modulation frequency of 100 kc/s. However for maximum sensitivity it can be shown [1] that the modulation amplitude should be twice the line width, although a distorted line shape results from such a modulation. The optimum modulation amplitude is therefore taken to be about one quarter of the line width, which in the case of the haemo-proteins means up to about 150 gauss. To produce such a modulation at the sample using a frequency of 100 kc/s would be very difficult and the power lost through eddy current heating would be considerable even if the modulation coil were placed inside the cavity. In general the modulation amplitude obtainable with spectrometers working at 100 kc/s is around 10 gauss. For very wide lines, therefore, the full advantage of using high frequency modulation is not felt.

By working at an audio frequency such as 400 c/s it is a simple matter to produce field modulation amplitudes of about 100 gauss so that the detection system can work under optimum conditions. This partly offsets the increased crystal noise at low intermediate frequencies. Another distinct advantage is that the skin depth in brass at 400 c/s is about 50 thousandths of an inch as against 4 at 100 kc/s, so that the modulation can be applied from outside the cavity and dewar; eddy current heating

will be reduced with a consequent saving in liquid coolant.

As a result of these arguments the spectrometer used for most of the measurements on haemo-proteins, carried out in this work, operates at Q or K band frequencies with 400 c/s field modulation and phase sensitive detection. It can also be used with 50 c/s crystal video detection.

4.2.2. The Microwave System

4.2.2.1. Klystron

The spectrometer is able to work at both Q and K band frequencies since the electronics including the klystron power supply are identical in each case and only the waveguide runs are separate. The microwave system is essentially the same for both frequencies so that only one need be described in detail.

The K band klystron used is the 2K33 with a frequency of 24.kMc/s and a power output of 40 milliwatts. The Q band klystron is an E.M.I. Type R5146 with a frequency of 36 kMc/s and maximum power output of 60 milliwatts, which varies considerably over the tuning range. The frequency of each klystron can be varied by about 10% by mechanically distorting the resonant cavity and also by a few tens of megacycles by varying the reflector voltage.

The power supply for both klystrons is a conventional series stablized type [2], capable of delivering 2000V (variable) for anode-cathode potential, the anode being earthed. Another

similarly stabilized 650V supply has its positive line at -2000V so that negative voltages of 650V (variable) for the reflector to cathode and 200V (variable) for grid to cathode may be obtained through a resistor chain in the output. The heater supply is a 6V lead-acid accumulator. A diode is fitted in the reflector circuit to prevent positive voltages being applied to the reflector which would result in its being burnt out by the electron bombardment.

The klystron is air cooled by an electric blower mounted on a separate stand so that vibration of the klystron and waveguide assembly is kept to a minimum.

4.2.2.2. Automatic Frequency Control

In order to obtain an accurate comparison of results taken over periods of up to one or two hours it is necessary for the frequency of the klystron to remain constant during that time. This is achieved by locking the klystron frequency to an external high "Q" reference cavity. At the same time there should be an appreciable reduction in the noise from the klystron.

The klystron is frequency modulated at 33 kc/s and a discriminator curve is obtained from the reference cavity. This is used to apply error voltages in the correct phase to the klystron reflector.

The block diagram Fig. (4.1) shows the arrangement of the locking system.

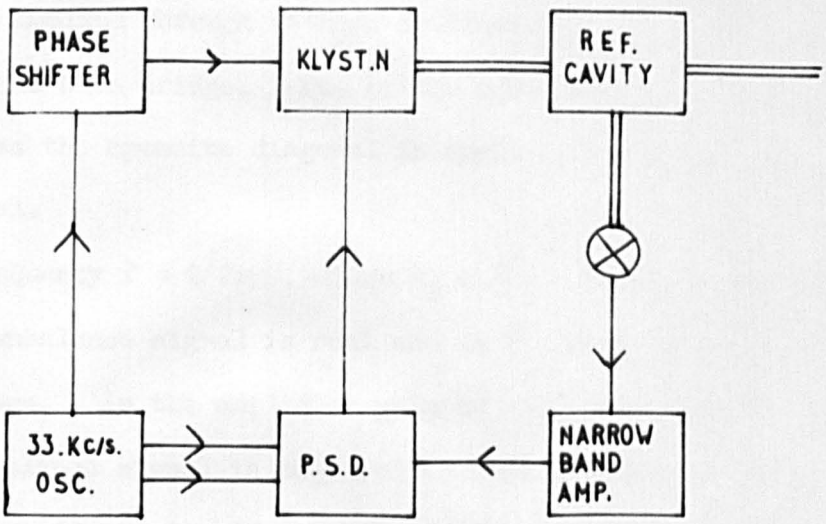

KLYSTRON LOCKING SYSTEM

FIG. 4.1

The oscillator [3] Fig. (4.2) supplies an adjustable voltage for the modulation of the klystron frequency and a two-phase voltage for the phase sensitive detector. A wien bridge, shown in the dotted square, is driven by two separate amplifiers V_1, the output being applied through cathode followers V_2 across one diagonal of the wien bridge. The bridge unbalance signal which appears across the opposite diagonal is applied to the amplifier input terminal.

At a frequency $f \simeq 1/2\pi RC$, where $R_2 = 2R_3 = R$, $C_2 = \frac{C_1}{2} = C$, this bridge unbalance signal is real and in the same phase as the driving voltage. As the amplifier gain is high only a small amount of unbalance signal is required to just maintain oscillation. The thermistor adjusts itself so that the above conditions are realized. The oscillator output amplitude is largely independent of amplifier characteristics and depends mainly on the wien bridge.

Variations in the ambient temperature of the thermistor will cause fluctuations in the oscillator output. To reduce this to a minimum the wien bridge is enclosed in a separate aluminium box and connected to the rest of the circuit by a standard octal plug. The switch in the input to the bridge enables the oscillations to be 'stopped' whilst tuning the klystron. This was found to be necessary because of an intermittent and untraced 33 kc/s pick up which tended to keep the klystron locked even when the 33 kc/s modulation was disconnected from the reflector. After tuning

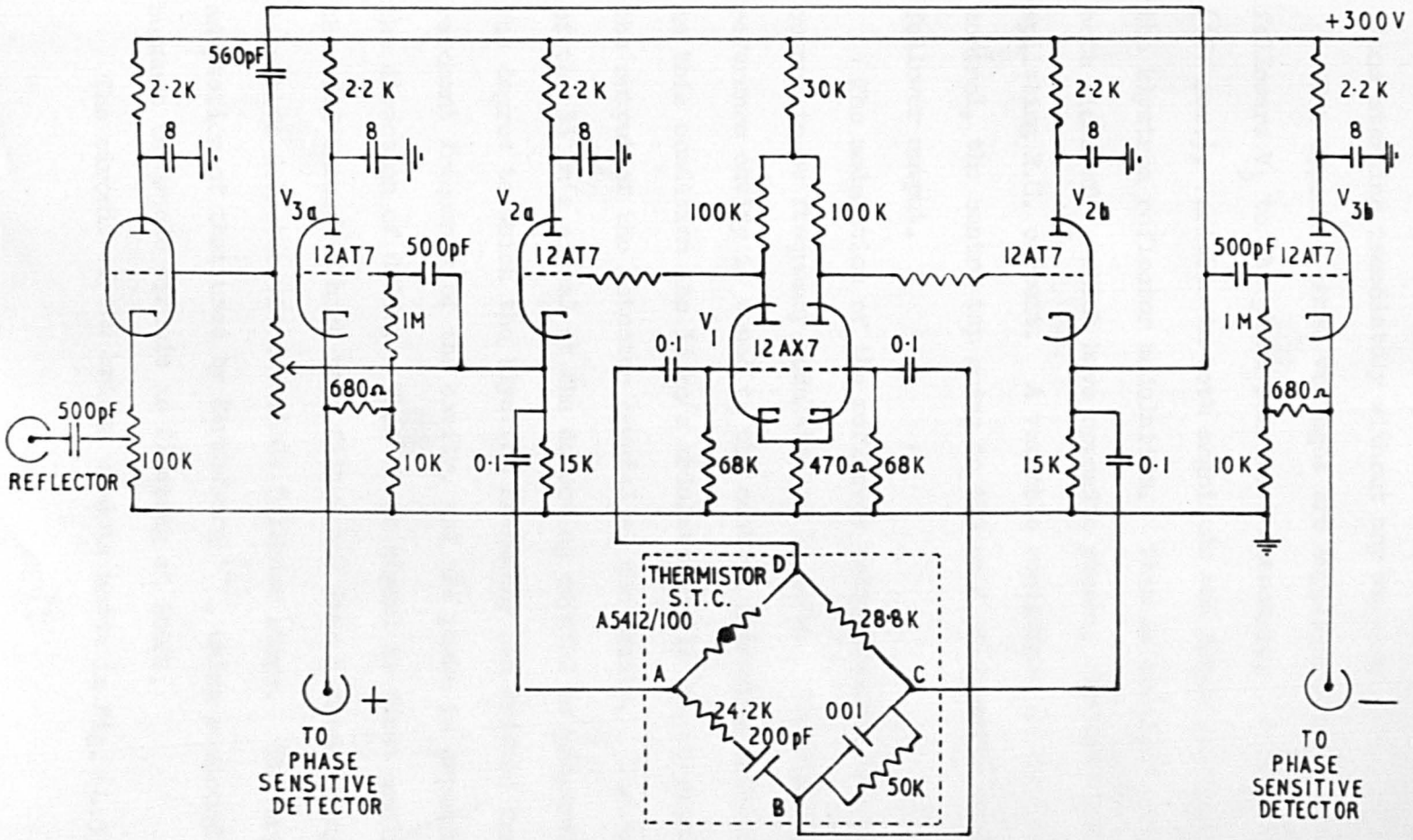

FIG. 4.2
33Kc/s. OSCILLATOR

the klystron, the oscillator could be switched on again, oscillations starting immediately without any warming up period.

Two opposite phase voltages are supplied through cathode followers V_3 to the phase sensitive detectors. A small voltage (15V max.), variable in both magnitude and phase is supplied for the klystron reflector modulation. This is arranged by connecting both sides of V_2 which have opposite phases, through a phase splitting R.C. circuit. A variable resistance is the phase control, the centre tap going to the grid of a triode with cathode follower output.

The modulation of the reflector voltage causes the microwave output to be frequency modulated at 33 kc/s. The high "Q" reference cavity is tuned to the central microwave frequency and in this condition the 33 kc/s modulation will not be present in the output of the detector crystal at the cavity. The amplitude of the 33 kc/s signal at the detecting crystal is proportional to the degree to which the klystron frequency has drifted from the resonant frequency of the cavity, and the phase is dependent on the direction of drift. This error signal is first amplified then fed through a high pass filter and into a diode bridge phase-sensitive-detector via a cathode follower stage. The bridge is an adaptation of that used by Strandberg [4], using semiconductors because the whole circuit is floating at 2000V.

The circuit of the bridge used is shown in Fig. (4.3).

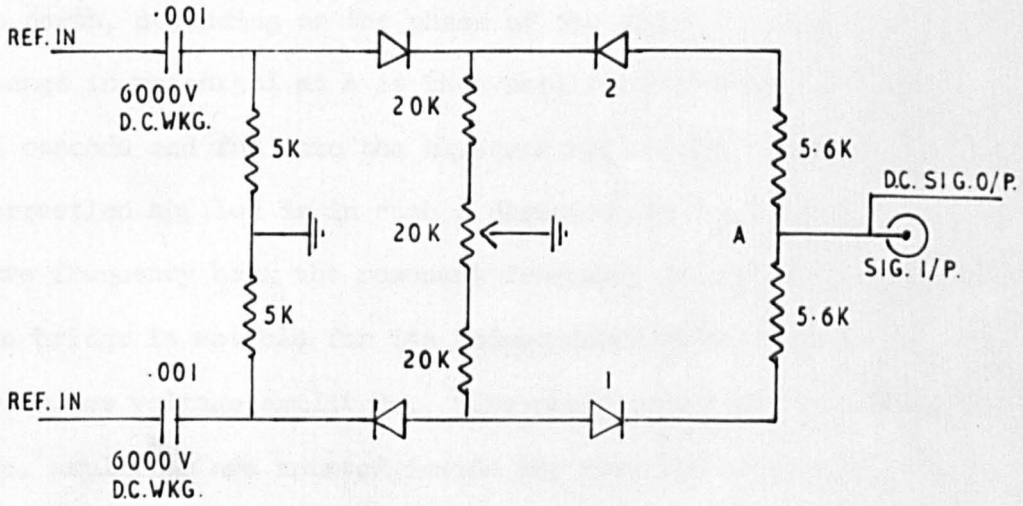

FIG.4.3
DIODE PHASE SENSITIVE DETECTOR

A sufficiently large reference voltage is able to effectively "switch off" the detecting diodes, independently of the magnitude of the signal voltage. Thus the detecting diodes may only conduct during every other half cycle. Then, depending on the phase of the signal voltage, either diode (1) or diode (2) will conduct. That is, the potential of A will either rise or fall with respect to earth, depending on the phase of the signal voltage. This change in potential at A is then amplified by a double triode in cascode and fed onto the klystron reflector. The voltage correction applied is in such a direction as to bring the microwave frequency back the resonant frequency of the reference cavity. The bridge is notable for its independence from variations in the reference voltage amplitude. The phase sensitive detector and d.c. amplifier are mounted inside the klystron power supply and are floating at the reflector voltage. Reference and signal voltages come in through 6000V d.c. isolating condensers.

When locked to the reference cavity the reflector volts on the klystron can be varied over a 30 volt range without the microwave frequency changing. The signal to noise ratio is improved by a factor of about 3/2 and drift is negligible over long periods. This degree of stability could not be obtained by locking to the sample cavity since this has a low "Q", being of the transmission type. Once cooled down to liquid nitrogen or hydrogen temperatures, the sample cavity stayed on tune, since temperature fluctuations

are the chief cause for changes in its resonant frequency and these should then be very small. The procedure for locking the klystron is to tune the frequency to that of the sample cavity and then to adjust the reference cavity to resonate at this frequency.

4.2.2.3. Waveguide Components

Since K and Q band systems are identical except in the size of components and since Q band was used for all the myoglobin measurements, only this system will be discussed in detail.

(a) Isolator

This component is a microwave gyrator so designed that it offers practically no attenuation (less than 1 db) to microwave power when flowing in one direction but over 30 db attenuation in the reverse direction. The isolator is situated just after the klystron and in this position prevents reflections from the waveguide system reaching the klystron. The insertion of such an element should therefore increase the amplitude and stability of the klystron by a large factor.

(b) Wavemeter and Reference Cavity (5)

The wavemeter and reference cavity is a cylindrical transmission cavity of 4.0 cms. diameter operating in the H_{03p} mode. It is heavily constructed from brass so that it is insensitive to mechanical and thermal changes. The movable plunger which forms one flat face of the cavity is driven directly by a rotating

micrometer screw. The microwave power is fed into the cavity through two holes, in the narrow side of the main guide, which are spaced $\frac{\lambda_g}{2}$ apart along the centre line. These two holes are situated symmetrically along a diameter of the end face of the cavity. The output coupling is located in the same face at a distance 0.55r from the centre along a diameter which makes 45^o with the line joining the input holes. The wavemeter is used by rotating the micrometer screw head until a resonance absorption occurs in the cavity at at least two different positions. The guide wavelength λ_g is measured directly from the micrometer readings. The free space wavelength λ, is then given by the relation

$$\frac{1}{\lambda^2} = \frac{1}{\lambda_g^2} + \frac{1}{\lambda_c^2} \qquad (1)$$

where λ_c is the critical wavelength and is given by $\lambda_c = 0.618r$ for this mode, r being the radius of the cavity in millimetres. Thus the free space wavelength for the cavity is

$$\frac{1}{\lambda^2} = \frac{1}{\lambda_g^2} + 0.0065 \qquad (2)$$

where λ and λ_g are measured in millimetres.

(c) Matching Units

It is necessary to have matching units on either side of the sample cavity to compensate for discontinuities in the guide at the input and output coupling holes. These matching units are

phase shifters using waveguide 'squeeze' sections. These consist of a waveguide with slots cut in each broad face $6\frac{1}{2}$" long and $\frac{1}{32}$" wide. A simple clamping screw enables the narrow sides to be compressed inwards. This alters the width of the guide and hence the guide wavelength and impedance over the compressed section. This effectively alters the phase of the wave arriving at the end of the 'squeeze' section.

(d) Sample Cavity

Two cylindrical transmission cavities, operating in different modes are used. The diagram Fig. (4.4) shows the direction of the microwave magnetic field in the two cavities, since it is the position of the maximum of this field which is of importance in electron resonance. The two modes are the lowest order modes which can be set up in cylindrical cavities and the patterns are determined as H modes. The first two subscripts of the H indicate the type of travelling wave pattern the mode represents and the third subscript, the number of complete patterns (i.e. the number of half guide wavelengths) which are accommodated in the length of the cavity. The cavities are excited by iris coupling holes and are of the transmission type. The diagram shows the method of coupling to the guides in the respective modes. The black dot shows the position of maximum magnetic field at which the sample is placed. Since the microwave magnetic field in the H_{011} mode is perpendicular to the d.c. field regardless of the

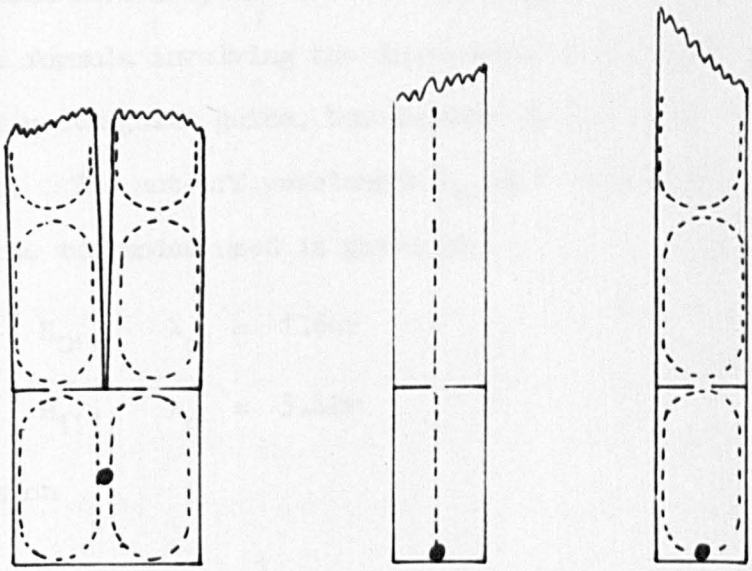

FIG. 4.4

CAVITY MODES

rotation of the magnet the transition probability remains constant as the magnet is rotated. However for the $H_{1;1}$ mode cavity the transition probability falls to zero when the microwave and d.c. fields are parallel.

For cylindrical cavities, the cut-off wavelength λ_c is not given by a simple formula involving the dimensions of the guide as in the case of rectangular guide, but depends on the roots of a Bessel function. The cut-off wavelength λ_c in a circular guide of radius r for the two modes used is given as

$$H_{01}, \quad \lambda_c = 1.64r$$

$$H_{11}, \quad \lambda_c = 3.42r$$

using the expression

$$\frac{1}{\lambda^2} = \frac{1}{\lambda_g^2} + \frac{1}{\lambda_c^2}$$

gives the resonant wavelengths of these modes in a cylindrical cavity of radius r and length d as

$$\frac{1}{\lambda_{111}^2} = \left(\frac{1}{3.42r}\right)^2 + \left(\frac{1}{2d}\right)^2 \qquad (3)$$

$$\frac{1}{\lambda_{011}^2} = \left(\frac{1}{1.64r}\right)^2 + \left(\frac{1}{2d}\right)^2$$

where the length d is an integral number of half guide wavelengths.

It has been mentioned earlier that the magnet gap must be as narrow as possible for the production of large homogeneous magnetic fields. This requires that the sample cavities be as narrow as possible. It is obvious from the equations 3 above that the radius may be made small by increasing the length, however the limiting measurement is that of the waveguides into and out of the cavity. The positions of these guides at the coupling holes is chosen so that the correct mode is excited preferentially in the cavity. In the H_{111} mode the guides must have their broad faces together and in the H_{011} mode they must have their narrow faces together. The H_{111} mode cavity can therefore be narrower than the H_{011} mode cavity. The actual dimensions of these cavities are for Q band.

H_{111} cavity internal diameter 7.14 mms.

H_{011} cavity internal diameter 10.25 mms.

Although it would be more convenient to use the H_{01} cavity for single crystal study, since full 180° measurements can be made in a crystal plane with only one mounting, better signals are obtained using the H_{111} mode cavity. This is probably due to the fact that the H_{111} mode is dominant in a cylindrical cavity and also because the H_{111} cavity has a smaller volume at resonance than the H_{011} cavity. The latter fact results in a better filling factor when working with the very small myoglobin crystals in the H_{111} mode cavity.

The photograph Fig. (4.5) shows the H_{111} cavity used. The waveguides, which are of thin german silver for low temperature work, are soft soldered into a circular threaded brass block, the diameter of which is only just greater than the diagonal of the waveguide square. A thin brass collar screws onto this, holding firmly in place the iris coupling hole diaphragm which is of brass 0.5 mm. thick. The cavity, also of brass, screws into this collar tightly up against the end diaphragm to make good electrical contact. The bottom face of the cavity forms the top face of a screw plunger which runs in a fine screw thread in the lower part of the cavity wall. A choke joint of length $\lambda_{g/2}$ is used between the plunger and cavity wall so that the actual contact between them is at a point of zero current in a half-wave shorted line, and the contact does not have to be good. A microwave leak between the two parallel guides above the coupling holes was stopped by building up the dividing waveguide wall with soft solder which was flattened on screwing the assembly tightly together. The iris coupling holes are drilled in positions such that they are at the centre of the waveguide cross section. The optimum diameter of these holes was determined empirically as that which gave the best electron resonance signal. This diameter was found to be 2 mm., which resulted in the cavity having a rather low "Q" but a smaller hole and higher "Q" would result in insufficient microwave power reaching the detecting crystal.

This type of cavity assembly makes it possible to clean not

Q BAND CAVITY
FIG. 4.5

only the cavity but both sides of the coupling hole diaphragm and the waveguides. It was found that accumulated dirt just above the coupling holes could produce a broad resonance absorption around $g = 2$, at low temperatures, which frequently obscured the broad myoglobin lines. Cleaning the whole cavity system usually cured this. Dirt in the waveguide outside the magnetic field can also absorb microwave power due to dielectric loss.

The upper ends of the german silver waveguide go into a dewar head assembly and are vacuum sealed with transparent plastic adhesive tape. The cavity itself is sealed with grease on the screw threads, a rubber 'O' ring between cavity and brass collar and a coned brass cup over its end. The cavity can thus be evacuated to prevent the formation of liquid air inside it at low temperatures.

(e) Crystal Detector

The crystal detector is of the 'open' type, G.E.C. SIM 8 which is mounted across the waveguide, the case forming a continuation of the guide walls. Both the silicon crystal and the tungsten wire are located in this aperture, the latter being placed in a position of maximum electric field and acting as a pick up probe. The rectified current is taken out from the crystal holder by coaxial cable.

The crystal holder is insulated from the rest of the waveguide run in order to break the low frequency path which could

result in 50 c/s pick up. This can make it impossible to use high amplification on crystal video detection.

The end of the waveguide is terminated in a movable plunger which is used to eliminate the wave reflected by the detector back along the waveguide.

4.2.2.4. Magnetic Field

The magnetic field is produced by a Newport Type D 8" magnet. This magnet has interchangeable pole pieces and is mounted on a calibrated turntable for single crystal work. With flat unconed pole pieces and a 10 cm. gap the field homogeneity is at least 1 in 10^5 over 1 cm^3 but the maximum field obtainable is less than 8 kilogauss. For Q band frequencies, fields of at least 14 kilogauss are required and these are achieved using 60° conical tips. The face diameter is then reduced to 10 cms. with a gap reduced to 3 cms. which maintains a homogeneous field over the sample. This gap just allows room for a tailed dewar and absorption cavity.

The power supply is a Newport Type B Mark II current stabilized unit. This has three current ranges which for the type D magnet are (0.5 - 12) amps, (2.5 - 13.5) amps and (5.0 - 15.5) amps. The field ripple produced by this unit is quoted as 0.25 gauss peak to peak for the 8" magnet.

The field is swept using a Newport Type A sweep unit which has variable range and time. The maximum sweep possible is 2.5 amps the smallest 0.25 amps, sweep times are variable from

32 minutes to 8 secs..

Field modulation at both 50 c/s and 400 c/s is applied externally through a modulation coil mounted on the yoke. This coil is described more fully in connection with the 400 c/s electronic system.

4.2.3. Electronic System

4.2.3.1. Crystal Video Detection Fig. (4.6)

Field modulation at 50 c/s is supplied from the mains through a variable transformer. This is adjusted so that the total sweep is greater than the width of the resonance line under investigation. Thus when the d.c. field is at the resonance value the signal is passed through twice in every cycle. The output from the crystal is fed through a wide band amplifier onto the Y plates of an oscilloscope. A 50 c/s voltage is applied to the X plates and adjusted to be in phase with the a.c. component of the magnetic field. Consequently a graph of absorption against magnetic field is traced out on the oscilloscope screen.

The wide band amplifier is a normal R.C. coupled amplifier Fig. (4.7) with a gain of about 10^4 and a reasonably flat response from 20 c/s to 10 kc/s. There is a variable input impedance of 500 Ω to 20 kΩ and a variable output attenuator.

4.2.3.2. 400 c/s Phase Sensitive Detection

The advantages of using this method of detection have been discussed earlier and the layout of the spectrometer is shown in the block diagram Fig. (4.8).

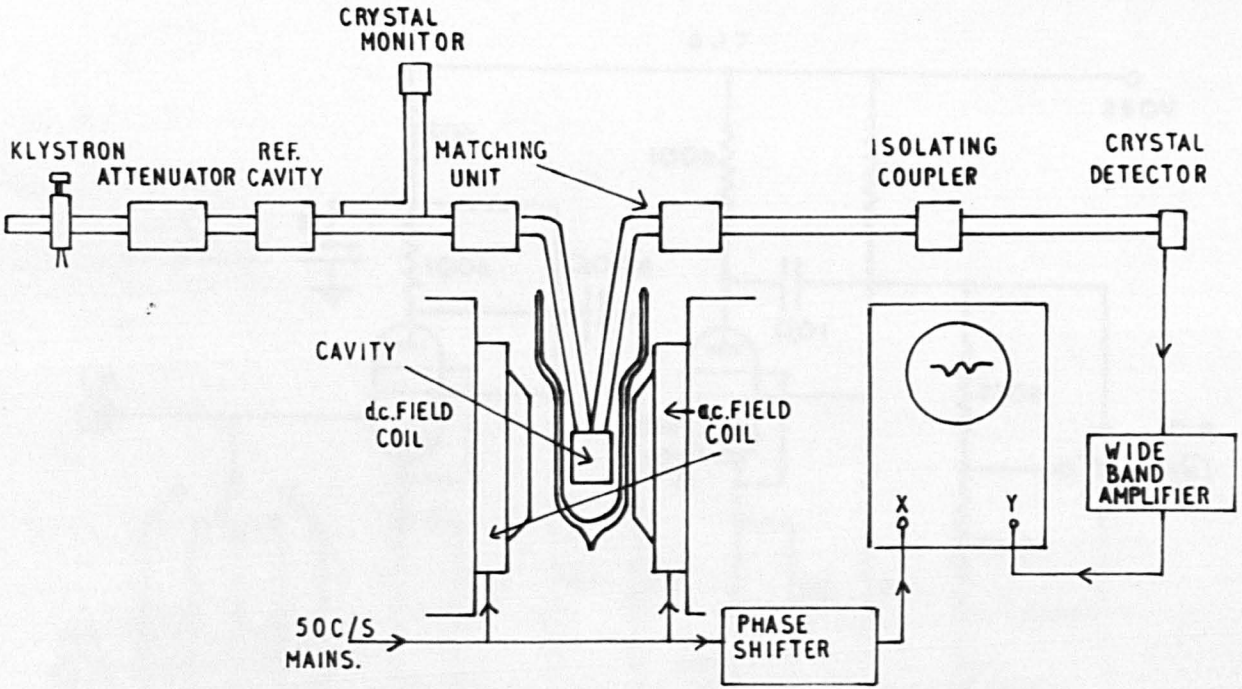

FIG.4.6
CRYSTAL VIDEO SPECTROMETER

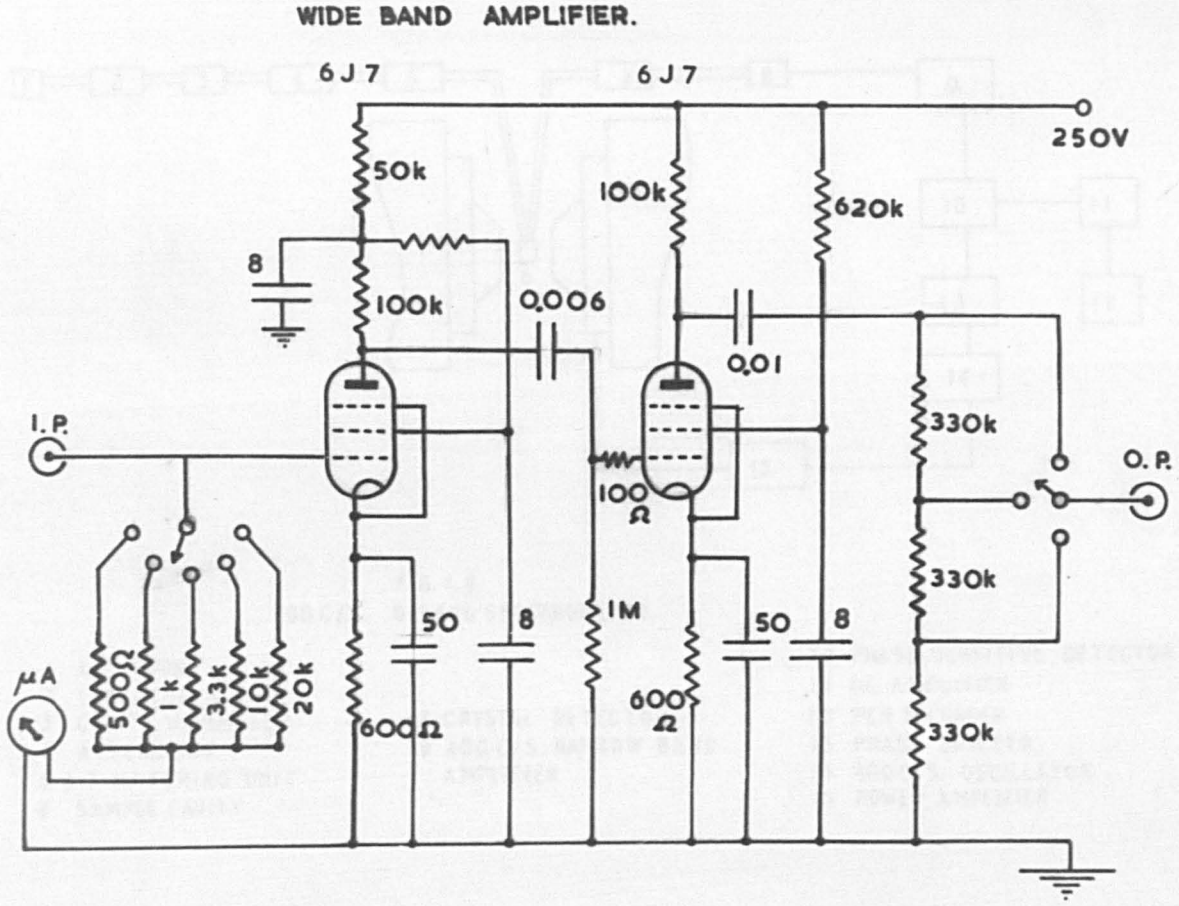
WIDE BAND AMPLIFIER.
6J7
6J7
250V
50k
100k
620k
8
100k
0.006
0.01
330k
I.P.
O.P.
100 Ω
330k
50
8
1M
50
8
μA
500Ω
1k
3.3k
10k
20k
600Ω
600 Ω
330k

FIG. 4.7

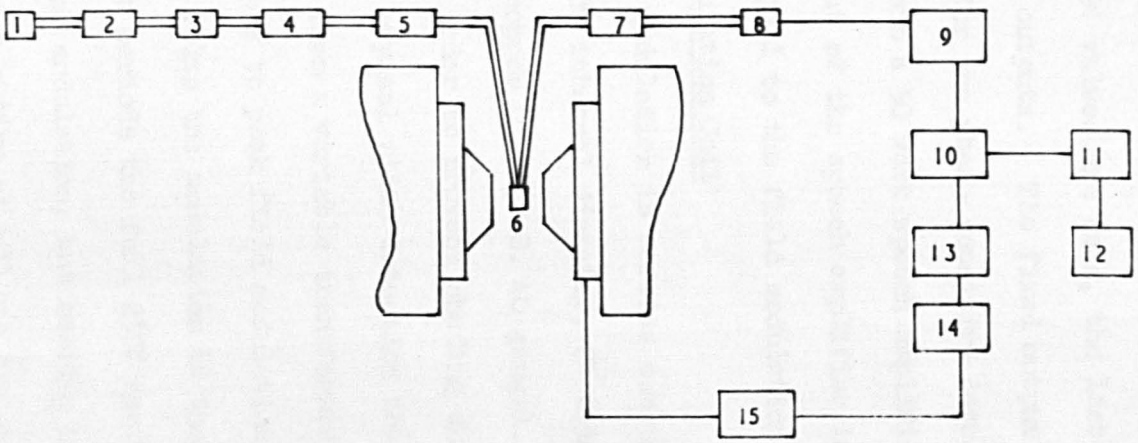

FIG. 4.8.
400 C/S. Q BAND SPECTROMETER

1 KLYSTRON
2 ISOLATOR
3 CAVITY WAVEMETER
4 ATTENUATOR
5 & 7 MATCHING UNIT
6 SAMPLE CAVITY
8 CRYSTAL DETECTOR
9 400 C/S. NARROW BAND AMPLIFIER
10 PHASE SENSITIVE DETECTOR
11 D.C. AMPLIFIER
12 PEN RECORDER
13 PHASE SHIFTER
14 400C/S. OSCILLATOR
15 POWER AMPLIFIER

(a) 400 c/s Oscillator Fig. (4.9)

This is an R.C. oscillator of conventional design in which the frequency determining network is a Wien bridge. A thermistor in one arm of the bridge stabilizes the amplitude of oscillation. Three EF91 valves are used, the last acting as a cathode follower with two outputs. The fixed output serves as the reference voltage for the phase sensitive detector and the variable output is fed into a 50 watt speech amplifier (Admiralty pattern 12522A). The output of the speech amplifier is delivered by two 807 valves in push pull to the field modulation coil.

(b) Modulation Coil

The modulation is carried out using one single modulation coil of 8" internal diameter, 2" thickness and 600 turns of glass covered copper wire (B.S. 40 gauge). The coil is cast in epoxy resin in order to prevent chafing due to vibration in the field.

For crystal video detection the 50 c/s current is fed through the coil from a variable transformer. With 50 volts across the coil a peak to peak field modulation of 200 gauss is produced and with 100 volts the modulation is increased in direct proportion. For short periods the full 230V can be used, producing nearly 1000 gauss modulation, but heating in the coil is considerable.

For operation at 400 c/s the maximum field modulation will only be produced if the impedance of the load matches the output impedance of the power amplifier. This was

400 c/s OSCILLATOR.

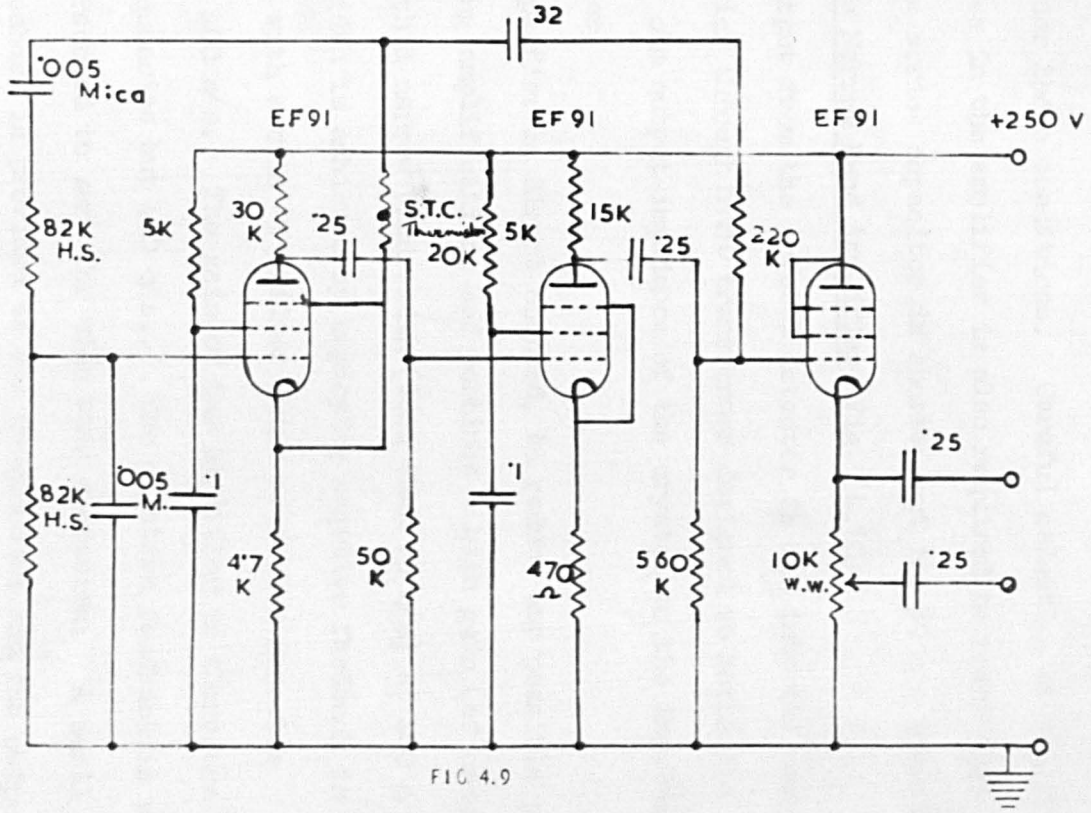

FIG 4.9

found to be much less than the impedance of the coil, due to the coil's self induction at 400 c/s. Matching was achieved by adding series capacitance to the coil until there was a maximum voltage across it. With 2.5 μF in series with the coil the maximum is 200 volts. A 400 c/s field modulation of 75 gauss is obtained under these conditions. Careful selection of the 807 output valves in the amplifier is also required to reach this value. The series capacitor is shorted out for 50 c/s operation.

(c) 400 c/s Narrow Band Amplifier Fig. (4.10)

The output from the crystal detector is fed into the narrow band amplifier through a 1:10 transformer designed to match the nominal 350 ohm output impedance of the crystal to the input of the amplifier.

The amplifier is direct coupled, to reduce any possible phase shifts during amplification, and combines a high gain (of order 5×10^4) with a narrow band width (less than 15 c/s) at 400 c/s.. This band width is achieved by employing negative feedback in conjunction with a twin 'T' filter which acts as a rejector circuit for 400 c/s. The gain of the amplifier is therefore low for all frequencies but 400 c/s.. The negative feedback is variable and can be reduced to zero for wide band operation. A small positive feedback is provided at all frequencies and the output is from a cathode follower stage.

(d) 400 c/s Phase-Sensitive-Detector Fig. (4.11)

The phase-sensitive-detector is a modified form of Schuster's

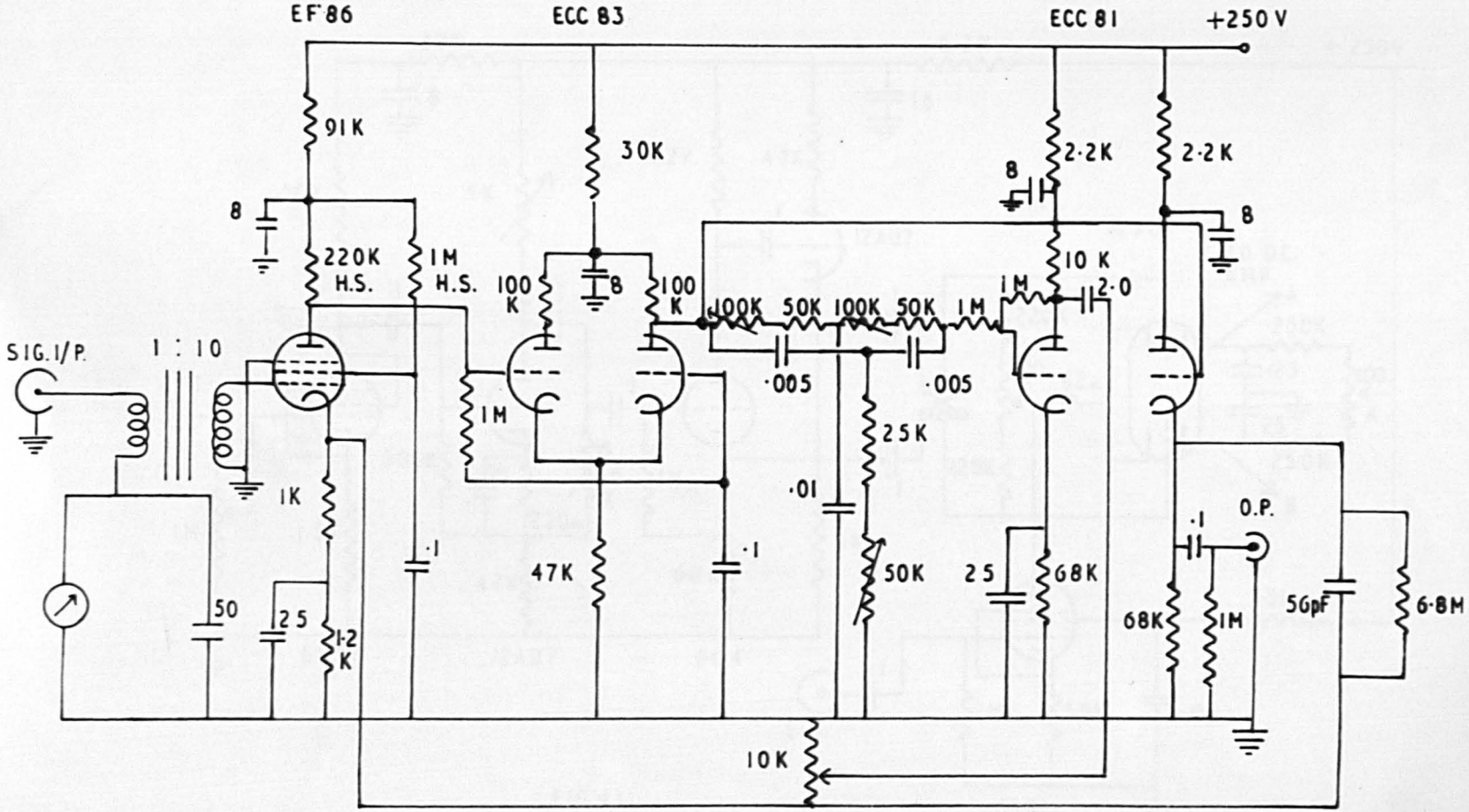

FIG. 4.10
400 C/S. NARROW BAND AMPLIFIER

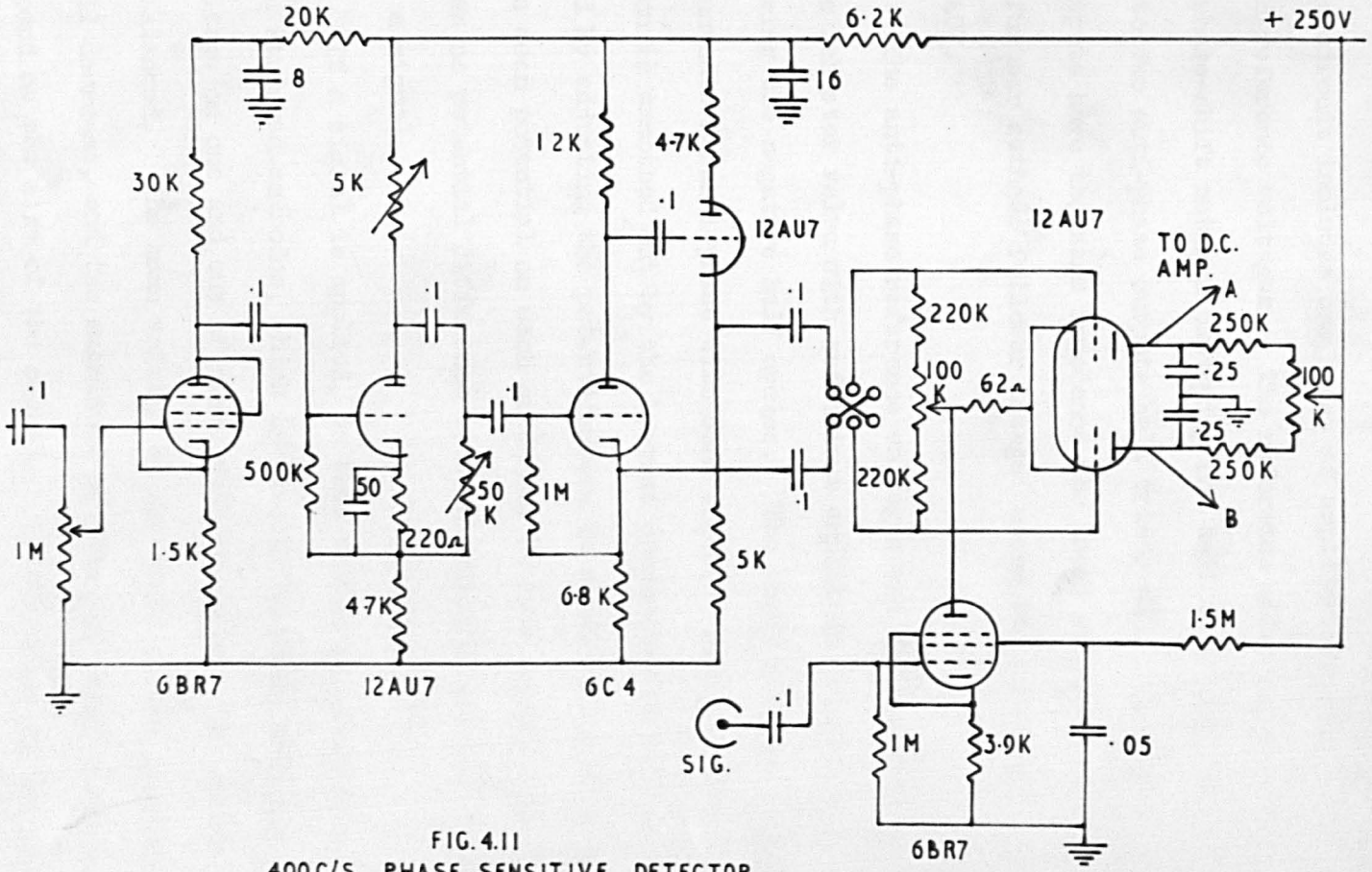

FIG. 4.11
400 C/S. PHASE SENSITIVE DETECTOR

circuit using a double triode 12AU7. Apart from this valve, the circuit includes one stage of amplification for both signal and reference voltages. The reference phase can be varied in a phase-shift network employing one half of a 12AU7 and is split into two anti-phase outputs by a triode 6C4. In order that both outputs have the same impedance the anode output is taken through a further cathode follower stage using the other half of the 12AU7.

The anti-phase reference voltages are fed onto the grids of the Schuster valve with sufficient amplitude to bias each valve off during the negative half cycles. The anode voltages therefore fluctuate in anti-phase with each other. However, this fluctuation is smoothed out by the by-pass condensers on each anode, and by adjusting the potentiometers in anode and grid circuits, the mean potential on each anode may be made equal. There is then no potential difference between points A and B in the absence of a signal.

If a signal is applied, to both valves simultaneously through the strapped cathodes, which is exactly in phase with the grid voltage on one and out of phase with the other, the system is unbalanced. The mean voltage on the anode of the in-phase valve will decrease, and the magnitude of this potential difference will depend on the size of the signal. If the phase of the signal is reversed, the size of the potential difference is also reversed.

The electron resonance signal therefore emerges as a slowly varying potential difference between the points A and B, and is passed through a variable time constant circuit to a d.c. amplifier. The gain of this amplifier is made sufficient to operate the pen recording ammeter on which the resonance absorption is traced.

(e) D.C. Amplifier Fig. (4.12)

The d.c. amplifier uses two stages of amplification with a cathode follower output to the recording ammeter which has a range of 0 - 5 milliamps and a resistance of 350 Ω . A jack plug socket is so arranged that when the ammeter is disconnected a 350 Ω resistance replaces it across the output. In series with the recording ammeter is a centre zero microammeter, with variable shunt, which is used when balancing the amplifier. In general the gain of the d.c. amplifier is kept fixed and the magnitude of the output signal controlled by an attenuator between narrow band amplifier and phase-sensitive-detector.

4.3. Experimental Techniques

4.3.1. Measurement of Magnetic Field Strength

The magnetic field strength is measured by a proton resonance meter. The protons are those present in a water sample to which a paramagnetic salt has been added in order to reduce the spin-lattice relaxation time and prevent saturation. This is con-

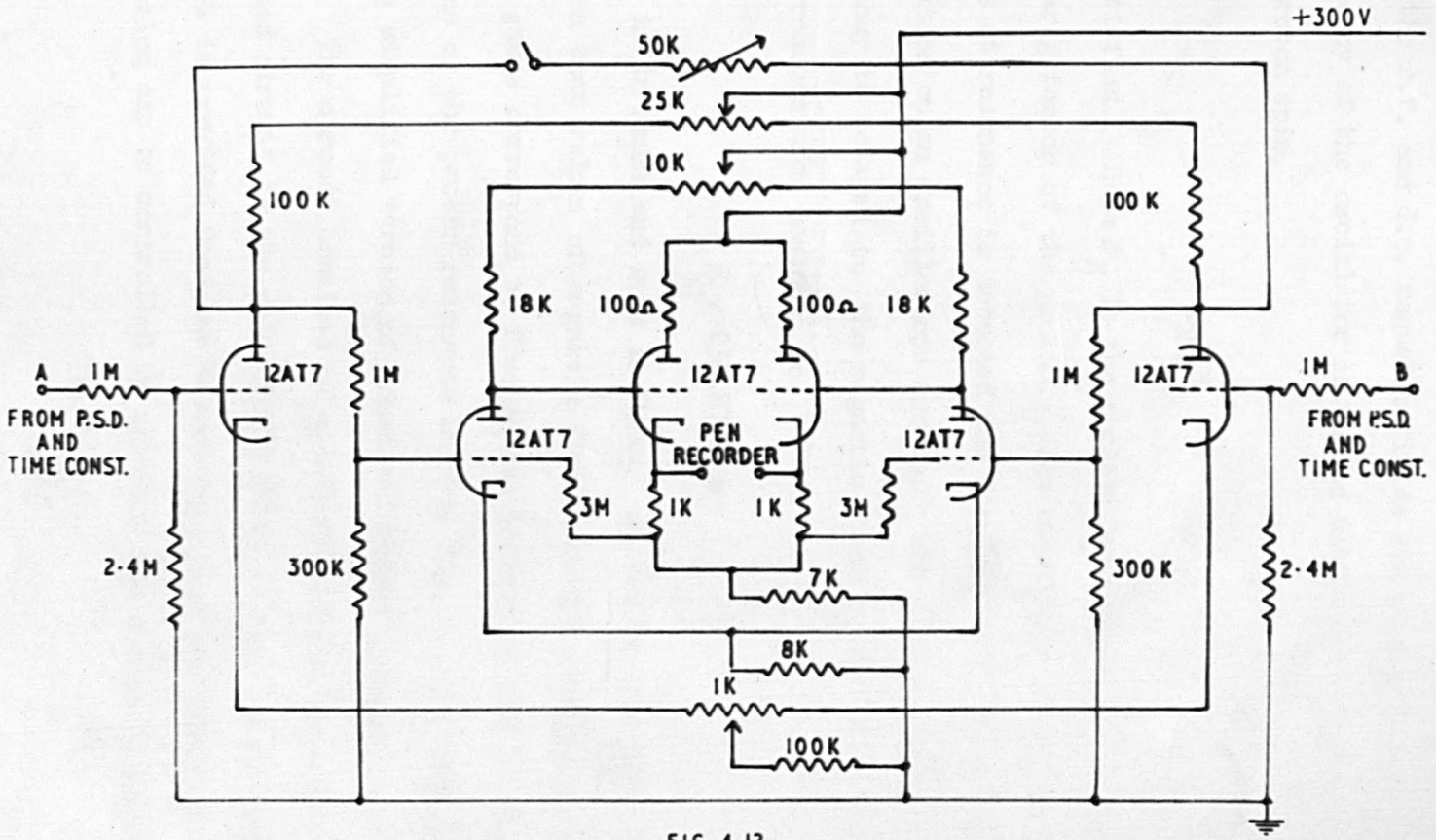

FIG. 4.12.
D.C. AMPLIFIER

tained in a small coil which forms part of the tuned circuit of a marginal radio-frequency oscillator. The coil is oriented so that the r.f. and d.c. magnetic fields are perpendicular and the frequency of the oscillator is varied until the resonance condition for proton spin,

$$h = g_I \beta_N H$$

is satisfied. Here β_N is the nuclear Bohr magneton and g_I is the nuclear g factor of the proton. The absorption of energy which occurs at resonance is detected and displayed with 50 c/s field modulation on an oscilloscope screen. The proton resonance frequency is related to the magnetic field by the above equation which reduces, for protons, to

$$H = 234.87 \times \nu$$

where H is in gauss and ν is in Mc/s. It can be seen from this equation that values of magnetic field strength from 2,000 to 20,000 gauss correspond to frequencies between 10 and 100 Mc/s..

One of the proton resonance meters, Fig. (4.13), used is, in fact, a simplified version of Pound and Knight's n.m.r. spectrometer. The circuit consists of a cathode coupled amplifier with the tuned circuit in the grid of the first valve. A positive feedback is provided from the second anode and the level of oscillation can be controlled by altering the amount of negative

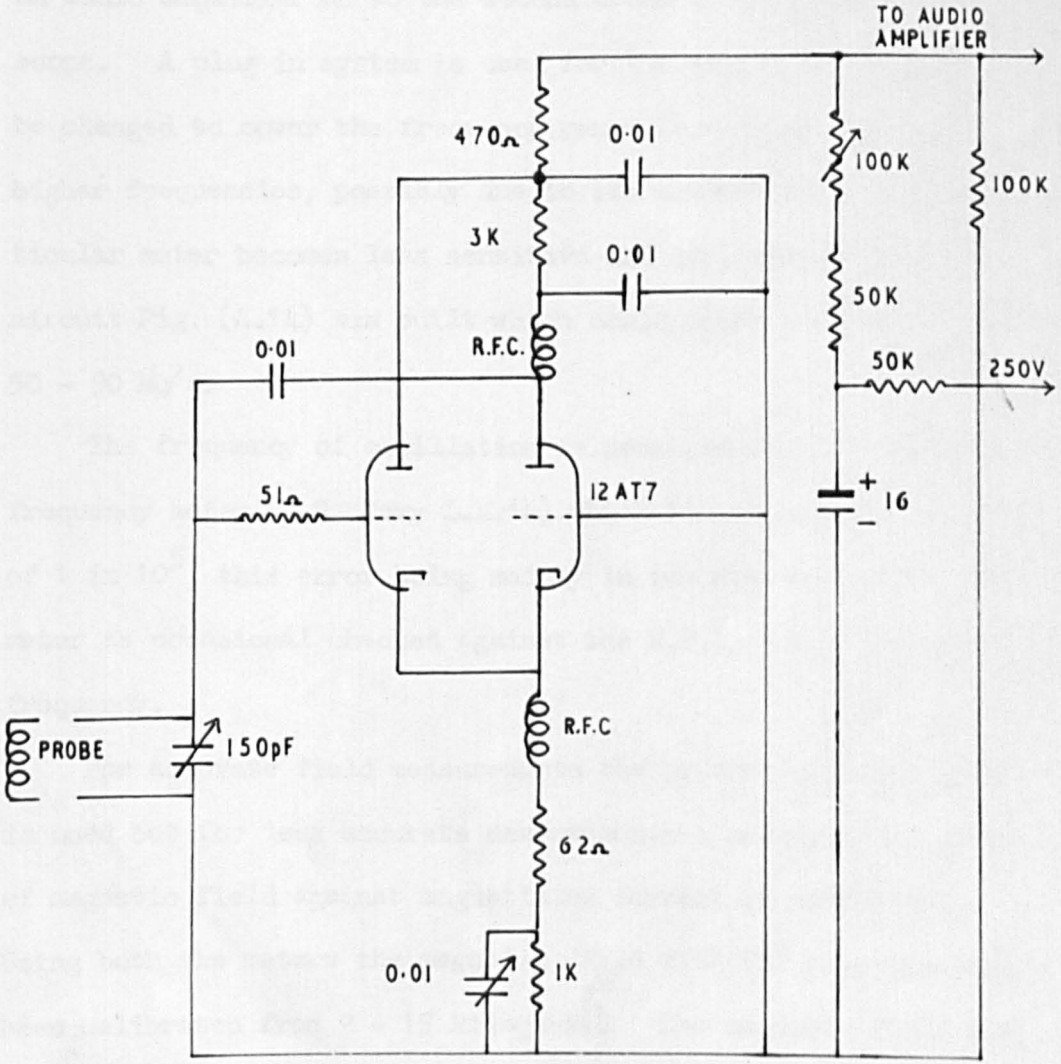
TO AUDIO AMPLIFIER
470Ω
0·01
100K
100K
3K
0·01
50K
0·01
R.F.C.
50K
250V
51Ω
12AT7
16
PROBE
150pF
R.F.C
62Ω
0·01
1K

FIG. 4.13

feedback in the common cathode lead. The absorption of energy at resonance is detected by means of the change in voltage across the resistor in the H.T. lead, and this voltage is passed through an audio amplifier on to the second trace of a double beam oscilloscope. A plug in system is used for the sample coils which can be changed to cover the frequency range 10 - 60 Mc/s.. At the higher frequencies, possibly due to its construction, this particular meter becomes less sensitive and one using a Hopkins circuit Fig. (4.14) was built which could cover the range 50 - 90 Mc/s.

The frequency of oscillation is measured with a hetrodyne frequency meter (U.S. Navy L.M.14) which has an overall accuracy of 1 in 10^5, this error being mainly in reading the dial. The meter is occasional checked against the N.P.L. 5 Mc/s standard frequency.

For accurate field measurements the proton resonance meter is used but for less accurate measurements a calibration curve of magnetic field against magnetizing current is sufficient. Using both the meters the magnetic field with 60° pole tips has been calibrated from 2 - 15 kilogauss. The magnetic field was taken through a complete cycle before each measurement to avoid the hysteresis effects and was set only from one direction which was chosen to be with current increasing. The calibration showed the field to be far from saturation even at 15 kilogauss.

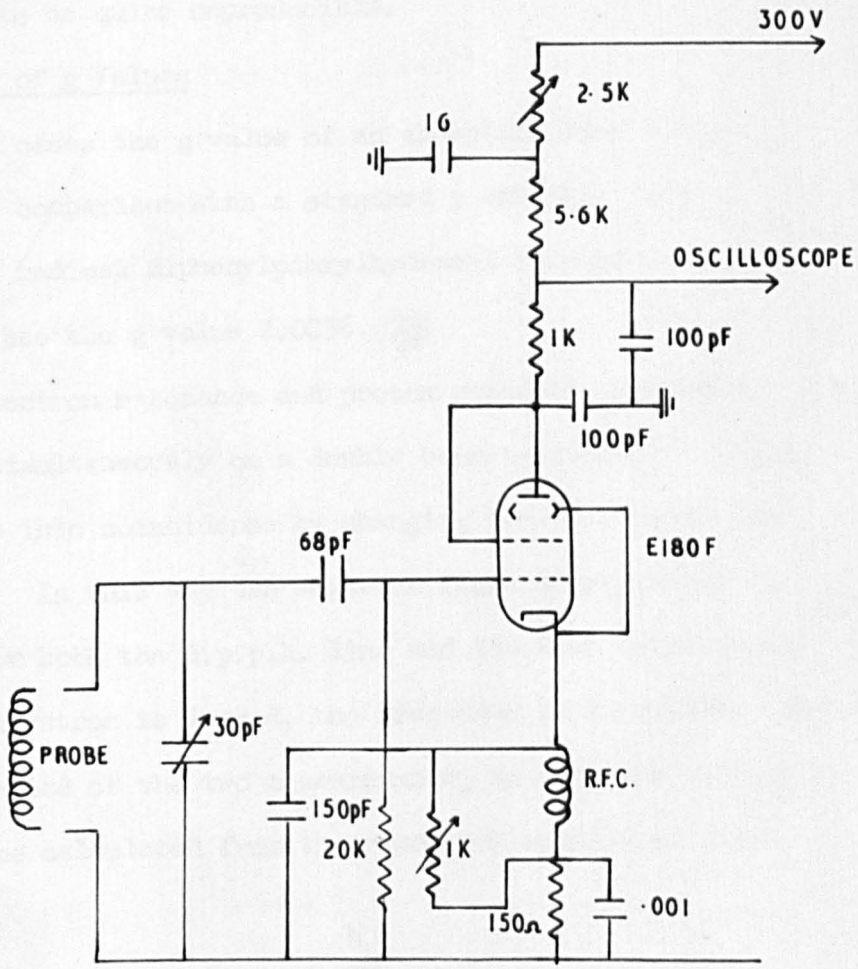
300V
2·5K
1G
5·6K
OSCILLOSCOPE
1K
100pF
100pF
68pF
E180F
PROBE
30pF
R.F.C.
150pF
20K
1K
150Ω
·001

FIG. 4.14

When using the curve, all current readings have to be taken with the field increasing after a full cycle. The pole pieces were not disturbed once the calibration was made and the curve has proved to be quite reproducible.

4.3.2. Measurement of g Values

In all cases the g value of an abosption line has been measured by comparison with a standard g marker. This is the stable free radical diphenylpicrylhydrazyl (d.p.p.h.) which in the powder has the g value 2.0036.

The electron resonance and proton resonance absorptions are displayed simultaneously on a double beam oscilloscope screen and brought into coincidence by changing the r.f. oscillator frequency. In this way the magnetic field at resonance is measured for both the d.p.p.h. line and the line under study. Since the klystron is locked, the frequency is accurately constant over the period of the two measurements, so that the unknown g value can be calculated from the resonance conditions which reduce to

$$g_x = g_h \frac{H_h}{H_x}$$

where the subscript (h) denotes the values for d.p.p.h. and the subscript (x) the sample.

In these measurements care is taken to position the proton sample as close as possible to the electron resonance cavity in

order to minimise any errors caused by difference in field at the two positions.

4.3.3. Measurement of Line Widths

Two methods have been used to measure line widths of the myoglobin crystals. With wide lines it is often sufficiently accurate to mark magnet current readings on the recorder chart and translate these into field values using the magnet calibration chart.

The magnetic field is swept slowly through resonance whilst the magnetizing current is measured on an accurate diagonal scale ammeter. Precise readings can be made every 0.05 amps (roughly 50 gauss) and markers are put on the recorder chart by a 1.5 volt dry battery connected across the meter and operated with a bell-push. Examination of the marker spacings enables the linearity of the sweep to be checked and interpolation between the markers can then give the actual line width.

Whenever necessary the accuracy of line width measurement can be increased by using proton resonance calibrated markers. This involves the use of a communications receiver which has crystal controlled check points at 100 kc/s intervals. The frequency of the proton resonance meter is set by beating it with one of these check frequencies, whilst the magnetic field is increasing. As the field passes slowly through the proton resonance value, the absorption signal crosses the oscilloscope screen and a mark is put on the recorder chart with the bell-push.

The proton resonance meter is then turned to the next highest check frequency and a further mark is made at resonance. The electron resonance line is thus calibrated by a series of marker lines corresponding to accurately known proton resonance frequencies. The line width can be measured this way in terms of proton resonance frequency over the whole range of field values 2 - 15 kilogauss.

4.3.4. Measurements on Broad lines

In all the measurements on very broad lines, the greatest source of error lies in determining, precisely, the positions of the centres and the peaks of the derivation curves. In general the area under the curve will remain constant as the line width changes with direction through the crystal. Therefore it can happen that the peak height will be very reduced in the broad line and the signal-to-noise ratio made low. A faster sweep makes the peak sharper but the field markers become less frequent or less accurate in proportion. Working at liquid hydrogen temperature ensures the maximum signal intensity for the broadest lines but the results in many cases have to be the average of several measurements.

The estimated error in the line width measurements was as follows:-

For lines of width 0 - 150 gauss about 5%
150 - 600 gauss about 10%
600 and over about 15%.

The accuracy with which the g value of a line can be

measured also depends on its width. Using crystal video detection on lines more than 50 gauss wide the g value cannot be measured with less than 0.75% error. Using proton resonance markers on the pen chart this error can be reduced to about 0.2%.

REFERENCES

(1) J. Roch, Académie des Sciences, Feb. 1959.

(2) D. J. Ingram, Radio Frequency Spectroscopy, Butterworth.

(3) J. Goldberg, Electronic Engineering, Dec. 1959, p. 732.

(4) M. W. P. Strandberg, Rev. Sci. Inst. 25, 1954, pp. 776-792.

(5) B. Bleaney, J. H. H. Loubser & R. P. Penrose, Proc. Phys. Soc. A59, 1947, p. 185.

(6) R. V. Pound & W. D. Knight, Rev. Sci. Inst. 21, 1950, p. 219.

(7) N. J. Hopkirs, Rev. Sci. Inst. 20, 1949, p. 401.

Chapter 5

Myoglobin - Its Structure and Properties

5.1. Haemoproteins

The haemo-proteins are so called because they each consist of a globular protein molecule containing one or more haem prosthetic groups. The structure of this group varies only slightly from one haemo-protein to another and consists basically of a tetrapyrrolic ring (porphin) surrounding an iron atom Fig. (5.1). The protein molecules, however, vary considerably in molecular weight and also in amino-acid composition.

Myoglobin is of particular interest because it is one of the smallest protein molecules and is closely related to the blood pigment haemoglobin. Because of its size it was chosen by Kendrew for the first detailed X-ray analysis of a protein. It is contained within the cells of the tissues and its function is to combine reversibly with oxygen, brought by the haemoglobin in the blood, storing it until it is required. As might be expected the tissues of diving mammals contain a particularly large proportion of myoglobin. The myoglobin studied by Kendrew and that used in this work was in fact that of the Sperm Whale. X-ray measurements however indicate that the myoglobin molecules obtained from different species are, apart from minor differences in amino acid composition, more or less the same. Conclusions drawn from the study of any one, therefore, may be applied to the

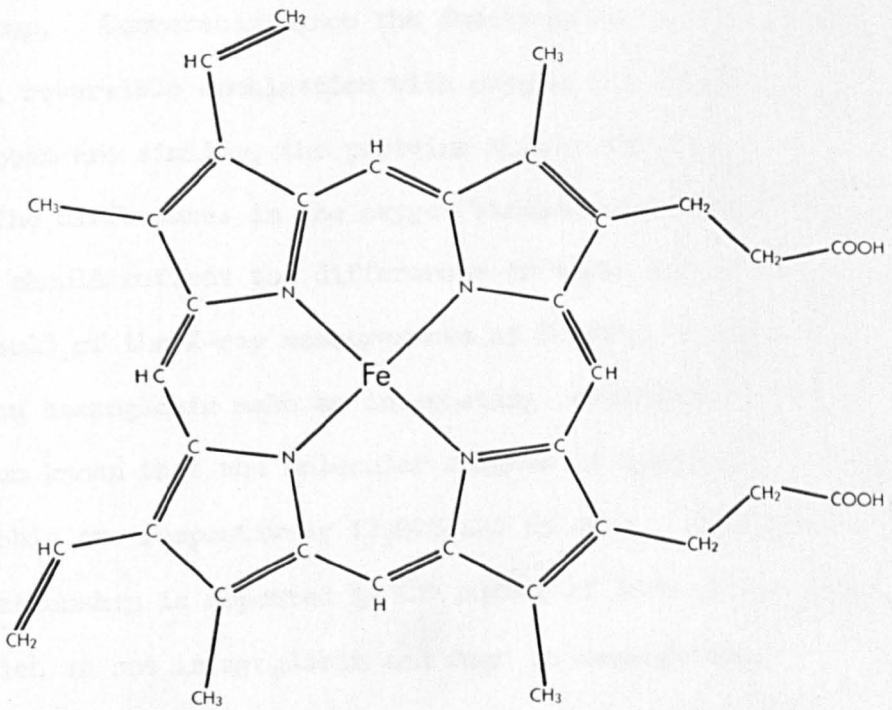

FIG.5.1
CHEMICAL FORMULA OF HAEM GROUP

elucidation of the structure of the other.

Since the haem group is basically the same in each haemoprotein it must be the protein which modifies the function of the haem group. Conversely since the functions of the haem groups, i.e. reversible combination with oxygen, in myoglobin and haemoglobin are similar, the proteins should also be similar. The differences in the oxygen binding characteristics of the two, should reflect the differences in their structure.

The result of the X-ray measurements of Kendrew on myoglobin and Perutz on haemoglobin make an interesting comparison. It has long been known that the molecular weights of myoglobin and haemoglobin are respectively 17,000 and 65,000. This one to four relationship is repeated in the number of haem groups per molecule which is one in myoglobin and four in haemoglobin. These facts, considered with the similar functions of the two proteins strongly suggest that one molecule of haemoglobin could be made up of four subunits, each one similar to a myoglobin molecule. Foetal haemoglobin with a molecular weight of 34,000 seems to consist of two of these subunits. X-ray measurements show that the haemoglobin molecule is in fact made up of four polypeptide chains in two sets of identical pairs, whilst the myoglobin molecule has only one. Models of the myoglobin molecule and of the subunits of the haemoglobin molecule, at 5.5A resolution, do show a remarkable similarity. It is there-

fore surprising that the amino acid sequences of the polypeptide chains should be found to be different. The exact way in which the characteristic tertiary structure of these proteins arises, is not fully understood. However it is certain that the haem group plays an important part in providing the nucleus, as it were, around which the globin chain is folded.

The structure of myoglobin has been determined at 2A resolution and where possible the amino acid sequence has been fitted to the three dimensional electron density distribution. The model which resulted Fig. (5.2) shows clearly the course of the polypeptide chain, the position of the haem group and how it is bonded to the rest of the protein molecule.

5.2. The Iron Atom

The principal bond between the haem group and the protein is that between the iron atom and a nitrogen atom in a histidine ring side chain. Chemical evidence had suggested that this might be so, some years before the X-ray results. There are no other strong bonds to the protein. Hydrogen bonds link the proprionic acid groups of the haem to side chains extending from the polypeptide chains on either side of the haem group. Elsewhere the haem group rests at the Van der Waals distance from various atoms in the protein molecule. The haem group is in this type of contact with about 90 different atoms in the protein.

The sixth coordination site is the one which combines

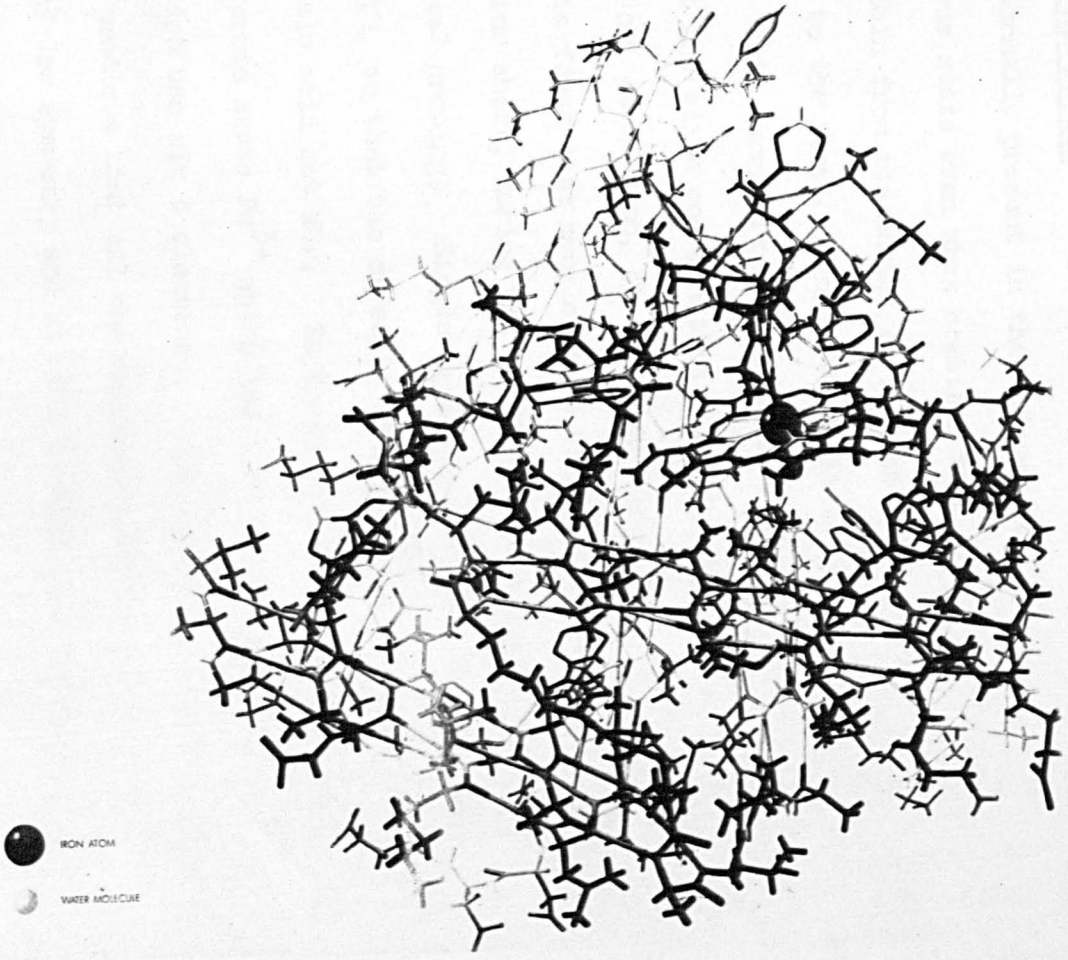

FIG. 5.2

reversibly with molecular oxygen. In the absence of oxygen the site can be occupied by various other molecules usually water.

5.2.1. State of the Fe ion

As normally present in the body myoglobin contains iron in the ferrous state even when combined with oxygen. On removal of myoglobin from its normal environment, the iron atom is easily oxidised to the ferric form in which it no longer combines with oxygen. This ferric form is known as ferri- or metmyoglobin, and in it the sixth coordination point is taken up by a water molecule or, at high pH, by a hydroxyl group.

It is found that myoglobin is converted to metmyoglobin, met Mb. ior short, during the purification processes necessary for crystal growing. Single crystals are found to grow best at acid pH, so that the crystals studied so far have been of sperm whale acid met Mb.. In these crystals the iron atom is in the ferric state Fe^{3+} which has five d electrons, whilst the ferrous ion has six d electrons. Application of Kramers theorem to Fe^{2+} predicts that all the degeneracy will be removed by fields of low symmetry and it will be difficult to observe electron resonance.

It was shown in Chapter 2 that a $3d^5$ complex can have a spin value of either 5/2 or 1/2 with possibly an intermediate configuration of spin 3/2. These configurations correspond to 5, 1 and 3 unpaired electrons respectively. From magnetic susceptibility measurements on the various complexes it is

possible to estimate the number of unpaired electrons on the iron atom in each.

5.2.2. Susceptibility Measurements

The results of measurements of paramagnetic susceptibility are usually represented by Curie's formula,

$$x = \frac{N\mu^2}{3kT} \qquad 5.1$$

where N is the number of magnetic ions per unit volume and μ denotes the absolute magnitude of the magnetic dipole moment, Thus

$$\mu = \mu_B \cdot \beta \qquad 5.2$$

where μ_B is the magnetic moment measured in Bohr magnetons or the "number of Bohr magnetons". When the magnetic moment comes from the parallel coupling of spins of n electrons,

$$\mu_B = \sqrt{n(n+2)} \qquad 5.3$$

The usual procedure used in the analysis of x is to measure x at a certain temperature T. From this result the value of μ is found and then from (2) a value of μ_B. An integer n is then chosen, which can give μ_B most closely which is then taken to be the number of unpaired electrons.

These arguments hold only on condition that the magnetic moment due to the orbital motion of electrons has been completely quenched and that the spin of the electrons is completely free.

If these conditions are satisfied the number of Bohr magnetons for 1, 2, 3 etc. electrons are, using (3)

No. of electrons:	0,	1,	2,	3,	4,	5.
μ_B:	0,	1.73,	2.83,	3.87,	4.90,	5.92.

Departures from these values indicate that the above conditions have not been satisfied and are usually interpreted in terms of orbital contribution.

A great deal of work has been done on the susceptibilities of haemoproteins since the first precise measurements by Pauling and Coryell [1] in 1936. Much of the work up to 1946 has been reviewed by Hartree [2]. These measurements showed that haemoproteins could be expected to have values of magnetic moment roughly equal to one of the following:-

$$\mu_B = 5.80;\ 5.43;\ 4.47;\ 2.84$$

which are for acid methaemoglobin (acid met Hb), ferro Hb, alkaline met Hb, and met Hb azide, respectively. The first of these indicates the presence of five unpaired electrons with an orbital contribution of 0.12. The others however differ considerably from the values to be expected from the possible numbers of spins. The results have been taken to indicate the presence of 4, 3 and 1 unpaired electrons respectively.

In explaining the measured values, Pauling rejected the idea of large orbital contributions and attributed both high

and low values to a magnetic interaction between the four haem groups in the molecule. Measurements then followed on myoglobin which showed μ_B for acid met and ferro Mb to be 5.85 and 5.46 respectively. Since the molecules were in solution there could be no interaction between the haem groups in myoglobin. The similar results from haemoglobin and myoglobin therefore indicated that there was little magnetic interaction between the haem groups in haemoglobin and that departure from the spin only values, must be due to a large orbital contribution in these particular derivatives.

It must be mentioned here, however, that an interaction between the haem groups in haemoglobin is indicated by the shape of the oxygen dissociation curve, which is a plot of the percentage of oxy Hb against the partial pressure of oxygen. The slope of this curve increases with the partial pressure of oxygen, until about 60% is converted to oxy Hb. This means that the oxygen affinity of haemoglobin, up to this point, is dependent on the percentage of oxy Hb present. Interpreted in terms of one molecule this implies that the oxygen affinity of any one haem group is influenced by the state of oxygenation of the other three. The curve for myoglobin is quite different, very low partial pressures of oxygen resulting in a high percentage of oxy Mb, and no interaction is indicated. Since the interaction in haemoglobin is not magnetic its actual nature remains unknown.

The suggestion by Pauling that the magnetic moment (μ_B = 4.47) of alkaline met Hb indicates a spin of 3/2 has been questioned by Griffith [3]. His calculations suggest that if there is one compound with S = 3/2, there can be none with S = 5/2 or that there cannot be complexes with all three kinds of spin. The magnetic moment in the alkaline met Hb might therefore be due to a thermal equilibrium between molecules with S = 5/2 and S = 1/2. This could be tested experimentally by measuring the temperature variation of the magnetic susceptibility or by electron resonance. There has been little success with the latter, however, due to the difficulty of converting large enough crystals to the alkaline form.

Table 1

derivative (group attached to Fe at 6th coordination point)	form	no. of unpaired electrons
	acid met	
H_2O		5
F		
CN		1
N_3		
iminazole		
SH		
NH_3		
	reduced	
H_2O		4
O_2		0
CO		
CN		

Besides those derivatives already mentioned, several others have been studied; the high and low spin complexes are listed in Table 1 above.

5.3. Electron Resonance Measurements

No attempt will be made, in this section, to exhaustively survey all the work which has been done on the haemoproteins using electron resonance techniques. Only two examples are considered which are typical of the results from high spin and low spin complexes. These results are discussed only in connection with the information they can give on the state of the Fe^{3+} ion. The structural information obtained at the same time will be discussed later in the chapter.

5.3.1. Acid Metmyoglobin

Susceptibility measurements indicate that in this form, the iron atom has five unpaired electrons and that the orbital contribution to magnetic moment is not large. The d shell is thus exactly half filled giving a $^6S_{5/2}$ ground state. The splitting of this ground state in Mn^{2+} has been described in the section on S state ions, Chapter 2, and the same type of splitting has been observed in high spin ferric ions. No hyperfine structure is observed since the most abundant isotope of iron has zero nuclear magnetic moment.

The orbital singlet ground state, of the iron atom in acid met Mb, might therefore be expected to be split into three

Kramers doublets separated by roughly 0.2 cm^{-1}. The electron resonance spectrum should then consist of five lines centred on the free spin value of g = 2.

In fact only one transition is observed [4]. The electron resonance spectrum from single crystals of acid met Mb [5] consists of two lines, one from each of the differently oriented haem groups in the unit cell, whose g value varies from 2 to 6. The value of g = 2 occurs when the magnetic field is parallel to the crystalline electric field, which is assumed to be perpendicular to the haem plane. Thus $g_{\parallel} = 2$ whilst the g value in the haem plane is found to be approximately isotropic, $g_{\perp} = 6$. This same g value variation is found in all types of acid met Mb and Hb.

It is immediately apparent from the electron resonance spectrum that the splitting between the three Kramers doublets must be very much greater than that found in most ferric complexes. If the splitting is much greater than the microwave quanta ($h\nu$), a single resonance from the lowest lying doublet, assumed to be $S_z = \pm \frac{1}{2}$ as in Mn^{2+}, will be observed. The result has been considered by Griffith [3] and more recently Kotani [6]. Calculations show that a splitting of at least 10 cm^{-1} between the Kramers doublets is required to explain a value of $g_{\perp} = 5.90$.

A variation from $g_{\parallel} = 2$ to $g_{\perp} = 6$ can be explained simply provided that the splitting between the three Kramers doublets is very much larger than that between the two spin levels of the

lowest doublet.

When the magnetic field is parallel to the axis of quantization or z axis, the Hamiltonian reduces to the form

$$\mathcal{H} = g_o \beta H_z S_z \qquad 5.4$$

where $g_o \beta S_z$ is the component of the electronic magnetic moment in the z direction and therefore $g_o = 2$.

The operation of the spin on the $\pm \frac{1}{2}$ states gives

$$\mathcal{H} \left| \tfrac{1}{2} \right\rangle = \tfrac{1}{2} g_o \beta H_z \left| \tfrac{1}{2} \right\rangle$$

$$\mathcal{H} \left| -\tfrac{1}{2} \right\rangle = -\tfrac{1}{2} g_o \beta H_z \left| -\tfrac{1}{2} \right\rangle$$

and hence the difference in energy between the $+\frac{1}{2}$ and $-\frac{1}{2}$ states is $g_o \beta H_z$. The results of the electron resonance measurements are written in the form of a spin Hamiltonian

$$\mathcal{H} = g_{\parallel} \beta H_z \qquad 5.5$$

so that by comparison

$$g_{\parallel} = g_o = 2.$$

When the magnetic field is perpendicular to the z direction the Hamiltonian has the form

$$\mathcal{H} = g_o \beta H_x S_x \quad . \qquad 5.6$$

S_x is expressed more conveniently in terms of the "step up" and "step down" operators as $\frac{1}{2}(S_+ + S_-)$ where

$$S_{\pm} = \left\{ S(S+1) - M_S(M_S \pm 1) \right\}^{\frac{1}{2}}$$

No interaction with the higher spin states is included so that with $S = 5/2$ and $M_s = \pm \frac{1}{2}$ the matrix elements are,

$$\mathcal{H}\,|\tfrac{1}{2}\rangle = g_o\beta H_x \tfrac{3}{2}|-\tfrac{1}{2}\rangle$$

$$\mathcal{H}\,|-\tfrac{1}{2}\rangle = g_o\beta H_x \tfrac{3}{2}|+\tfrac{1}{2}\rangle$$

and the matrix is therefore

	$\lvert\frac{1}{2}\rangle$	$\lvert-\frac{1}{2}\rangle$
$\lvert\frac{1}{2}\rangle$	0	$\frac{3}{2}\,g_o\beta H_x$
$\lvert-\frac{1}{2}\rangle$	$\frac{3}{2}\,g_o\beta H_x$	0

The eigenvalues are the roots $E_1 E_2$ of the secular equation

$$\det.(H - EI) = 0$$

where H is the determinant and I the unit matrix of the same order.

Therefore

$$E = \pm \tfrac{3}{2}\, g_o\beta H_x$$

and the energy difference between the spin levels is now

$$E_1 - E_2 = 3g_o\beta H_x$$

which is expressed in the spin Hamiltonian as $g_\perp \beta H_x$.

Thus

$$g_\perp = 3g_o = 6.$$

Any departure from this value of 6 will indicate the

extent to which the assumption that there is no interaction with the higher spin states holds for a particular complex. Thus taking $g_{\perp} = 5.90$ Griffith obtained a lower limit of 10 cm^{-1} to the size of the zero field splitting. An upper limit to this parameter has been provided by susceptibility measurements made on single crystals of acid met Mb [7]. The magnetic anisotropy in the ab plane of the crystal was measured at temperatures from 90°K to room temperatures. A measurable anisotropy was observed below 150°K increasing rapidly as the temperature was lowered. This was compared with theoretical curves calculated for various values of D. The experimental values lay between D = 2.5 and 5.0 cm^{-1} and an upper limit was set at 7.5 cm^{-1}, which corresponds to a splitting between the Kramers doublets of 15 cm^{-1}.

The origin of this large zero field splitting is as yet unexplained but a few possibilities have been put forward by Griffith.

The splitting may be due to admixture of excited states with S = 5/2, in particular $3d^4 4s$ and $3d^4 4p$, by the crystalline field and spin orbit coupling. Alternatively it may be due to bonding d_{yz} and d_{zx} orbitals being partially delocalized into the empty π-orbitals on the porphyrin ring system.

5.3.2. Acid met Mb azide derivative

Susceptibility measurements have indicated that this is a 'low spin' complex. The five d electrons must all be in the t_{2g} orbitals which suggests a large value of Δ. The orbital degeneracy is thus reduced from 5 to 3 making the effective orbital moment $L' = 1$. The total degeneracy of the ground state is therefore six, and this should be split by the crystalline field into a quartet and a doublet. Electron resonance transitions should be observed from this lowest doublet giving a single line with g factors spread across the free spin value.

The experimental results [8] agree with these predictions and from the g values obtained Griffith [9] has been able to deduce the splittings between the t_{2g} levels and their order. A full account of these measurements is reserved until it can be given in conjunction with a discussion of the present work.

5.4. Crystal Structure

Sperm whale myoglobin is found to crystallize readily in either of two forms [10] depending on the salting out process. From ammonium sulphate solution the crystals are monoclinic and known as Type A, whilst from concentrated phosphate buffer they are orthorhombic and known as Type B. The crystals which have

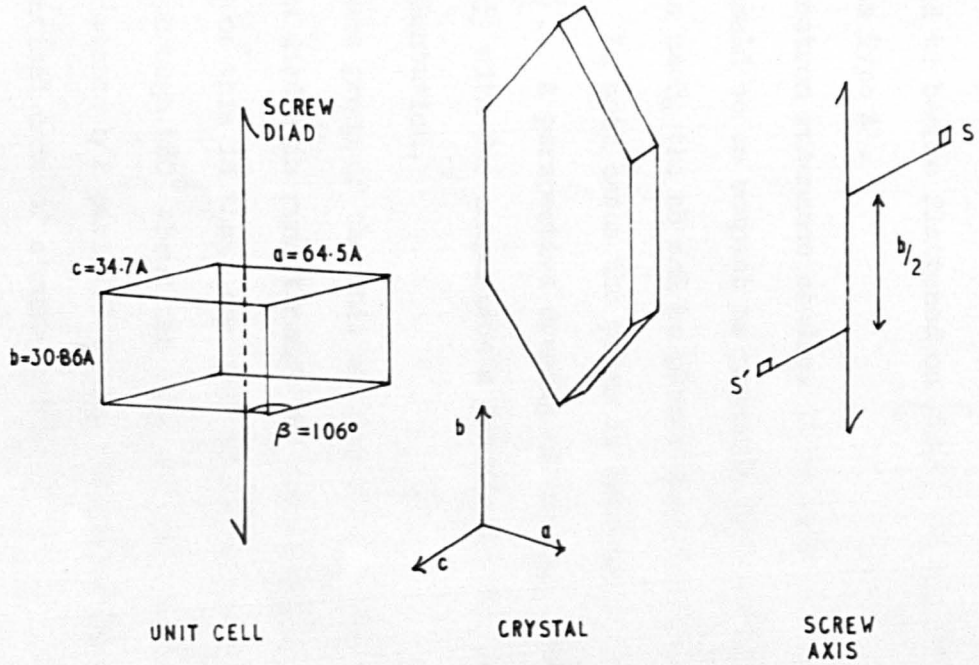

FIG. 5.3

TYPE A SPERM WHALE
ACID MET MYOGLOBIN

been studied in most detail are Type A and it was crystals of this type which were used in the present work.

These crystals normally form flattened four-sided prisms whose axis is b: at pH values below 7 they are flattened on $\{001\}$, that is to say in the ab plane, but if grown at higher pH they tend to become flattened on $\{100\}$ or the bc plane and are known as Type A'.

For electron resonance studies it is better that the crystal should be as compact as possible for its volume and in the crystals used, the ab and bc planes were almost equally developed. In both cases the prism is terminated by dome faces $\{110\}$. A perspective drawing of the unit cell is given in Fig. (5.3) with for comparison a drawing of the crystal in the same orientation.

The space group of the unit cell is $P2_1$. This implies that a screw diad axis runs through the cell parallel to b. The meaning of this is that, any unit of structure S Fig. (5.3) if rotated through 180° about the axis and then translated through a distance b/2 parallel to it, must come into coincidence with an identical unit of structure S'.

The X-ray analysis of the three dimensional structure of myoglobin has so far been completed at a resolution of 2A. This is too coarse to resolve individual atoms but sufficient to show the haem group, the configuration of most of the polypeptide chain

and the shape of the majority of side chains.

Figure (5.4) shows two sections through the three dimensional electron density distribution of the haem group, one parallel and the other perpendicular to the haem plane. The known chemical structure is superimposed upon these patterns and by careful fitting, the positions of the various atoms have been estimated. The position of the iron atom is fixed to within $\frac{1}{4}$A and of the other atoms to within $\frac{1}{3}$A.

The coordinates of the positions of the atoms in the haem group, the histidine ring and water molecule are listed in Table (2) as supplied by the M.R.C. Molecular Biology Unit, Cambridge. These coordinates are given as fractions of the unit cell edges. The dimensions of the unit cell and the monoclinic angle β are also given in this table. The distance between two atoms in a monoclinic unit cell is given by the relation

$$d^2 = a^2\Delta x^2 + b^2\Delta y^2 + c^2\Delta z^2 + 2ac\Delta x\Delta z \cos\beta$$

where the coordinates of the two atoms $(x, y, z)(x', y', z')$ are such that $x' - x = \Delta x$ etc.

From the coordinates of the iron atom (I) given in Table (2) it is possible to calculate the coordinates of all other iron atoms in the crystal and hence the distance of the nearest neighbour iron atoms. For example if the coordinates of the

Table 2

atom	x	y	z	
Haem section				
iron (I)	24.05	43.76	6.93	
nitrogen	23.59	41.64	8.85	
"	23.69	41.45	4.95	
"	25.30	45.58	5.21	
"	25.19	45.77	9.12	
Histidine				
nitrogen	18.38	46.09	6.96	
carbon (1)	20.33	45.60	7.80	
nitrogen	21.12	44.72	6.45	to iron
carbon (2)	19.61	44.67	4.75	
carbon	17.87	45.53	5.04	
Water Molecule				
oxygen	27.00	41.75	7.00	(accuracy doubtful)

x is in 96^{ths} of unit cell edge a

y is in 48^{ths} of " " " b

z is in 48^{ths} of " " " c

Unit cell dimensions

a = 64.5A, b = 30.86A, c = 34.7A, $\beta = 106^{\circ}$.

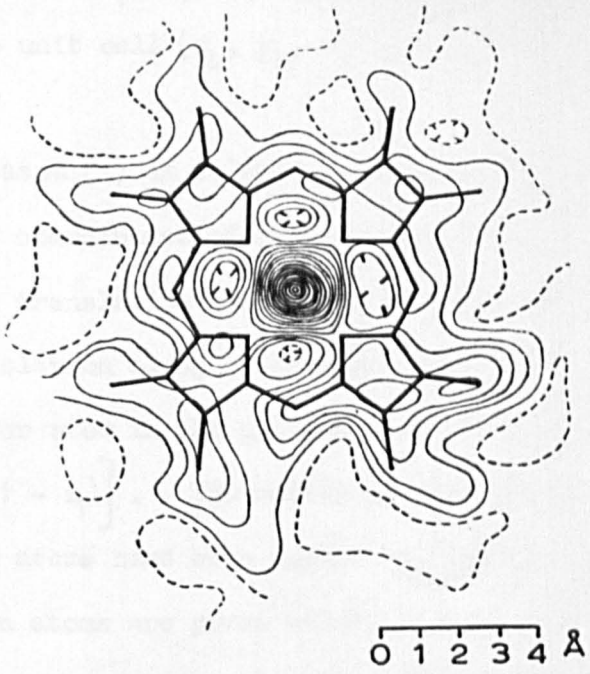

FIG. 5.4
CROSS SECTIONS THROUGH
HAEM GROUP

iron atom in Table (2) are (x_1, y_1, z_1) the coordinates of the other iron atom in the unit cell (x_4, y_4, z_4) can be calculated in the following way.

In Figure (5.5), atom (1) is related to atom (2) by the screw axis so that the coordinates of (2) are $(-x_1, \frac{1}{2} + y_1, -z_1)$. Atom (2) is related by translation along a to atom (3) and atom (3) is related by translation along c to atom (4). The coordinates of the other atom in the unit cell are therefore $\left\{(1 - x_1), (\frac{1}{2} + y_1), (1 - z_1)\right\}$. The coordinates of all the nearest neighbour iron atoms have been worked out and the distances between the iron atoms are given below.

The two nearest neighbours are related to (I) by a 360° rotation along the same screw axis. They are therefore separated from (I) by a translation through the distance b, which is 30.86A.

The next nearest neighbours are those related to I by a 180° rotation of the screw axis. At the same distance are two atoms related to (I) by translation along the c axis. Thus there are four iron atoms at a distance of 34.70A.

The other atom in the unit cell is at 38.01A and so is the atom related to it by a 360° rotation and upwards translation of b along the screw axis. This atom is denoted by the number (5) in Fig. (5).

Two atoms related to I by a translation in a positive

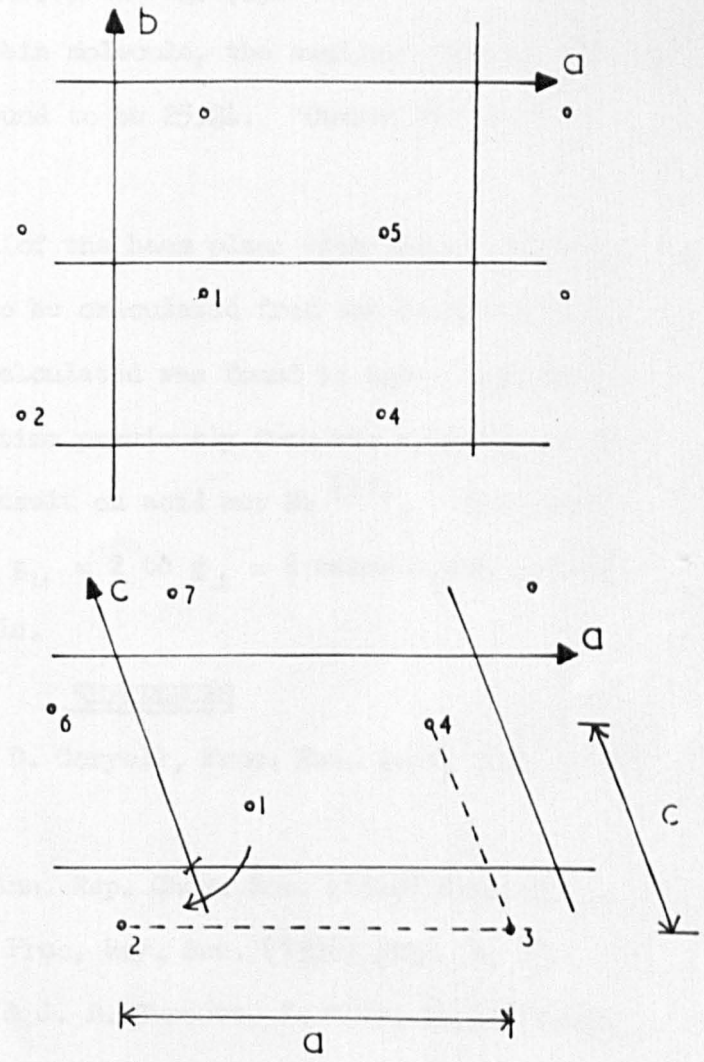

FIG. 5.5

NEAREST NEIGHBOUR
IRON ATOMS

direction along c and thence by a 180° rotation, up and down, of the screw axis are at a distance of just over 38A. These are positions (6) and (7) in Fig. (5).

In the haemoglobin molecule, the smallest distance between the iron atoms is found to be 25.2A. Others are at 33.4 and 36.0A.

The orientation of the haem plane with respect to the crystal axes can also be calculated from the X-ray results. The orientation so calculated was found to agree closely with that worked out sometime previously from the symmetry of the electron resonance result on acid met Mb [11]. The large g value variation from $g_{\parallel} = 2$ to $g_{\perp} = 6$ makes a very precise determination possible.

REFFRENCES

(1) L. Pauling & C. D. Coryell, Proc. Nat. Acad. Sci. (1936) 22 p. 210.

(2) E. F. Hartree, Ann. Rep. Chem. Soc. (1946) Vol. 43, p. 287.

(3) J. S. Griffith, Proc, Roy. Soc. (1956) A235, p. 23.

(4) D. J. E. Ingram & J. E. Bennett, J. Chem. Phys. (1954) 22, p. 1136.

(5) J. E. Bennett, D. J. E. Ingram & P. George, J. Chem. Phys. (1956) 24, p. 627.

(6) M. Kotani, Proc. of Theoretical Phys. Supp. No. 17 (1961), p. 4.

(7) F. R. McKim, Proc. Roy. Soc. (1961) A262, p. 287.

(8) J. F. Gibson, D. J. E. Ingram, Nature (1957) 180, p. 29.

(9) J. S. Griffith, Nature (1957) 180, p. 30.

(10) J. C. Kendrew & R. G. Parrish, Proc. Roy. Soc. (1956) A238, p. 305.

(11) J. E. Bennett, J. F. Gibson & D. J. E. Ingram, Proc. Roy. Soc. (1957) A 240, p. 67.

Chapter 6

Experimental Results and Discussion

6.1. Crystal Mounting

The crystals used in the electron resonance study vary considerably in size, the average having a maximum length along the b axis of about 2 mm with a 1 mm. cross section. They are dark reddish brown, almost black in colour and have a loose water filled structure which is extremely fragile. If allowed to dry the crystals frequently disintegrate, so that when mounting, a small drop of buffer solution is always allowed to remain with them. The faces are well defined, but crystals from the same batch have been found to be flattened in either the ab or bc planes, so that they must be carefully examined before mounting.

In general measurements are made with a particular crystal plane mounted parallel to the face of the electron resonance cavity plunger. These crystal planes are usually the ab, bc* and ac planes, where (a, b, c*) are mutually perpendicular axes. Of these, only the ab plane is parallel to an actual face of the crystal. To mount the crystal in the other planes requires the use of small wedges of a non absorbing material such as polystyrene or p.t.f.e.. The crystal is then mounted so that the ab plane is vertical with either the a or b axis horizontal. Since the two haem groups in the unit cell make the same angles with the ab and

c^{*} axes, the electron resonance signals from them coincide along these axes. This can be used as a check, since if the crystal is mounted correctly in a plane, such as the ab plane, the lines should coincide at points exactly 90^{o} apart around the plane. These "cross over" points can be quickly determined with crystal video detection and the mounting checked. If the cross over points are 90^{o} apart at least one crystal axis must be parallel to the face of the plunger. If the crystal is accurately mounted in the ac plane the lines from the two haem groups should coincide over the whole plane since they make equal angles with the plane.

The crystal has also been mounted in such a way that the haem plane is parallel to the face of the plunger. The correct angles for a wedge were calculated from the haem plane orientation in acid met Mb and a check on the accuracy of the mounting is given by the constancy of the g value of the signal. The crystal has been mounted in the same way with the haem plane perpendicular to the face of the plunger. A check is provided in this case by the fact that the signal should go through g = 2.

The normal way of tuning the electron resonance cavity of the Q band spectrometer is to adjust the klystron, mechanically, to give maximum power before bringing the cavity into resonance with that frequency. This is necessary because the output of the klystron is not constant over its entire frequency range.

Because of the water present in myoglobin crystals, however, the cavity cannot be tuned in the normal way at room temperature. This would be very awkward but for the fact that the crystals do not appreciably detune the cavity once frozen. The cavity tuning can therefore be 'calibrated' in the absence of the sample, in the following way.

The tuning plunger was screwed up to the end of the threads in the cavity wall and the klystron tuned to the resonant frequency. All the waveguide elements were then tuned at this frequency for maximum crystal current reading. This procedure was repeated every two turns down of the plunger and a curve of crystal current against number of turns showed two peaks. A more careful calibration over these peaks gave the exact positions of their centres in terms of the number of turns from the end of the threads. Optimum tuning is still possible after two whole turns of the plunger up or down from the centre of a peak.

Once the crystal is mounted on the face of the tuning plunger, where it is held partly by surface tension and partly by siliconegrease, the plunger is screwed to the end of its thread and then back the correct number of turns to bring it to the centre of a peak in the tuning curve. Allowance of half a turn is made for contraction in the cavity dimensions at low temperatures. The cavity is then sealed and immersed in liquid nitrogen just before pumping down.

With the H_{11} mode cavity measurements around the full 180° in a crystal plane cannot be made without rotating the crystal relative to the microwave magnetic field. This can be done by warming the cavity until the grease becomes plastic, removing the coned cup over the end of the cavity and rotating the plunger a quarter of a turn up or down. The method of tuning of the cavity ensures that it will still be within a peak power range of the klystron. The cap can be replaced and the cavity cooled down without the crystal warming above 0°C. This is necessary because the crystal tends to disintegrate upon repeated freezing and unfreezing. Remounting a frozen crystal in another plane is therefore difficult, but can be accomplished by working quickly and occasionally cooling the plunger with liquid nitrogen.

When measurements are to be taken with the azide derivative, one or two acid met crystals are seperated out along with a little ammonium sulphate solution and to this are added about 10 mgms. of sodium azide. This dissolves rapidly and permeates through the crystal. The azide ion reacts with the iron atoms to form met Mb azide. If the crystals are removed after about 10 mins. the electron resonance spectrum has two sets of lines, one from the azide and the other from the still unconverted acid met. Because of the large g value variation in the acid met it is easier to check the orientation of the crystal with these lines than those of the azide.

Throughout all the measurements the frequency of the klystron was determined by noting the field or magnet current at which the signal from d.p.p.h. occurs. A small quantity of d.p.p.h., just discernable with the naked eye, is put between the iris coupling holes in the roof of the cavity, and in this position can be left undisturbed for several days. It is then useful for comparing the day to day sensitivity of the spectrometer.

6.2. g Value Measurements

6.2.1. Azide Derivative

The g value variation in the three crystal planes of the azide derivative has been reported [1] and discussed previously [2]. However, it was considered necessary to check these measurements and compare the results of their analysis with the structural information now available from X-ray measurements.

What is wanted is the g value variation with respect to the surroundings of the iron atom. The crystalline electric field defines the direction of a principal g value $g_{\parallel}$, and in general there will be a maximum and a minimum g value, at right angles to each other, in a plane perpendicular to the crystalline field direction. These three principal g values when oriented in an unknown direction in the crystal would be difficult to measure, however their magnitude and directions can be determined from measurements in the ab, bc*, and ac planes.

The method used here is described by Schonland and requires the maximum and minimum g values in the ab, bc^{*} and ac planes together with the angle between the maximum g value and one of the axes in the plane.

The curves in Fig. (6.1) show the g value variation in the various crystal planes as determined by Gibson [3]. The numbers on the curves have been added to relate the curves obtained from the same haem groups in the unit cell. The normal to the plane of haem group (1) lies inside the quarter hemisphere formed by the positive directions of the three coordinate axes.

The actual values of the maximum and minimum g value are:-

Table (1)

Plane	$g_{max.}$	$g_{min.}$	σ_+
ab	2.79	2.19	30°, $^{(1)}\sigma_+$
bc^{*}	2.43	1.73	72.5, $^{(2)}\sigma_+$
ac	2.67	1.71	79.5, $^{(3)}\sigma_+$

Here $^{(1)}\sigma_+$ is defined as the angle between the maximum g value and the a axis in the ab plane, whilst $^{(2)}\sigma_+$ and $^{(3)}\sigma_+$ are the angles between the maxima and the c^{*} axis in the bc^{*} and ac planes respectively. Since there is only one line in the ac plane and no cross over points to define the a and c axes the position of the c^{*} axis must be determined from its g value

measured in the bc^* plane using proton resonance.

The actual calculation of the principal g values and principal axes is rather long and involved and will not be described here. Briefly, however, the problem can be defined more clearly as follows.

If the magnetic field has direction cosines (l, m, n) with respect to the (a, b, c^*) axes, the square of the corresponding g-value is given by an expression of the form

$$g^2 = A_{11}l^2 + A_{22}m^2 + A_{33}n^2 + 2A_{12}lm + 2A_{13}ln + 2A_{23}mn$$

where $A_{ij} = A_{ji}$. This expression is in fact a central quadric which when referred to its principal axes reduces to a simple form involving no cross turns.

$$g^2 = g_x^2 \cos^2\alpha + g_y^2 \cos^2\beta + g_z^2 \cos^2\gamma$$

where g makes angles (α, β, γ) with the principal axes. When the coefficients A_{ij} are known, the principal g-values and principal axes are found by diagonalizing the matrix A in the usual way. Schonland's paper describes how the coefficient A_{ij} may be determined from the data in Table (1).

The results of the calculation are given in Table (2), the angles are referred to the axes as shown in Fig. (6.2) and thus apply to haem group (1).

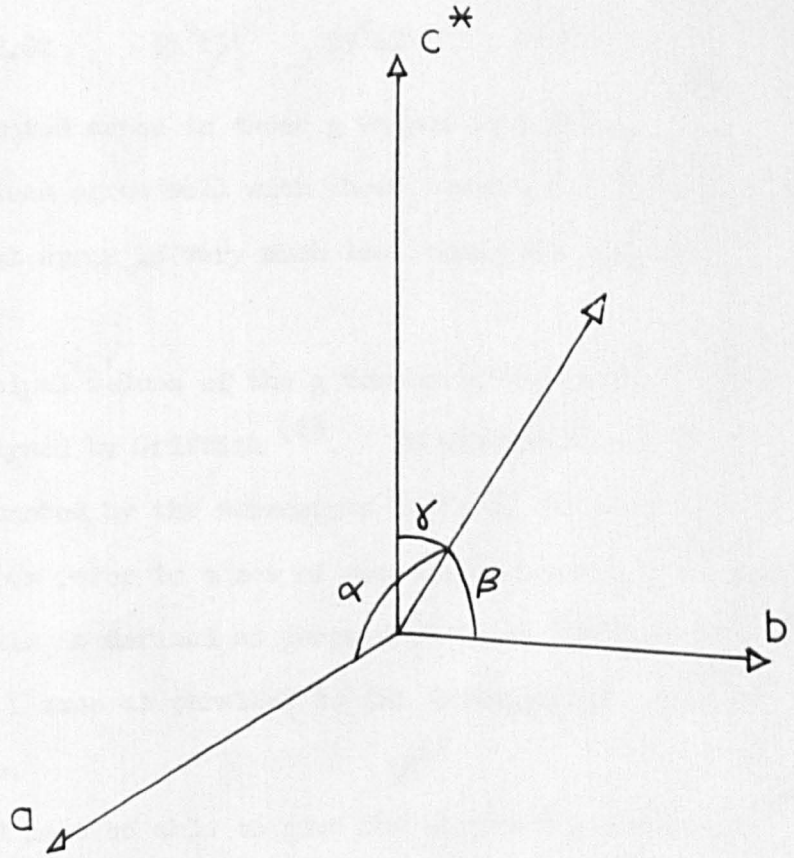

FIG. 6.2

Table (2)

	α	β	γ
$g_1 = 1.71$	$84^{\circ}33'$	$75^{\circ}42'$	$164^{\circ}40'$
$g_2 = 2.19$	$122^{\circ}20'$	$33^{\circ}35'$	$81^{\circ}54'$
$g_3 = 2.82$	$33^{\circ}13'$	$59^{\circ}42'$	$77^{\circ}40'$

The estimated error in these g values is 0.75%.

The g values agree well with those found by Gibson suggesting that the actual error is very much less than that estimated.

6.2.1.1. Discussion

The principal values of the g tensor in the azide derivative have been analysed by Griffith [2]. In this paper the g values 1, 2, 3 are denoted by the subscripts X, Y, Z, respectively. These subscripts refer to a set of coordinate axes X, Y, Z for which the Z axis is defined as perpendicular to the haem plane and the X and Y axes as parallel to the iron-nitrogen bonds in the haem plane.

Any model must be able to give the observed g values as closely as possible. For the theoretical determination of the g values it is necessary to calculate the magnitude of the splitting of the levels of the lowest Kramers doublet in the presence of an external magnetic field. Griffith does this by considering the effect of the spin-orbit coupling, magnetic field energy, and a rhombic distortion along the cartesian axes. Fitting the theoretical g values to the observed g values deter-

mines a parameter which by working back gives relations between the energies of the t_{2g} levels. The results are that d_{yz} lies 2.26λ above d_{xz}, and 4.45λ above d_{xy}, where λ is the spin orbit coupling parameter. The value of λ from the free-ion data is 435 cm^{-1} but in for example $K_3Fe(CN)_6$ it is 280 cm^{-1}.

In discussing the order of the levels so derived, Griffith suggests that the energies of the d orbitals are raised by π-interaction. The least stable orbital d_{yz} should therefore be that which is most exposed to π-interaction.

The nitrogen atom of the histidine ring bonded to the iron atom at the 5th. coordination point should therefore tend to π bond with the d_{yz} orbital so that the plane of the ring should be parallel to the xz plane. It follows therefore that the minimum g value in the plane should be parallel to the projection of the histidine ring in that plane.

Since the coordinates of the atoms in the histidine ring are known it is possible to check the above suggestion. The iminazole ring of histidine is shown bonded to the iron atom in Fig. (6.3). If the nitrogen atom makes σ bonds with two carbon atoms and the iron atom, using an sp^2 hybridized orbital, the carbon atoms can be assumed equidistant from the haem plane. A line joining them should therefore be parallel to the projection of the histidine ring on the haem plane. The coordinates of the carbon atoms (1) and (2) given in Chapter 5, Table 2, are referred to monoclinic

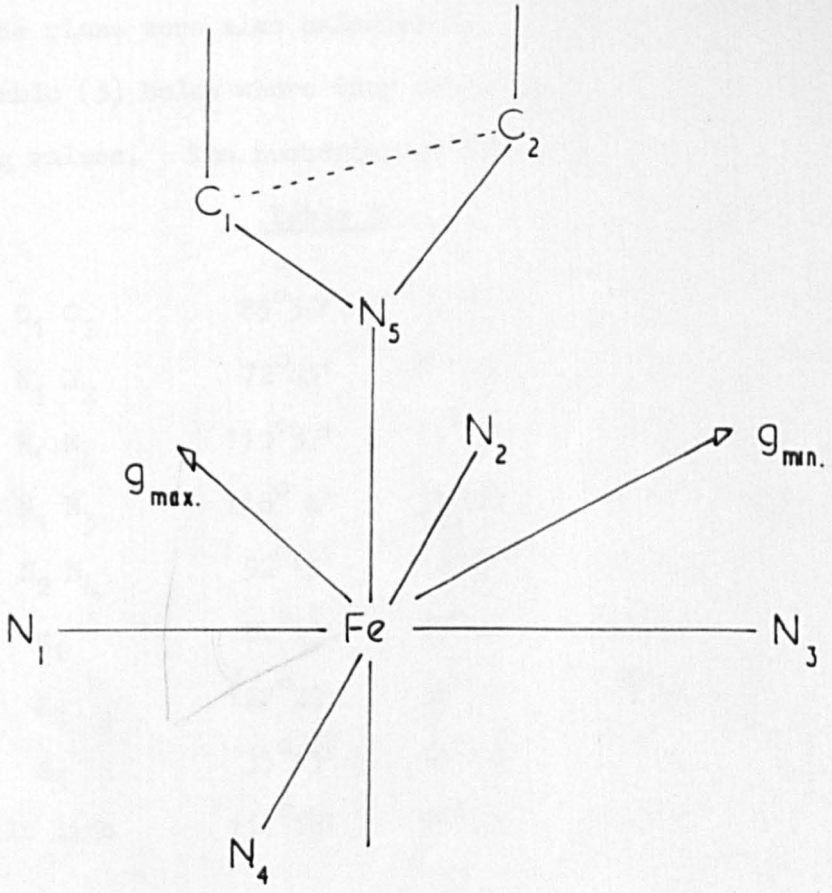

FIG. 6.3

THE DIRECTION $C_1 C_2$ IN THE HISTIDINE RING

axes. These were changed to refer to the axes a, b, c^* and the direction of the line joining C_1 and C_2 was calculated. At the same time the directions of the lines joining the four nitrogen atoms in the plane were also calculated. These directions are given in Table (3) below where they are compared with those of the principal g values. The numbering of the atoms is shown in Fig. (6.3).

Table 3

	α	β	γ
C_1 C_2	85°30'	74°23'	163°43'
N_1 N_2	72°43'	87°32'	162°32'
N_1 N_4	110°37'	21°16'	95° 2'
N_1 N_3	118° 4'	51°22'	51°26'
N_2 N_4	92°15'	46°48'	136°51'
g_1	84°33'	75°42'	164°40'
g_2	122°20'	33°35'	81°54'
g_3	33°13'	59°42'	77°40'
tilt line	117°16'	53°23'	48°19'

The results show that the minimum g value is indeed parallel to the plane of the histidine ring. However, the basis of this prediction was a calculation in which the minimum g value was assumed to be parallel to an iron-nitrogen bond in the plane. These are the directions N_1 N_3, N_2 N_4 in Table (3) and it can be seen that the minimum g value is not parallel to either of these but makes an angle of approximately 29° with N_2 N_4.

These directions are shown related to the haem plane and the b and c^* axes in Fig. (6.4).

It is difficult to see, in the light of the above results, how the histidine ring can π-bond with the d_{yz} orbital. However, since the direction C_1 C_2 is closer to N_2 N_4 than N_1 N_3 there is likely to be unequal interaction between the histidine ring and the d_{xz} and d_{yz} orbitals, causing one to have a lower energy than the other.

The situation is complicated still further by the fact that the maximum g value is not parallel to the haem normal as calculated from both electron resonance and X-ray measurements on acid met Mb. There is an angle of 9° between the two directions. There are two possible explanations for the change in the direction of the axis of quantization.

1. The haem plane has tilted and remains perpendicular to the axis of quantization.
2. The azide molecule at the 6^{th} coordination site has distorted the crystalline field.

1. The manner in which the haem group is held in a "pocket" of the protein molecule has been discussed in Chapter 5. From an examination of the molecular model in Cambridge it appears to be quite possible for the haem plane to adopt various attitudes in the protein provided that this is allowed by the bonding of the iron atom to the histidine ring.

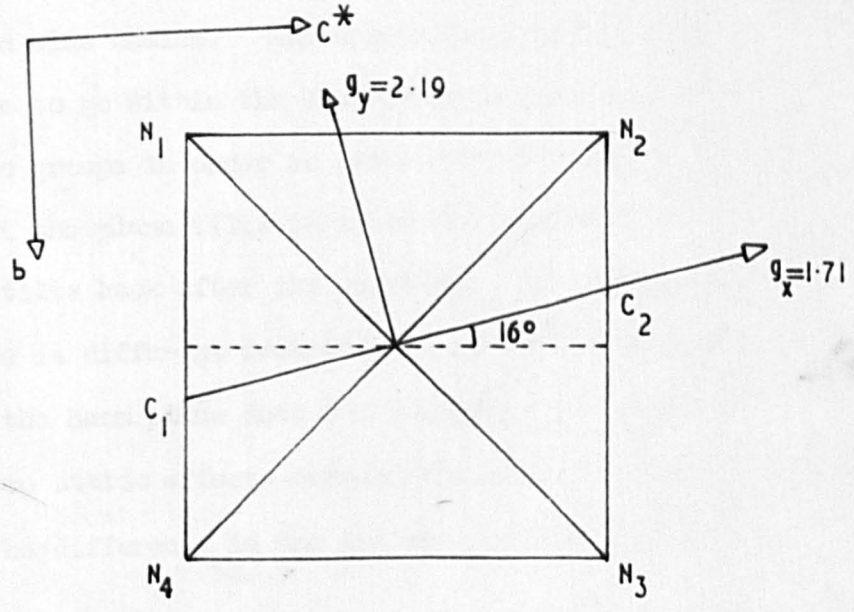

FIG. 6.4

HAEM PLANE AZIDE DERIVATIVE

This possibility has already been considered by Watson [4] in an attempt to explain the ability of molecules to approach the sixth coordination site of the iron atom. This site is not exposed at the surface of the protein as was once thought to be the case but is completely surrounded by various end groups of the amino acid side chains. Any approaching molecule would therefore have to go within the Van der Waals distance of the atoms in these groups in order to react with the iron. It is suggested that the plane tilts to allow the approach of the azide molecule and tilts back after the reaction. The shape of the azide molecule is different from that of the water molecule it replaces and the haem plane does not return to its original position due to steric effects between the azide and the protein molecule. The difference in the two orientations is the observed 9°.

Figure (6.5) is an enlargement of the haem group from a photograph of the molecular model. This photograph is taken from the "entrance" to the "pocket" containing the haem group, showing how the plane blocks access to the water molecule. There is no part of the protein molecule directly between the camera and the iron atom over the area enclosed by the broken line. The numbering of the nitrogen atoms in the plane is the same as that already used.

Assuming that the plane has tilted the direction of the

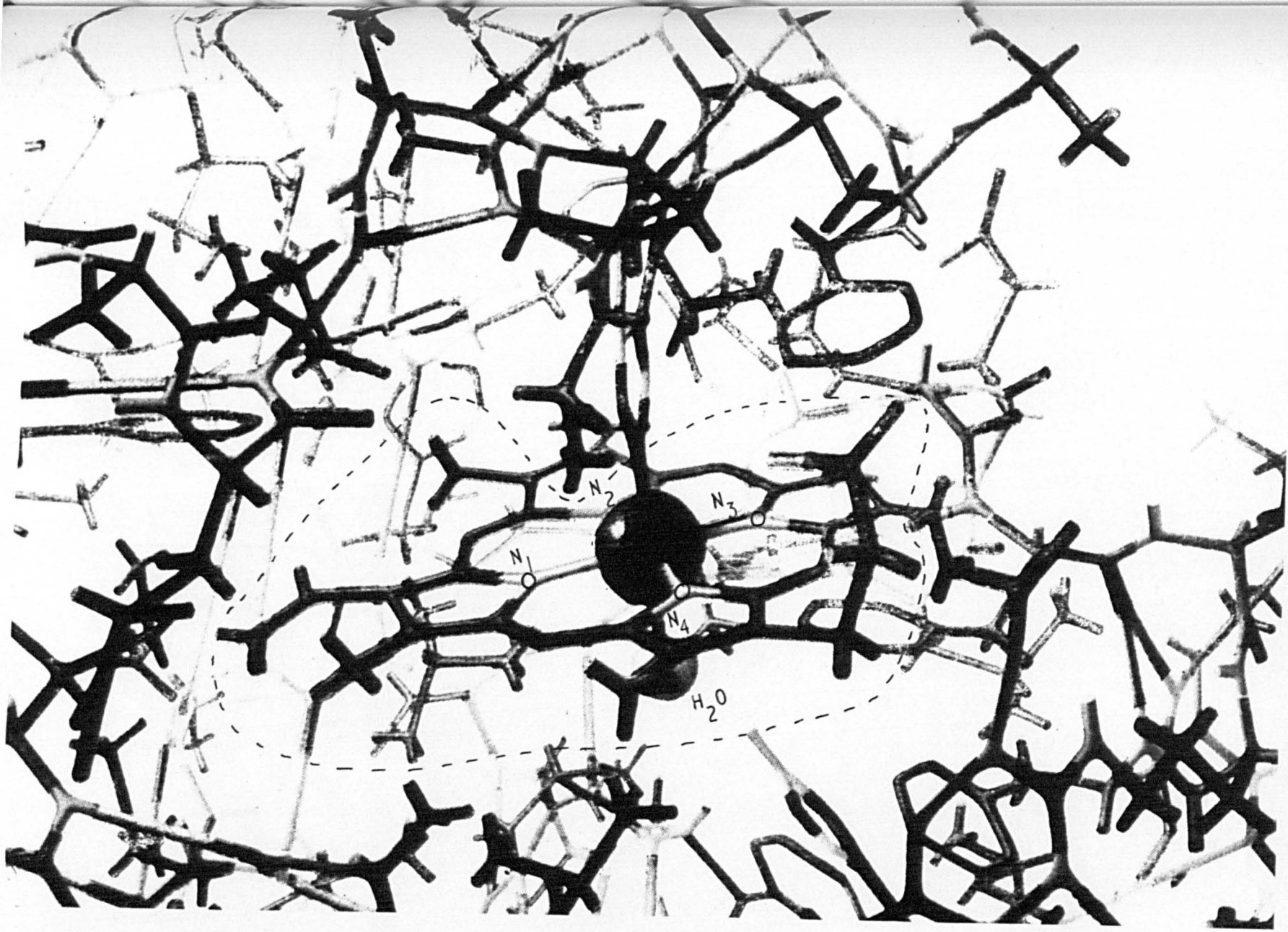

FIG. 6.5

diameter about which it does so can be calculated. This is the simple geometrical problem of the equation to the line of intersection of two planes defined by the angle cosines of their normals. The direction of this line referred to as the "tilt line" is given in Table (3) from which it can be seen to be almost parallel to the direction N_1 N_3.

Such a tilting of the plane would have an effect on the bond between the iron atom and the nitrogen atom in the histidine ring. If this nitrogen atom is to remain in the same position relative to the iron atom, the histidine ring as a whole must move. This might well in turn distort part of the helix of the polypeptide chain, transmitting the movement throughout its length. A movement of this type could possibly be the nature of the haem-haem interaction in the haemoglobin molecule.

2. The possibility that the plane does not tilt, poses the question as to what is defining the direction of the maximum g value. The effect of the ligand at the sixth coordination point is normally considered to be electrostatic and molecular orbital calculations made on the electronic structure of iron porphyrin complexes [5] show that a good model can be based on this assumption.

The azide molecule would not be expected to find the position of minimum energy anywhere but along the normal to the haem plane. The maximum g value would then be expected to lie in this direction

also. The fact that it does not, suggests that the azide molecule is prevented from taking up this exact position by the presence of the protein molecule. The maximum g value might therefore indicate the direction of the first nitrogen atom in the azide molecule relative to the iron atom. The direction of the movement of the axis of quantization suggests that the azide molecule might be displaced from the 6^{th} coordinateion site of the iron atom along the Fe - N_2 bond direction which may indicate therefore the direction of approach of the azide molecule,

A third possibility is that the presence of the azide molecule in changing the wave functions of the iron atom allows a small distortion of the haem plane.

6.2.2. Acid Met

The g value around the haem plane in acid met Mb is taken to be isotropic with a g value close to 6. An opportunity of checking the isotropy of the g value was provided by line width measurements around the haem plane. The crystal was mounted on a carefully cut wedge, the angles of which were considered accurate to 1°. The mounting was checked from the crystal video resonance signal which remained stationary on the oscilloscope screen as the magnetic field was rotated. The signal from the other haem group in the unit cell came into coincidence with this line only once in 180°. The line widths around the plane were measured by placing current markers rather than proton resonance

markers on the pen recorder trace.

The centres of the derivative curves at different orientations of the magnetic field were found to vary with respect to the current markers in a uniform way and this variation was plotted. The curve is shown in Figure (6.6), where the angles refer to the rotation of the magnet from the position in which both lines coincide. It can be seen that the angle between maximum and minimum g value is approximately 90°. The g values measured from this curve are not absolutely determined but the variation is such that if the maximum is considered to be 6 the minimum is 5.9.

The direction of these maximum and minimum g values in the haem plane is rather difficult to define since it is not known from which of the two haem groups, in the unit cell, the signal comes. A direction is, however, defined by the cross over point of the two lines. When the plane of one group is parallel to the face of the plunger the signals from both haem groups coincide when the magnetic field is parallel to both planes at once. This occurs when the field is parallel to the line of intersection of the planes containing the haem groups. This line makes the angles (α, $71^{\circ}57'$; β, 90°; γ, $161^{\circ}57'$) with the abc^{*} axes, which is thus very close (within 2.5°) to the direction N_1 N_2 in both haem planes.

The directions in the plane of maximum and minimum g value

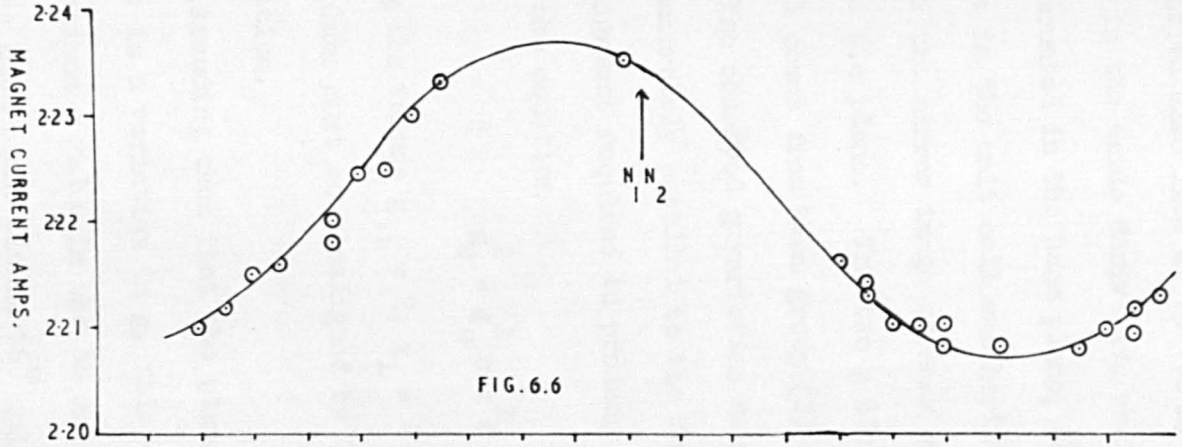

FIG. 6.6

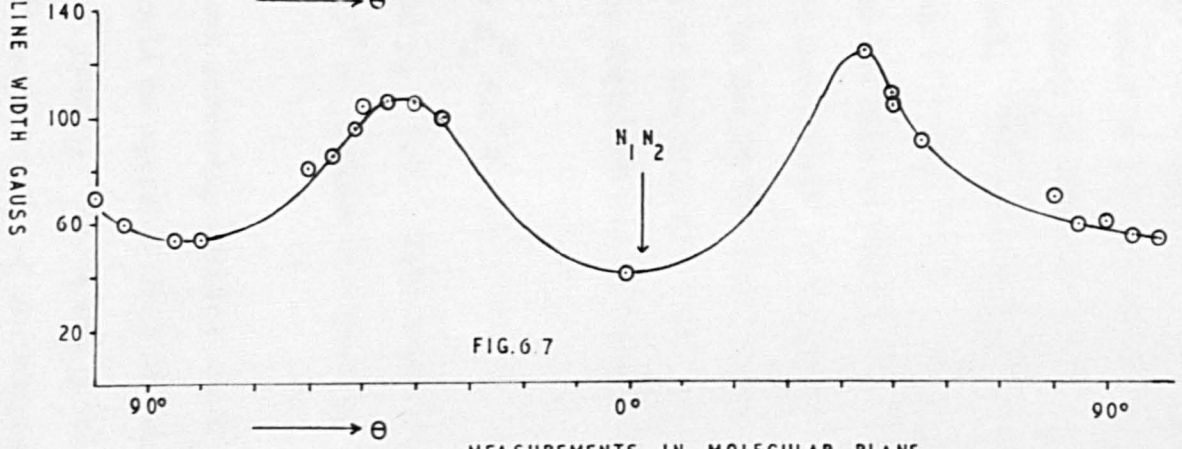

FIG. 6.7

MEASUREMENTS IN MOLECULAR PLANE
ACID MET Mb.

can now be referred to this direction and the minimum g value is seen to lie at 15° to the direction N_1 N_2. This is an interesting coincidence since the minimum g value in the azide derivative also lies at 15° to N_1 N_2. However, the minimum g value in the azide derivative would occur on either side of N_1 N_2, when mounted in the haem plane, depending on which of the haem groups in the unit cell was horizontal. The plan of haem group (2) is the mirror image of haem group (1) Fig. (6.4) reflected in the a.c plane. The two g minima can only be parallel if the signal comes from haem group (2) and this cannot be verified.

The observed g variation could be due to the plane being not accurately parallel to the face of the plunger. The angle of misalignment required to produce the variation can be calculated from the equation

$$g_\theta^2 = g_{\parallel}^2 \cos^2\theta + g_{\perp}^2 \sin^2\theta$$

using the values $g_{\parallel} = 2$, $g_{\perp} = 6$ and $g_\theta = 5.9$. This shows that the plane must be misaligned by 10.5° to produce the observed variation.

Assuming then that the plane was correctly mounted and that there is a variation in g, this should be apparent from the value of maximum g value in the ab and bc^* planes. These are g values in the haem plane within 16° and 6° respectively of the supposed maxima and minima. The maximum g value in the ab plane should therefore be greater than that in the bc^* plane.

The maximum g values in these planes were therefore measured very carefully by recording the resonance signals with proton resonance markers at 200 kc/s or 48 gauss intervals. The centre of the line could be determined to within a tenth of a marker separation or to within 5 gauss. This is an error of about 1 part in 700. The measurement of the field at the d.p.p.h. resonance is very much more precise because of the narrow line and an accuracy of 1 part in 10^4 may be expected.

The g values measured in this way are therefore accurate to within one part in 700 and are:-

ab plane $g_{max} = 5.98 \pm 0.01$

bc* plane $g_{max} = 5.86 \pm 0.01$.

These measurements thus confirm that there is a g value variation in the haem plane of acid met Mb, with maximum and minimum roughly equal to those above and oriented relative to the haem plane in the same way as those in the azide derivative. They are therefore parallel and perpendicular to the projection of the plane of the histidine ring on the haem plane.

6.3. Line Width Measurements

All measurements of line width were made at either liquid nitrogen or hydrogen temperatures and no change in width was observed on going from one temperature to the other. Q band frequencies were used throughout but the frequency dependence of the line widths was checked by repeating certain measurements at

X band frequencies.

6.3.1. Acid Met Mb

Line width measurements in acid met Mb were made around the (ab) plane and the haem plane. Since the haem normal is known to make an angle of 17° with the ab plane, these two sets of measurements determine the line width variation around the haem plane and around a plane at 73° to it. In order to determine the variation around a plane perpendicular to the haem plane, a single measurement was also made with the crystal mounted so that a haem normal was parallel to the face of the plunger. The line width was measured at g = 2 that is along the haem normal.

The line width variation in the (ab) plane and in the haem plane is shown in Figures (6.8) and (6.7). The general features of the variation are that, the line width is a minimum in the haem plane and increases out of the plane towards the haem normal. In the (ab) plane the nearest approach to the normal is 17° at 23° to the (a) axis and here the line width is 800 gauss. However the line width measured along the haem normal is 175 gauss. In a plane perpendicular to the haem plane, therefore, the line width increases to a maximum close to the normal and decreases very rapidly towards the normal.

In the haem plane itself there is a line width maximum at 45° on either side of the cross over point, marked 0° in the

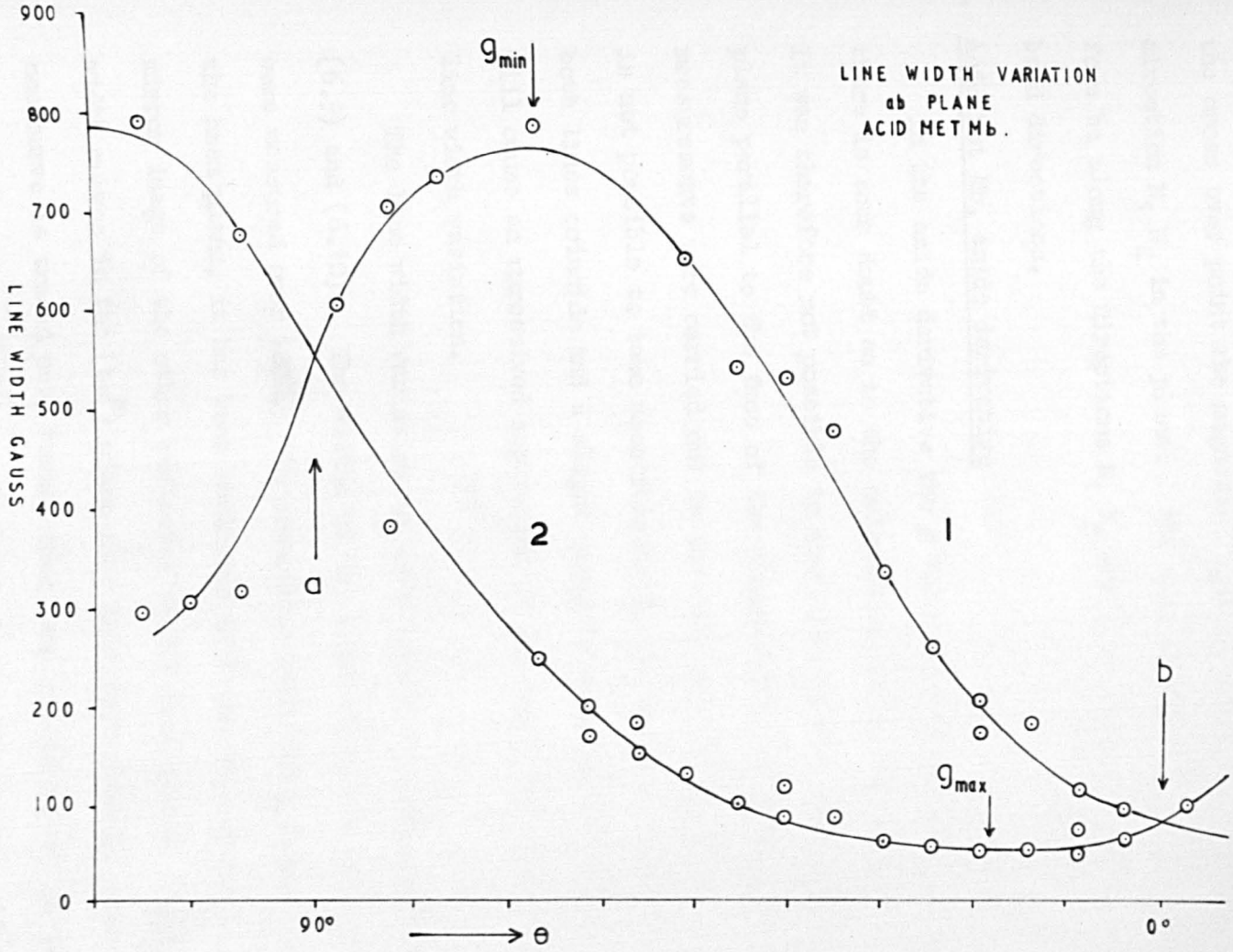
LINE WIDTH VARIATION
ab PLANE
ACID MET Mb.
LINE WIDTH GAUSS
900
800
700
600
500
400
300
200
100
0
g_{min}
g_{max}
a
b
1
2
90°
θ
0°

FIG. 6.8

Figure. The question of direction in the haem plane has been discussed already in connection with the g value variation. At the cross over point the magnetic field is very close to the direction N_1 N_2 in the plane. The line width maxima must therefore be along the directions N_1 N_3 and N_2 N_4 which are Fe - N bond directions.

6.3.2. Acid Met Mb, azide derivative

In the azide derivative the g value measurements show that there is some doubt as to the orientation of the haem plane. It was therefore not possible to mount the crystal with one haem plane parallel to the face of the plunger as in acid met, and the measurements were carried out in the (ab) and (bc^{*}) planes. It is not possible to take measurements in the ac plane because here both lines coincide and a slight error in mounting the crystal will cause an unresolved separation of the lines and consequent line width variation.

The line width variation in these planes is shown in Figures (6.9) and (6.10). The widths of the lines from both haem groups were measured over 180°. In connection with the g values in the haem plane, it has been mentioned that one haem group is the mirror image of the other reflected in the (ac) plane. The line width curves in the (bc^{*}) plane show this fact clearly, since if one curve is traced out, turned over, and placed on top of the other, they agree closely over their entire length, Fig. (6.11).

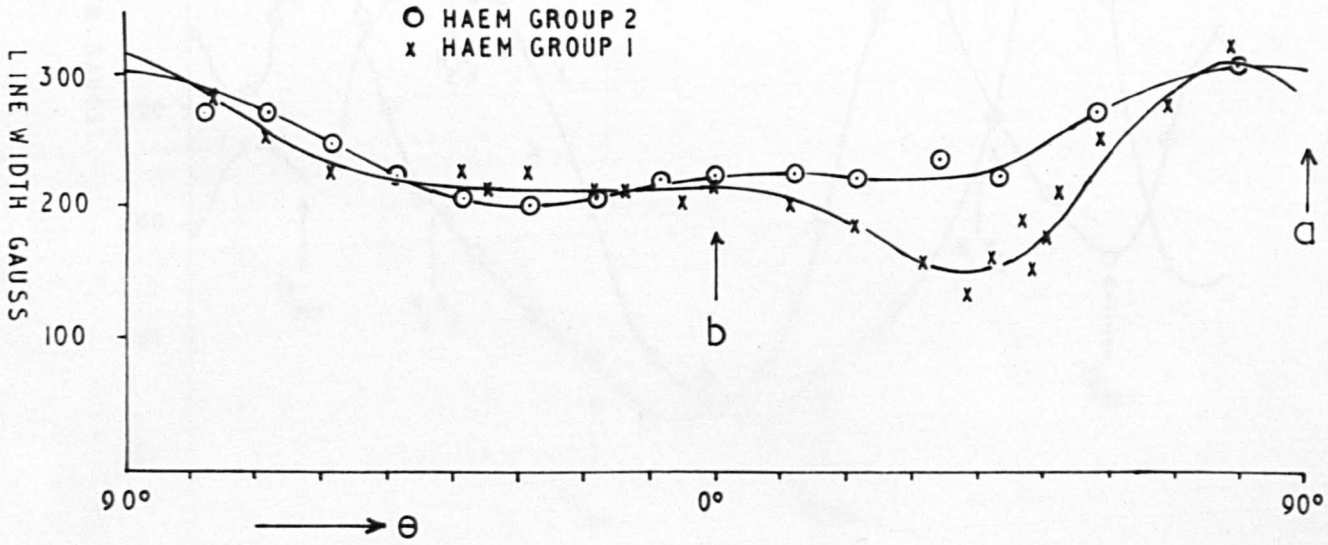

FIG. 6.9
LINE WIDTH VARIATION ab PLANE
AZIDE DERIVATIVE

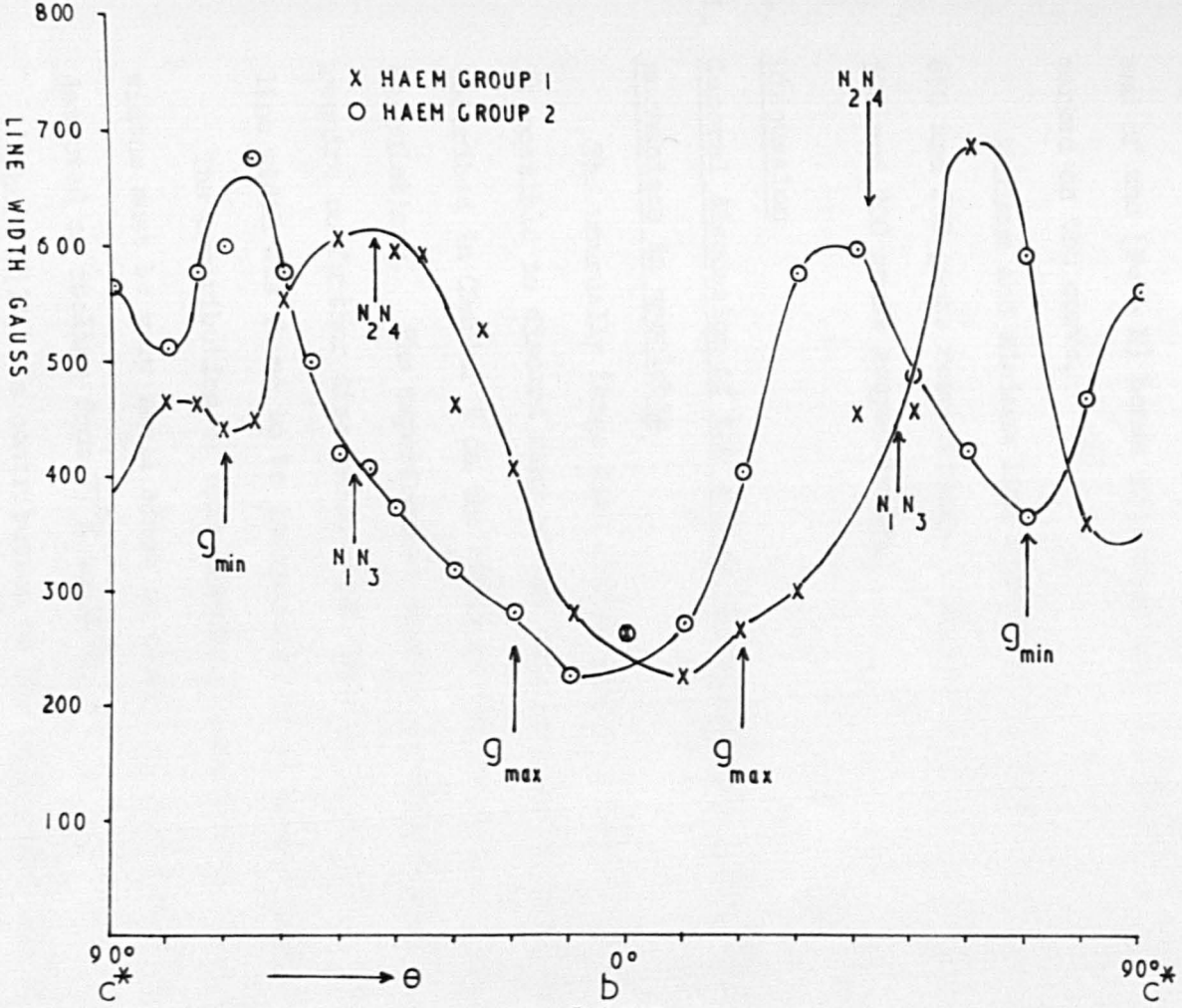

FIG. 6.10
LINE WIDTH VARIATION bc* PLANE
AZIDE DERIVATIVE

In discussing the line width variation in the (bc^{*}) plane, the mean of these two curves will be used.

In order to relate the line width variation to the surroundings of the iron atom, the directions of the principal g values and of the (Fe - N) bonds projected onto the (bc^{*}) plane, are marked on the curve.

Maximum and minimum line widths in the (bc^{*}) plane are 650 and 250 gauss respectively. In the (ab) plane they are 300 and 200 gauss respectively.

6.4. Discussion

6.4.1. General discussion of the effect of various line broadening mechanisms in myoglobin

The unusually large line widths found in myoglobin, make it possible to discard many of the line broadening mechanisms described in Chapter 3 on the basis of simple order of magnitude calculations. The experimental sources of line broadening require no further discussion other than to mention that the line width was found to be independent of microwave power level.

The contribution of spin-lattice relaxation to these line widths must be very small since no change in line width was detected on cooling from 77°K to 20°K.

There will be a contribution to the line width due to dipolar interaction between the electronic spins of neighbouring iron atoms. The magnitude of this interaction can be calculated

using Van Vlecks formula, Chapter 3, page 60, for each of the nearest neighbour iron atoms. An upper limit for the broadening, can be found by summing the individual contributions. For the six iron atoms within 35A, the maximum possible contribution to the line width is 14 gauss.

From the description of exchange interaction given in Chapter 3, it will be seen that the phenomenon is unlikely to occur between neighbouring iron atoms since these are separated by more than 30A.

If the observed line width variation is due to unresolved hyperfine structure, the structure must be due to interaction between the magnetic electrons and the magnetic moments of the surrounding nitrogen nuclei since the iron atom has no nuclear magnetic moment. The line width should be frequency independent.

The line widths in the (ab) plane acid met and in the (bc^{*}) plane, azide derivative were therefore measured at X band frequencies and found to be decreased in proportion to the decrease in frequency. It follows that the line width variation cannot be due to an unresolved hyperfine structure. However, molecular orbital calculations [5] do show that there is an appreciable probability of finding magnetic electrons at the nitrogen atoms part of the time, in both acid met and azide derivatives. An isotropic hyperfine structure is therefore to be expected but must be obscured by the line broadening process.

6.4.2. Proposed Mechanism for the broadening of the electron resonance lines

The mechanism proposed here for the explanation of the broad lines found in single crystals of myoglobin, is a result of the peculiar crystalline structure of these proteins. Essentially it supposes that the principal g values of the haem groups contributing to the resonance line are not strictly parallel to each other but are scattered about a mean orientation. The resonances from individual haem groups therefore occur over a range of magnetic field values, resulting in a broadening of the line.

The possibility that the haem group may change its orientation relative to the surrounding protein molecule has already been considered. If this does occur then it is only necessary to assume that the haem groups do not all have the same orientation with respect to the protein molecule. However, if there is no change in orientation of the haem group on going from acid met to azide derivative, the scatter in the directions of the principal g values must reflect the degree of disorder in the crystal structure as a whole.

The general features of a line width variation produced in this way are easily predictable. If the g value of the line is changing rapidly, as it does between principal g values, small

variations in their orientation will cause large changes in g and a broad line. Conversely at a turning point of the g value, the line will be narrow.

In acid met Mb therefore the line width should be a minimum around the haem plane. Out of the plane the line width should increase with the rate of change of g, rising to a maximum and falling again before the normal to the plane is reached. The variation in the azide derivative is rather harder to imagine due to the three principal g values. The theory thus predicts at least the basic features of the line width variation in acid met myoglobin.

6.5. Calculation of Line Width Variation

6.5.1. Acid Met Mb

In acid met Mb the g value at any angle θ to the principal g value $g_{\parallel}$, assuming $g_{\perp}$ isotropic, is given by the equation

$$g_\theta^2 = g_{\parallel}^2 \cos^2\theta + g_{\perp}^2 \sin^2\theta \quad . \qquad 6.1$$

The line width ΔH is proportional to the rate of change of g with θ so that

$$\Delta H \alpha \frac{dg}{d\theta} = \frac{(g_{\perp}^2 - g_{\parallel}^2) \cos\theta \sin\theta}{g} \qquad 6.2$$

Consider now two haem groups whose normals make angles of $\theta + \Delta\theta$ and $\theta - \Delta\theta$ with the magnetic field direction. The difference between their g values in this direction is given by

$$\Delta g = \frac{(g_\perp^2 - g_{||}^2)}{2g_\theta} \int_{\theta - \Delta\theta}^{\theta + \Delta\theta} \sin 2\theta \, d\theta$$

or

$$\Delta g = \frac{(g_\perp^2 - g_{||}^2)}{2g_\theta} \sin 2\theta \sin 2\Delta\theta + \text{const.} \qquad 6.3$$

but since

$$h\nu = g\beta H$$

$$\Delta H = \frac{h\nu}{\beta} \frac{\Delta g}{g_\theta^2}$$

and therefore

$$\Delta H = \frac{h\nu}{\beta} \frac{(g_\perp^2 - g_{||}^2)}{2g_\theta^3} \sin 2\theta \sin 2\Delta\theta + \text{const.} \qquad 6.4.$$

If ΔH is measured in kilogauss and if $2\Delta\theta$ is small the expression can be written as

$$\Delta H = 26.76 \frac{(g_\perp^2 - g_{||}^2)}{2g_\theta^3} \sin 2\theta \cdot 2\Delta\theta + \text{const.} \qquad 6.5$$

when $2\Delta\theta$ is in radians.

When instead of two haem groups there are many, their various orientations will be distributed about a mean value of θ. Since the resonance line widths are measured between the maximum slope points of the absorption line, $2\Delta\theta$ is the width of the angular distribution curve also measured between the maximum slope points. If the angular distribution of the haem group orientations is assumed to be Gaussian, $2\Delta\theta$ the

distance between the maximum slope points of the Gaussian curve is twice the standard deviation.

Equation 6.5 can be used to predict the line width variation in any of the crystal planes so long as the angle θ is known for every direction in that plane.

Using this equation the theoretical line width variation in the (ab) plane has been plotted. The angle θ was calculated using the equation

$$\cos \theta = \Sigma l_1 \, l_2$$

where l_1 and l_2 etc. are the direction cosines of the haem normal and the magnetic field. This was done at 10° intervals around the (ab) plane, over 180°. Once θ is known g_θ can be calculated from equation 6.1.

The shape of the curve obtained is shown in Figure (6.12) in which the (a) and (b) axes are marked. By an appropriate choice of $2\Delta\theta$ the curve has been made to agree quite well with the experimentally determined variation. Adjustment of the constant in equation 6.5 does not produce a better fit and the lack of agreement at the minimum can be taken to represent a residual line broadening, the nature of which cannot readily be explained.

The value of $2\Delta\theta$ required to match the curves is 0.055 radians or $3\frac{1}{3}^{\circ}$. The standard deviation of the angular distribu-

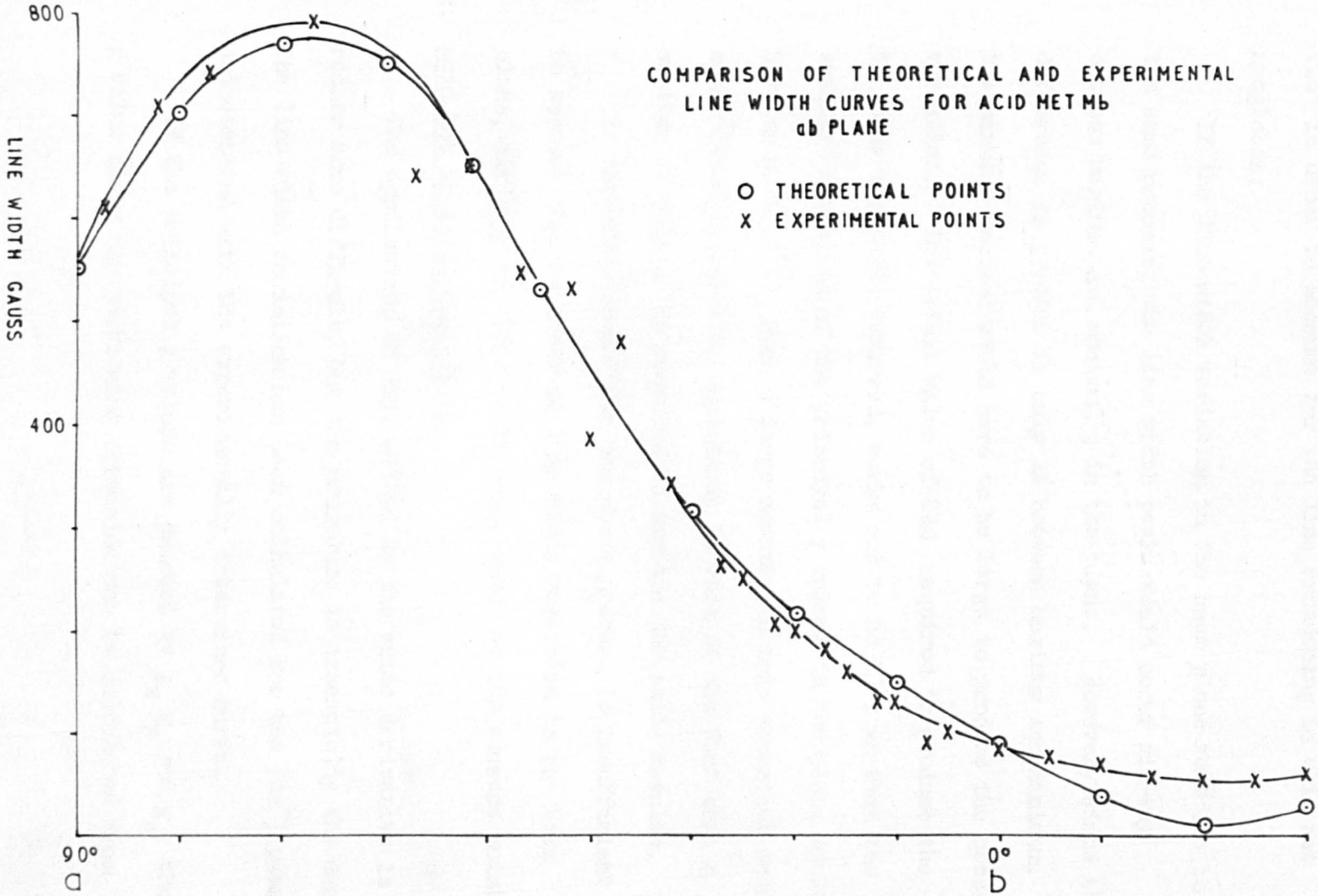
COMPARISON OF THEORETICAL AND EXPERIMENTAL
LINE WIDTH CURVES FOR ACID MET Mb
ab PLANE
O THEORETICAL POINTS
X EXPERIMENTAL POINTS
LINE WIDTH GAUSS
800
400
90°
a
0°
b

FIG. 6.12

tion of the haem group orientation would therefore have to be 1.6° in order to account for the line broadening in acid met myoglobin.

If the line width variation in the haem plane were due to the same process, the line width peaks would occur mid-way between maximum and minimum g in the plane. However, since the difference in g value is only 2% between maximum and minimum, the angular scatter would have to be large to produce the observed variation. The actual value of $2\Delta\theta$ required to produce the 50 gauss variation observed, works out to be 27°, so that the standard deviation of the principal g values in the plane would have to be 13.5°. Such a large scatter in this direction would seem rather improbable, especially in view of the fact that a scatter of only 4° is required to explain the azide results.

It therefore seems that the above process is insufficient to account for the observed line width variation in the haem plane, although the line width peaks occur at the correct points.

6.5.2. Acid Met Mb Azide Derivative

The application of this method to the azide derivative is rather more difficult, but the procedure is essentially the same. The line width variation has been calculated for the ($bc^{\#}$) plane and compared with the experimentally determined curve.

If the principal g values are denoted by g_x g_y and g_z, the g value along any particular direction can be calculated from

the following equation

$$g^2 = g_z^2 \cos^2\theta + g_x^2 \sin^2\theta \cos^2\phi + g_y^2 \sin^2\theta \sin^2\phi \quad . \quad 6.6$$

Here θ is the angle between the magnetic field and the z axis and ϕ is the angle between the projection of the magnetic field direction on the xy plane and the x axis. The coordinate axes and the ($bc^{\#}$) plane are shown in Figure (6.13). The angle α, in this diagram, represents the position of the magnetic field in the ($bc^{\#}$) plane and is zero when the magnetic field is parallel to the xy plane, that is when $\theta = 90^{\circ}$. The values of θ and ϕ were calculated for various values of α from 0 to 180° around the ($bc^{\#}$) plane.

The angle θ was determined as in the acid met Mb and the angle ϕ' calculated by simple geometry. The angle between $\phi' = 0$ (that is the direction of $\alpha = 0$) and the x axis was calculated by finding the direction of the line of intersection of the ($bc^{\#}$) and (xy) planes. Once this was known the angle ϕ was also known.

The line width in the azide derivative can be considered to be the sum of two line widths, one caused by variations in θ, and the other by variations in ϕ. The latter corresponds to small rotations of the xy plane about the z axis. Equation 6 can be differentiated with respect to θ and ϕ and a line width variation calculated for both. Thus,

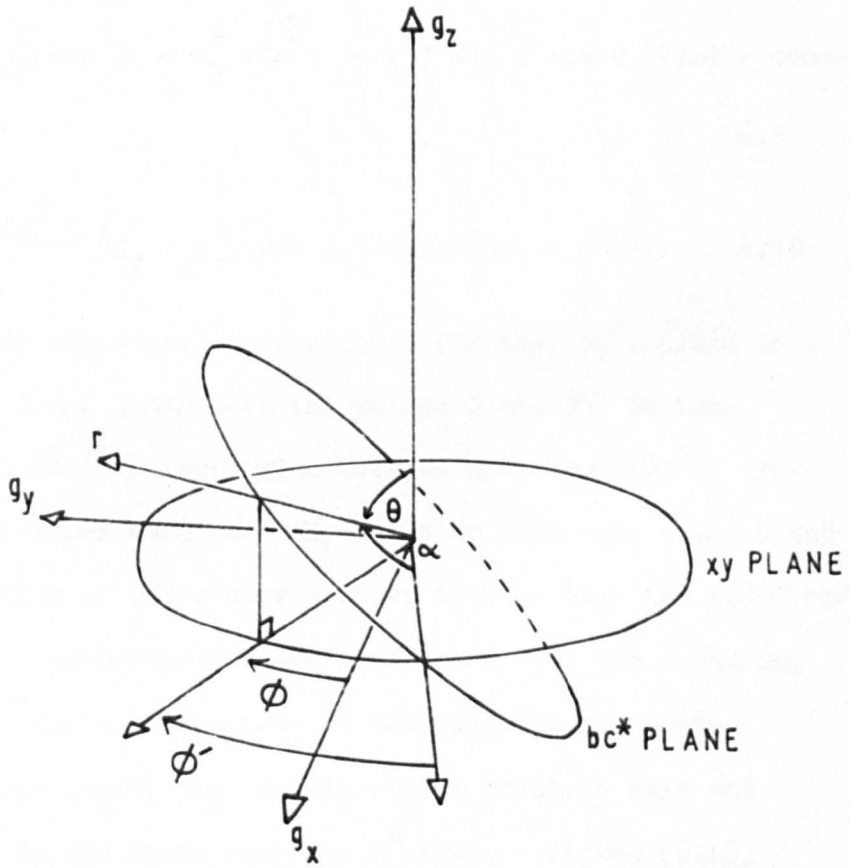

FIG.6.13

$$g \frac{\partial g}{\partial \theta} = (g_x^2 \cos^2\phi + g_y^2 \sin^2\phi - g_z^2) \sin\theta \cos\theta \qquad 6.7$$

and

$$g \frac{\partial g}{\partial \phi} = \sin^2\theta (g_y^2 - g_x^2) \sin\phi \cos\phi \quad . \qquad 6.8$$

The analogous expressions to equation 6.6 are therefore

$$\Delta H_1 = \frac{26.76}{g_{\theta\phi}^3} (g_x^2 \cos^2\phi + g_y^2 \sin^2\phi - g_z^2) \sin\theta \cos\theta (2\Delta\theta) + \text{const.} \qquad 6.9$$

$$\Delta H_2 = \frac{26.76 \sin^2\theta}{g_{\theta\phi}^3} (g_y^2 - g_x^2) \sin\phi \cos\phi (2\Delta\theta) + \text{const.} \qquad 6.10$$

These expressions are shown plotted for the ($bc^{\#}$) plane in Fig. (6.14). Since ϕ can have the values 0 and 90° in this plane, ΔH_2 will fall to zero twice between $\alpha = 0$ and 180°. However, θ never reaches zero and ΔH_1 falls to zero only at $\alpha = 0$ and 180°. Inspection of these curves shows that if they are added together with the appropriate values of $\Delta\theta$ and $\Delta\phi$, the resulting curve will show the main features of the experimental curve. Namely, two large peaks, one on either side of the b axis and two sharp dips in the curve near the $c^{\#}$ axis. Figure (6.15) shows the two curves summed with $\Delta\phi = 2\Delta\theta$.

This curve looks similar to the experimental curve, but differs from it in one important way. If the two dips in the experimental curve near the $c^{\#}$ axis do in fact correspond to the points at which $\phi = 0$ and $\theta = 90°$ then they are not in the

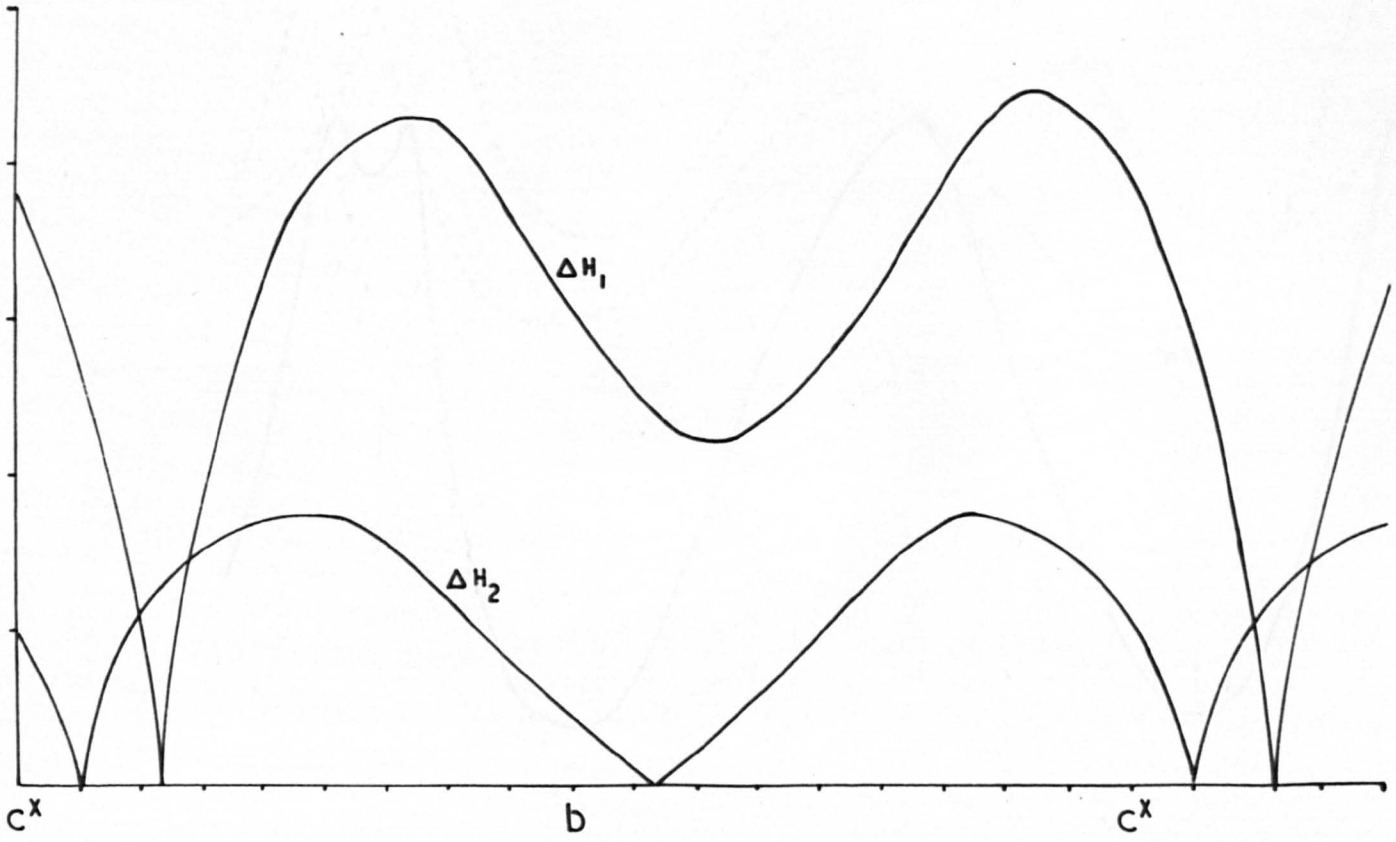

FIG. 6.14
VARIATION OF FUNCTIONS ΔH, & ΔH_2 $[\Delta\theta = \Delta\phi]$

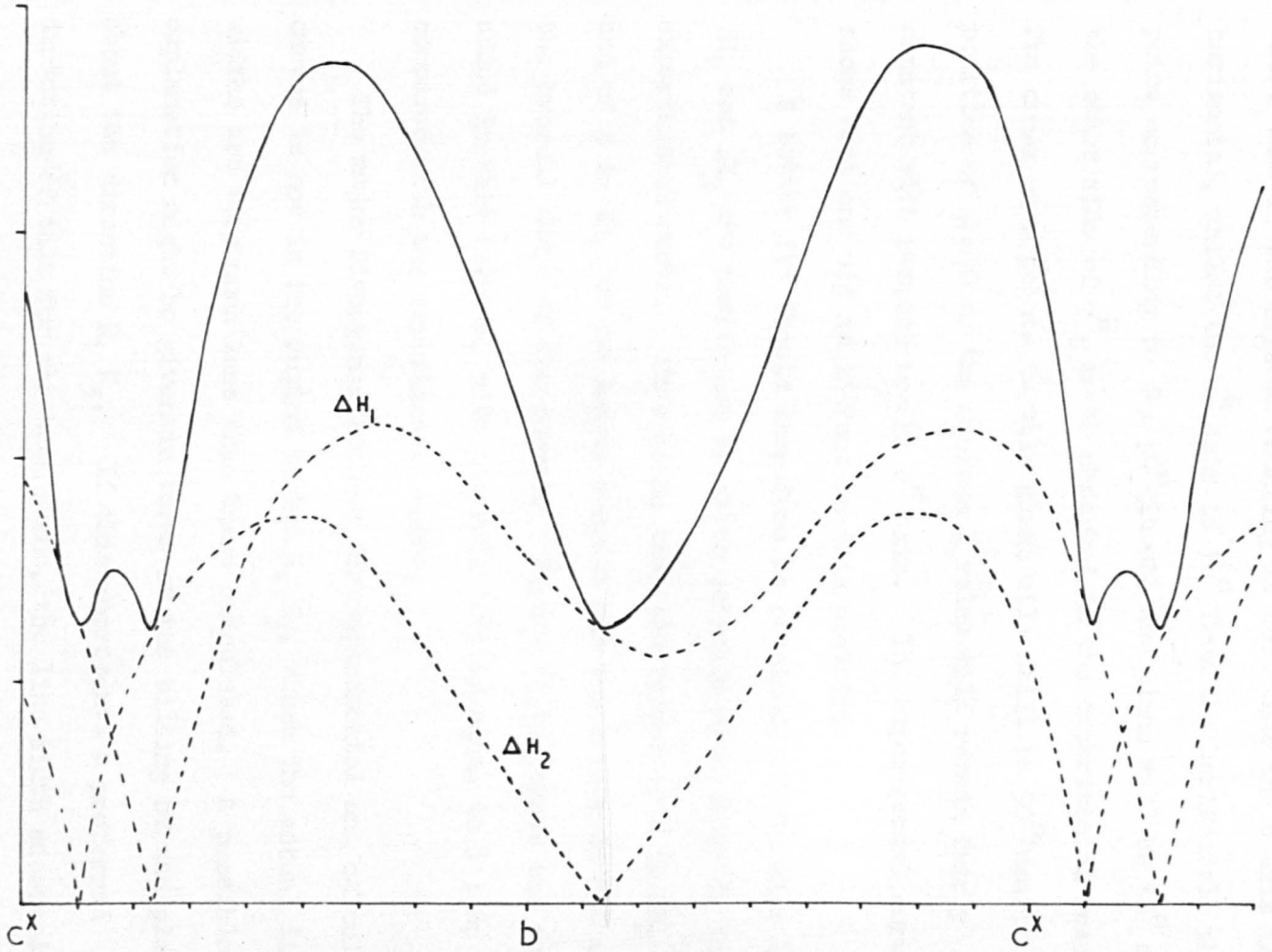

FIG. 6.15

THE SUM OF CURVES ΔH_1 & ΔH_2 $[2\Delta\theta = \Delta\phi]$

positions expected for the (bc^{*}) plane. This can be explained if it is assumed that the crystal was not mounted exactly in the (bc^{*}) plane whilst the measurments were being taken. Calculation shows that if the crystal mounting is such that the b axis is horizontal, whilst the c^{*} axis is 10° from the horizontal, the point corresponding to $\theta = 90^{\circ}$ in the new plane will be 10° on the other side of c^{*}, as is observed in the experimental results. The cross over points in this plane will still be 90° apart. The position of $\phi = 0$ or the minimum g value will remain fairly constant with respect to the c^{*} axis. The experimental curve shows that one dip is in fact in this position.

A better fit should therefore be obtained, if the dips in ΔH_1 and ΔH_2 are positioned so as to coincide with those in the experimental curve. This means that the values of θ in ΔH_2 and of ϕ in ΔH_1 are no longer correct but the errors do not alter the overall shape of the curves. Figure (6.16) shows the curves added in this fashion, with the ratio $\Delta\theta : \Delta\phi$ equal to 3 : 8, compared with the experimental curve.

The major divergence between the experimental and calculated curves is now in the region marked N_1 N_3, where the actual line widths are very much less than those calculated. A possible explanation might be given in terms of the tilting of the plane about the direction N_1 N_3. If this represents a preferred direction of tilt for the haem plane, the line width measured

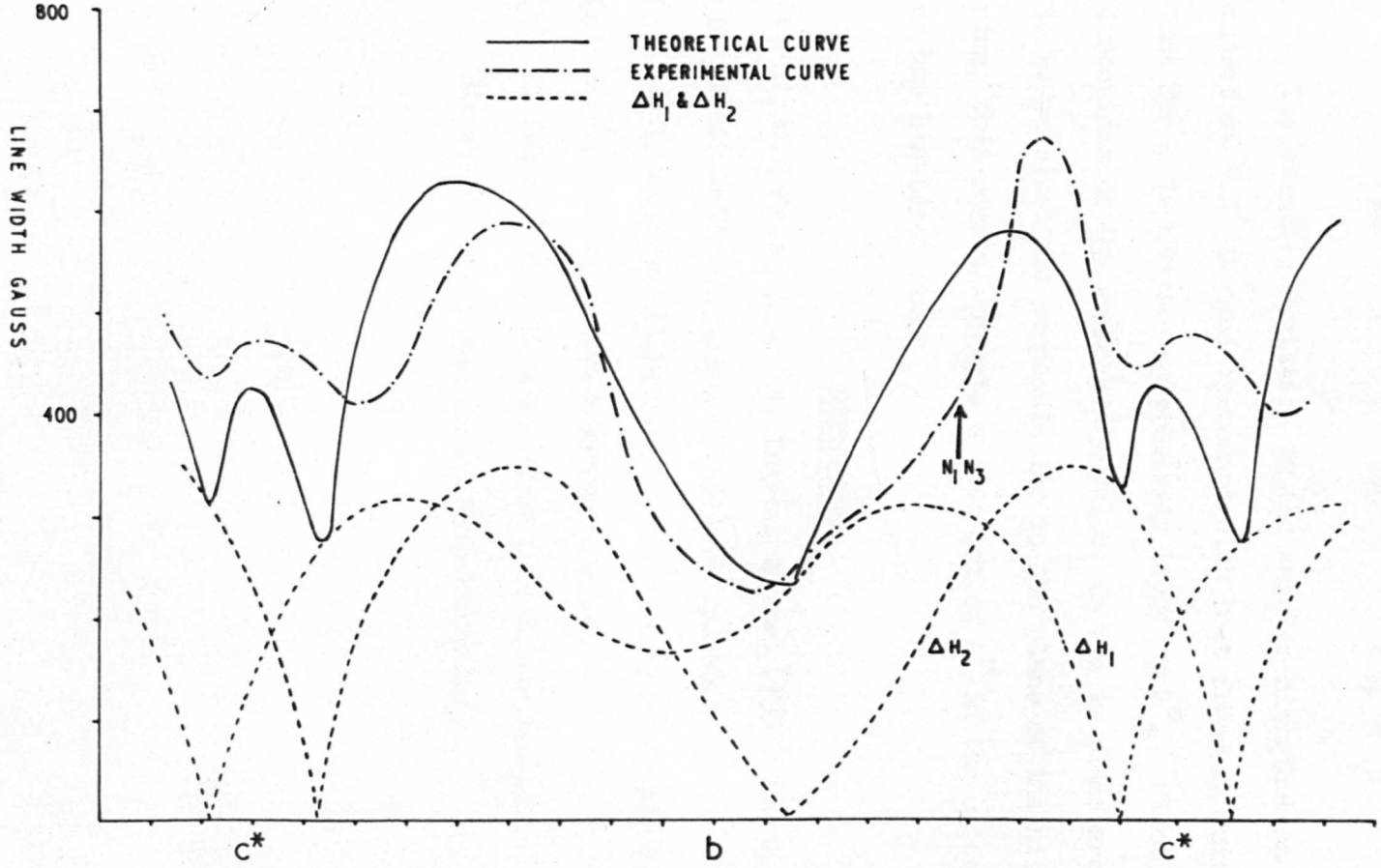

FIG. 6.16

THEORETICAL LINE WIDTH CURVE bc* PLANE AZIDE DERIVATIVE

with the magnetic field parallel to N_1 N_3 should be reduced.

The values of $\Delta\theta$ and $\Delta\phi$ necessary for Figure (6.16) are

$$2\Delta\theta = 3^\circ \qquad \text{and} \qquad 2\Delta\phi = 8^\circ .$$

The standard deviation in the angular distribution of θ is therefore 1.5° in good agreement with that found in acid met. That for ϕ is however surprisingly large at 4°. Since the directions of the principal g values in the xy plane are found to be parallel and perpendicular to the plane of the histidine ring, this result suggests a movement of 4° in the orientation of the histidine ring.

REFERENCES

(1) J. F. Gibson, D. J. E. Ingram, Nature (1957) 180 p. 29.

(2) J. S. Griffith, Nature (1957) 180 p. 30.

(3) J. E. Bennett, Ph.D. Thesis, University of Southampton.

(4) H. C. Watson, private communication.

(5) K. Ohno, Y. Tanabe & F. Sasaki, paper presented at Stockholm Conference on Quantum Chemistry.

Summary and Conclusions

A thorough analysis has been undertaken of the electron resonance measurements on the myoglobin derivatives and previous results have been considered in conjunction with the structural information now available. The g-value variation has been re-measured in acid met Mb. and its azide derivative. The results suggest that what was previously taken to be an isotropic g-value of 6 in the haem plane of acid met Mb. is very slightly anisotropic, with g-values varying from 5.86 to 5.98. The maximum and minimum g values in the plane seem to be parallel to those in the azide derivative.

The directions of the principal axes in the azide derivative have been related to the molecular structure as determined by X-ray measurements. The maximum g-value is found to make an angle of 9° with the haem normal as calculated from electron resonance and X-ray measurements on acid met Mb.. The possible implications of this fact have been considered in conjunction with a theory to explain the ability of molecular groups to react with the iron atom at its sixth coordination site. This site is shown by X-ray measurements to be screened from such reactions by the surrounding protein molecule.

The two other principal g-values in the azide derivative have been found to lie parallel and perpendicular to the plane of the histidine ring at the fifth coordination point of the

iron atom. The histidine ring thus appears to determine the directions of two principal g-values in both acid met and the azide derivative. The plane of this ring is not parallel to one of the iron-nitrogen bond directions in the haem plane, so that the splitting of the d_{yz}, d_{xz} orbitals cannot be due to straightforward π-interaction with the histidine ring.

The very great line width variations in both acid met Mb and the azide derivative have been measured in various crystal planes. These line widths have been explained in terms of a scatter in the orientation of the principal g-values of each iron atom, due to some form of disorder in the crystalline structure. On this basis, curves of the line width variation in certain crystal planes have been constructed and fitted to the experimental curves. Values for the standard deviation in the orientation of the g-values have been determined in this way.

The line widths observed in the haem plane, where there should be no broadening due to this process, have not been explained. Considering the magnetic dilution of the crystals, the line widths of from 40 to 120 gauss are very large and it would be of interest to discover the nature of the broadening process here. If the effect of the process could then be reduced it should be possible to observe any hyperfine structure

which might be present due to interaction with the nitrogen ligands.

If the line widths out of the haem plane are due to general disorder in the crystal structure, it would be interesting to make the same measurements on crystals containing the heavy elements used in solving the phase problem of the X-ray analysis. The presence of these heavy elements might well stabilize the structure and produce narrower lines.

When the X-ray analysis is taken to a higher resolution it should be useful to repeat this work for haemoglobin and compare the results with those from myoglobin. The effect of the closer packed structure might then be apparent.

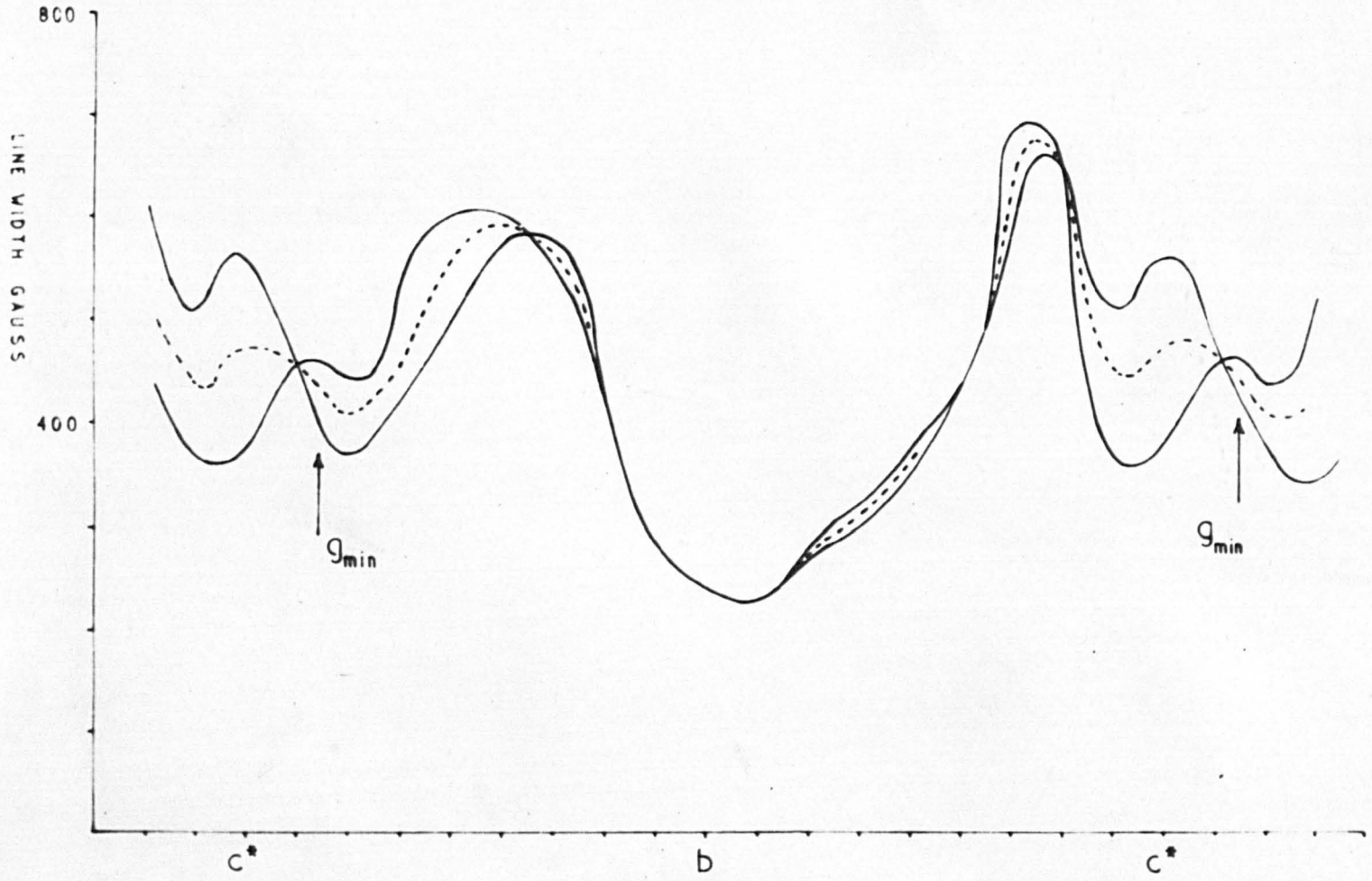

FIG.6.11

COMPARISON OF LINE WIDTH CURVES FROM HAEM GROUPS 1 & 2